

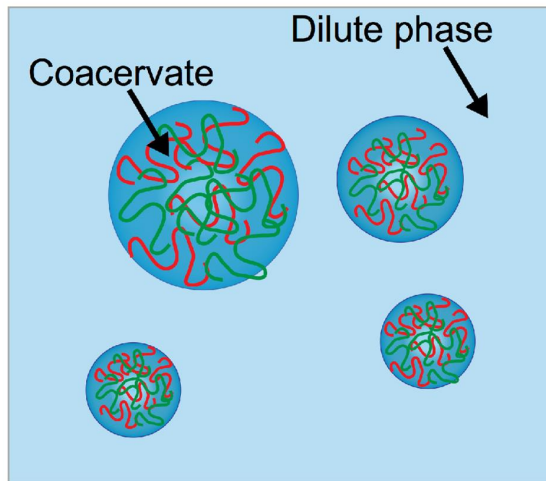
Liquid Liquid Phase Separation and Fibrillization of Intrinsically Disordered Peptides



Joan Shea, Department of Chemistry, UC Santa Barbara

Proteins can assemble in different ways

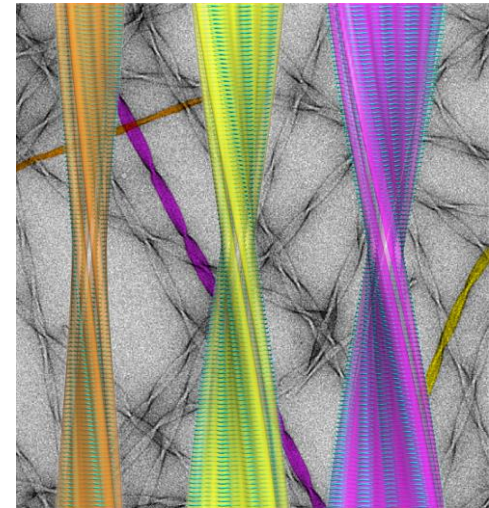
“Liquid”



Droplets
Biomolecular condensates
Coacervates

“Solid”

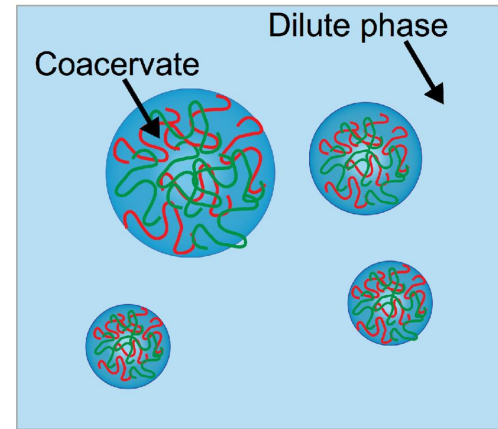
Aging



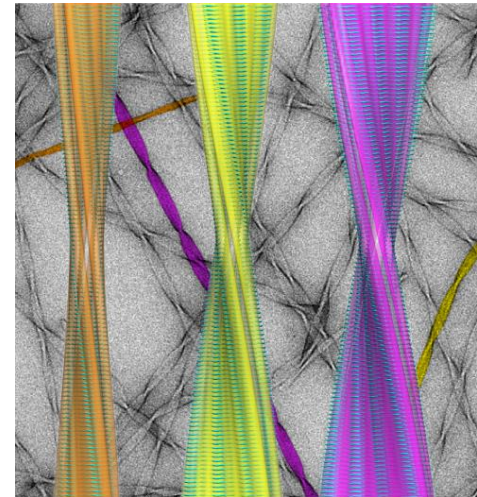
Amyloid Fibrils

Outline

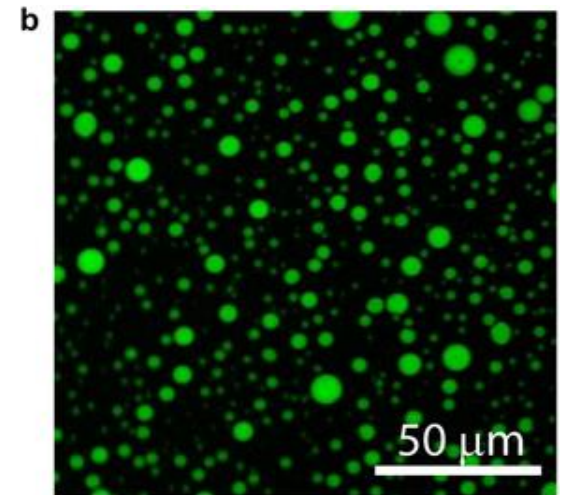
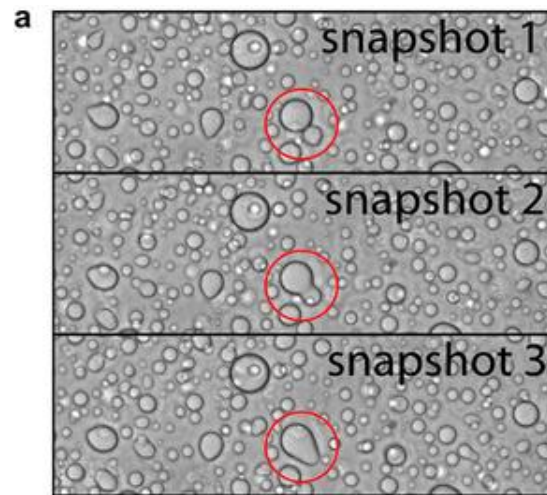
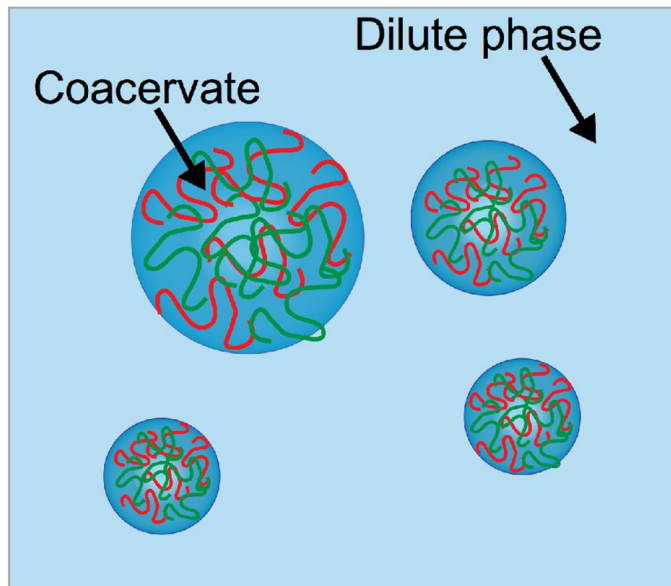
Part 1: Liquid-Liquid Phase Separation: From Model Systems to Tau



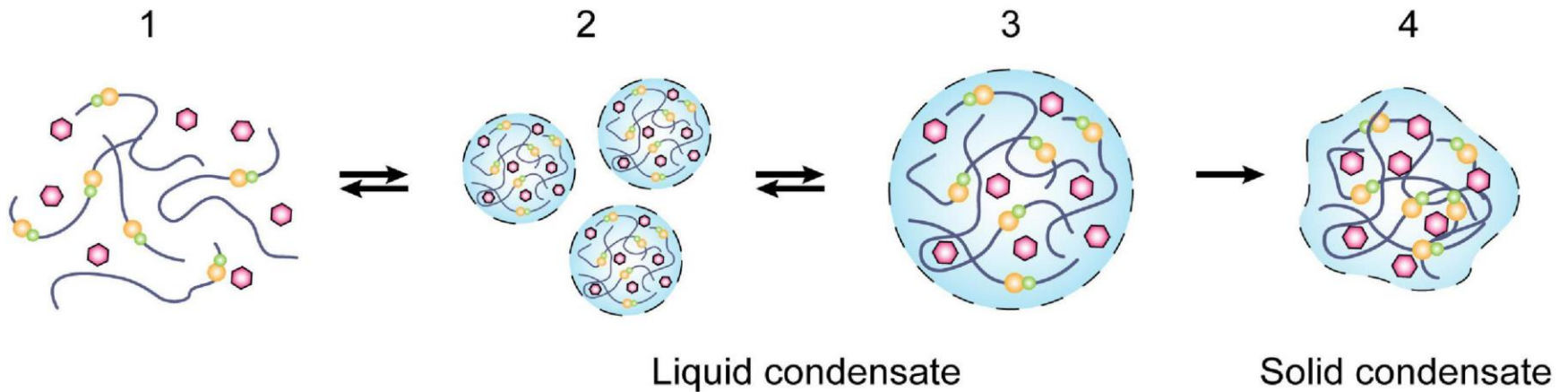
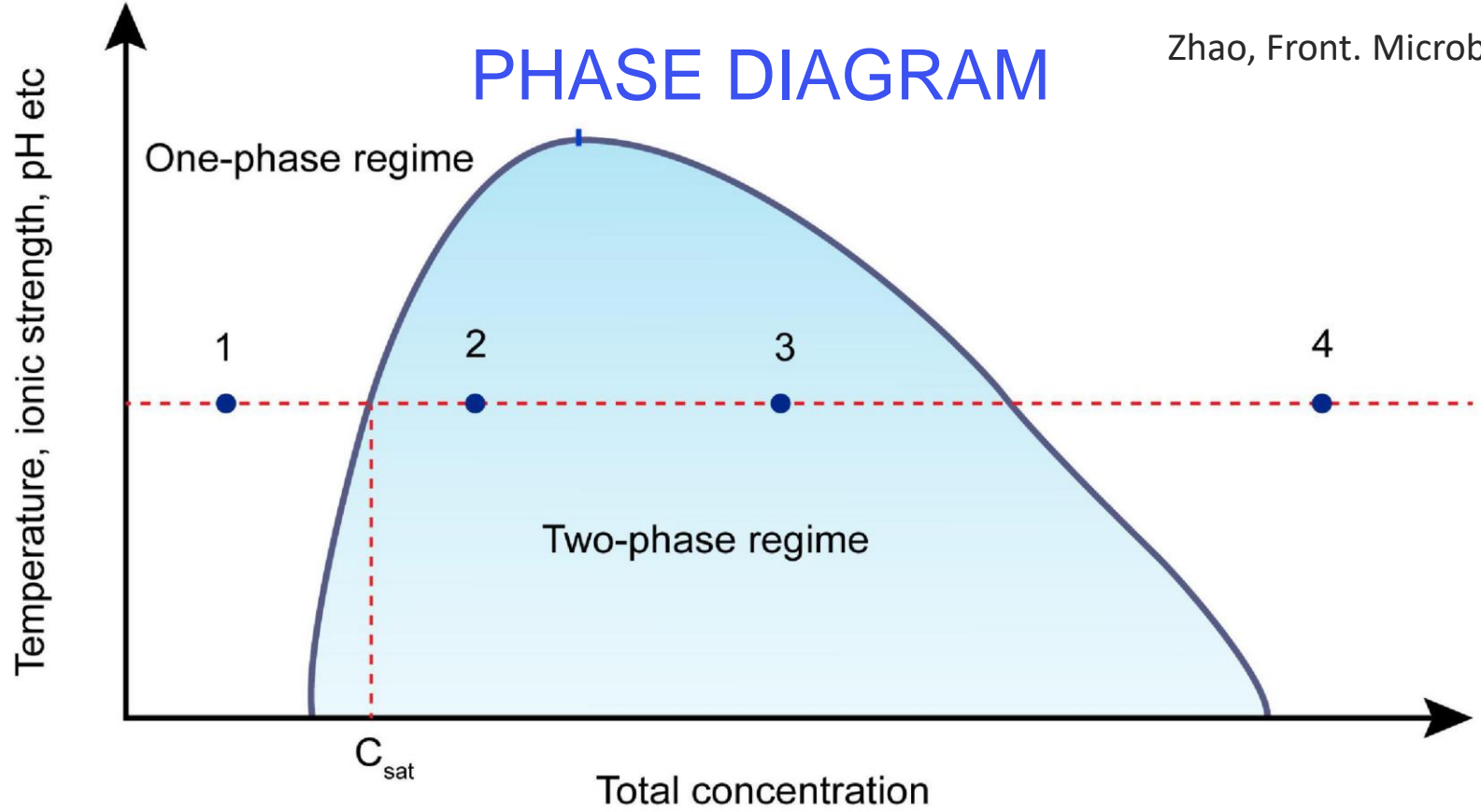
Part 2: Aggregation of the Tau Protein



Coacervation = liquid liquid phase separation
= formation of droplets
= formation of biomolecular condensates



PHASE DIAGRAM



What drives phase separation?

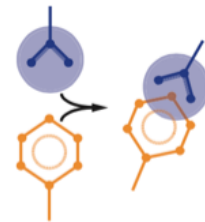
Charge pattern



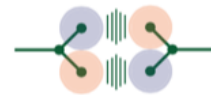
Chain charge density



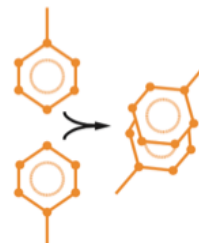
Short-ranged interactions



cation - π



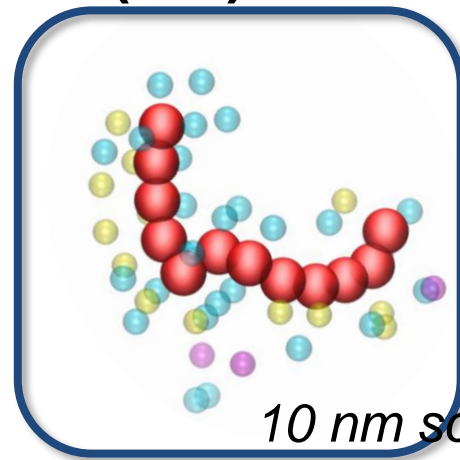
dipole - dipole



$\pi - \pi$ stacking

Computational Approaches

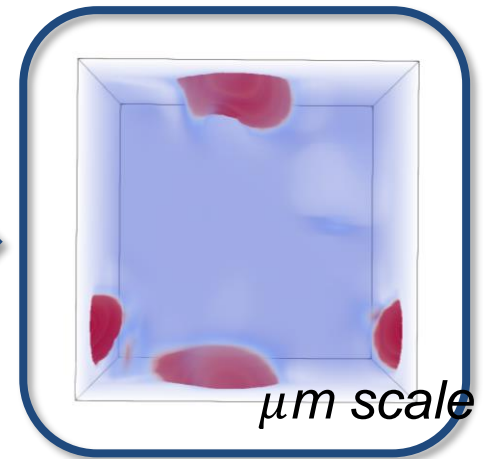
**Coarse-grained
(CG) MD**



10 nm scale



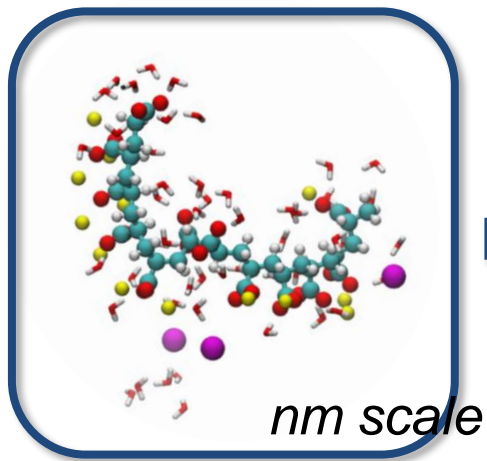
**Field theoretic
simulations
(FTS)**



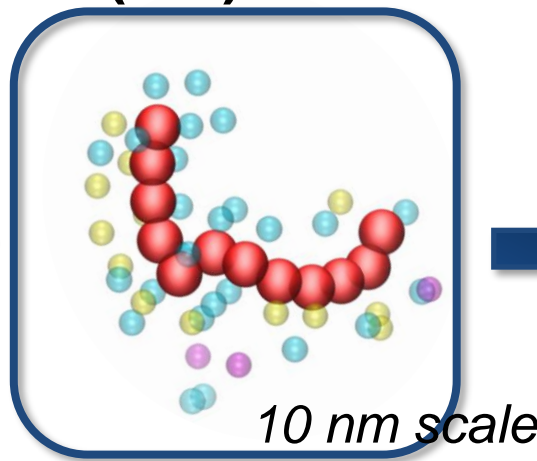
μm scale

Computational Approach

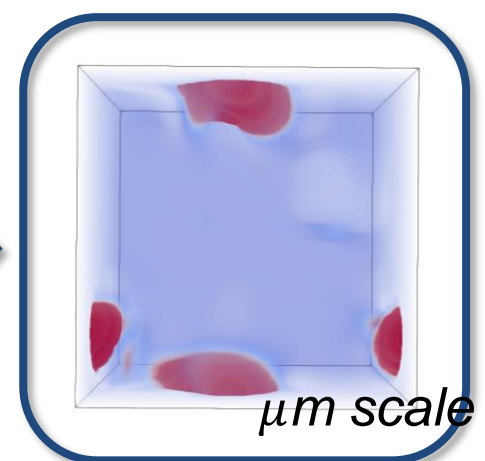
All-atom (AA) MD



Coarse-grained (CG) MD



Field theoretic simulations (FTS)



 **chemistry**

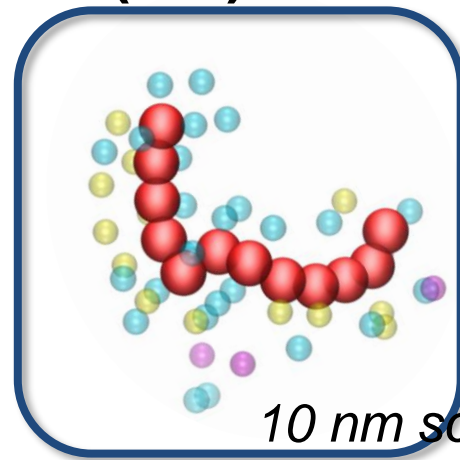
macroscopic properties 

- Clear connection to chemical details
- Short time/length scale
- Dilute conditions

- Can probe long time and length scales
- Efficient for high concentrations

Computational Approaches

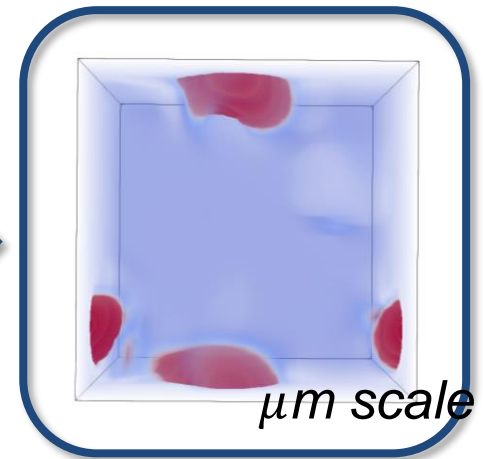
**Coarse-grained
(CG) MD**



10 nm scale

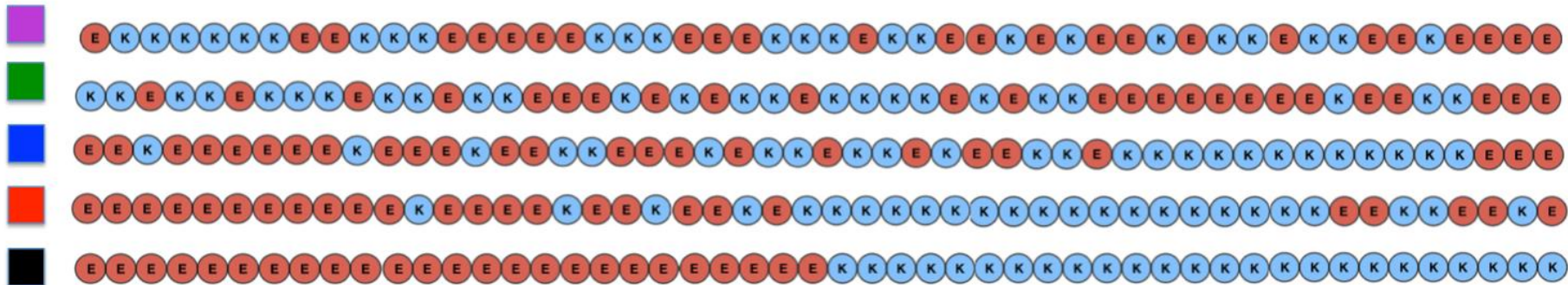
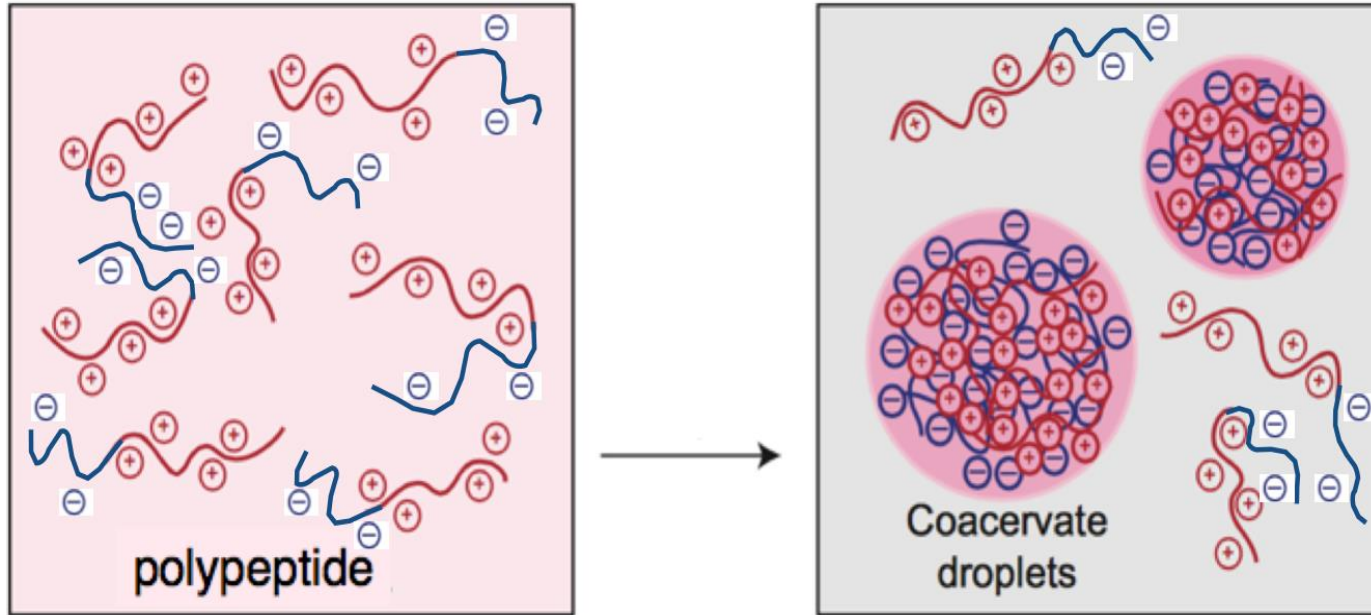


**Field theoretic
simulations
(FTS)**



μm scale

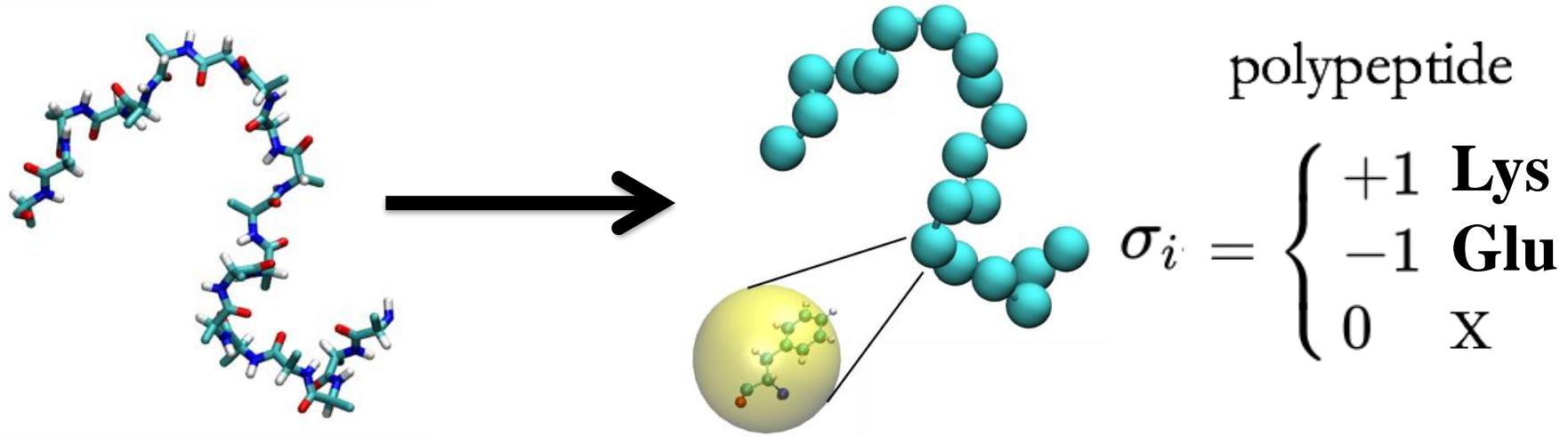
Simple Coacervation



Coarse-Grained Model

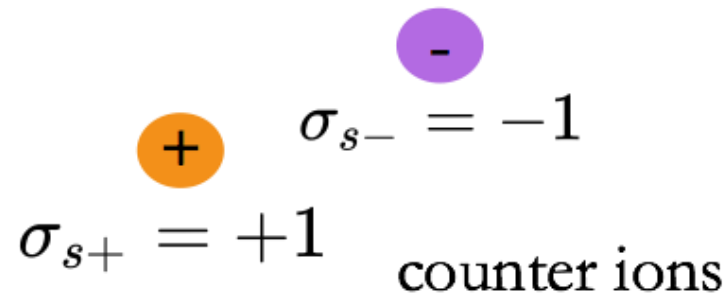
Coarse-grained peptide chain

Each amino acid represented by a single site

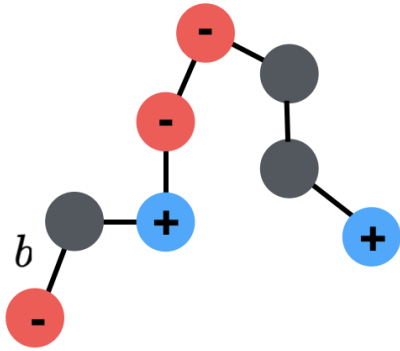


Implicit solvent

Explicit salt ions



Discrete Gaussian chain polyelectrolyte model



charge sequence

$$\{\sigma_i\} = \{\sigma_1, \sigma_2, \dots, \sigma_N\}$$

charge density

$$\frac{1}{N} \sum_i |\sigma_i|$$

N_l sites per molecule

σ_i charge on bead i

b segment length

Formally equivalent representations



Particle MD
simulation



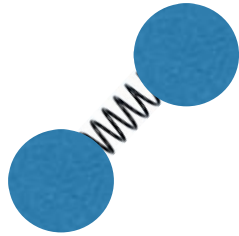
Field Theoretic
simulation

low polymer density

high polymer density

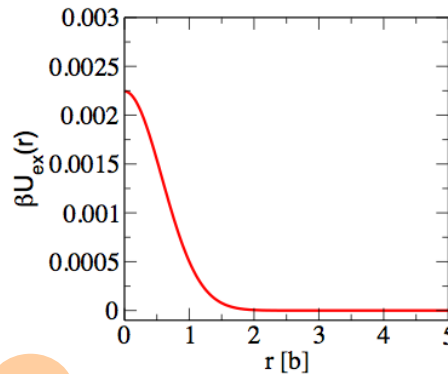
bond potential

$$\beta U_b = \frac{3}{2b^2} r^2$$



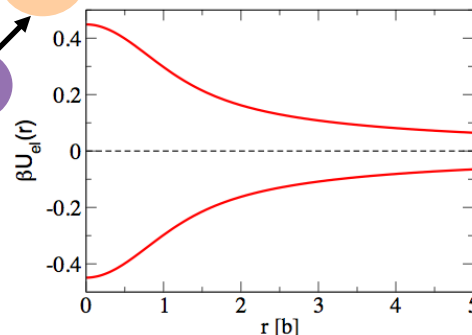
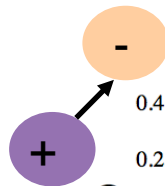
excluded volume parameter

$$\beta U_{ev}(r) = \frac{v}{8\pi^{3/2} a^3} e^{-r^2/4a^2}$$



electrostatic potential

$$\beta U_{es} = \frac{l_B z_i z_j}{r} \operatorname{erf}\left(\frac{r}{2a}\right)$$

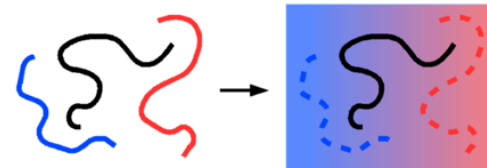


$$H[w, \psi] = \frac{1}{2B} \int d\mathbf{r} w(\mathbf{r})^2 + \frac{1}{2E} \int d\mathbf{r} |\nabla\psi|^2 - \sum_l \frac{CV\bar{\phi}_l}{N_l} \ln Q_l$$

Fluctuating
chemical
potential field

Fluctuating
electrostatic
potential
field

Single chain partition function
for polymers and salt ions



Polymers
decoupled!

Formally equivalent representations













Particle MD
simulation








Field Theoretic
simulation

low polymer density

high polymer density

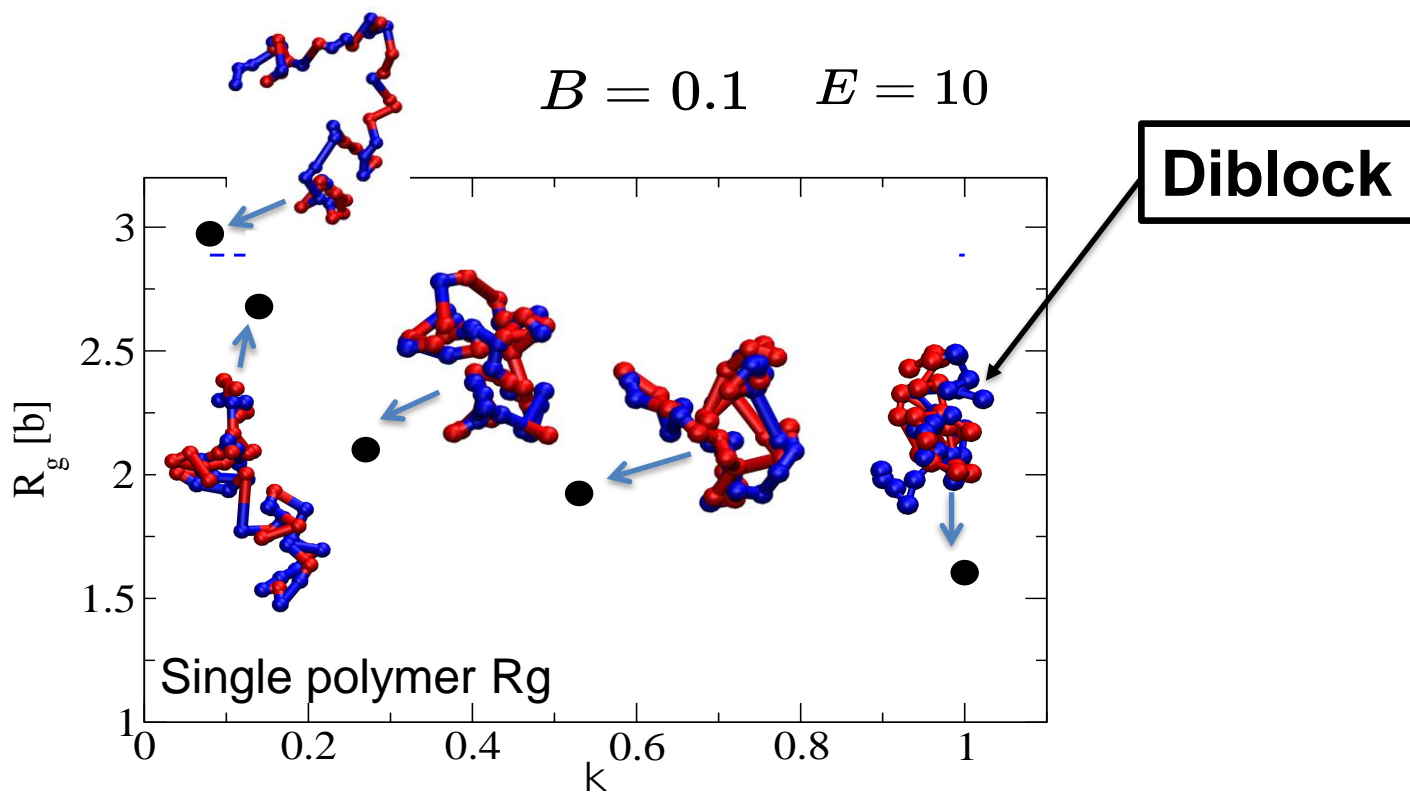
			SCD	κ
sv10			-2.10	0.08
sv15			-4.35	0.14
sv20			-7.37	0.27
sv25			-12.77	0.53
sv30			-27.84	1.00

Particle Based Simulations

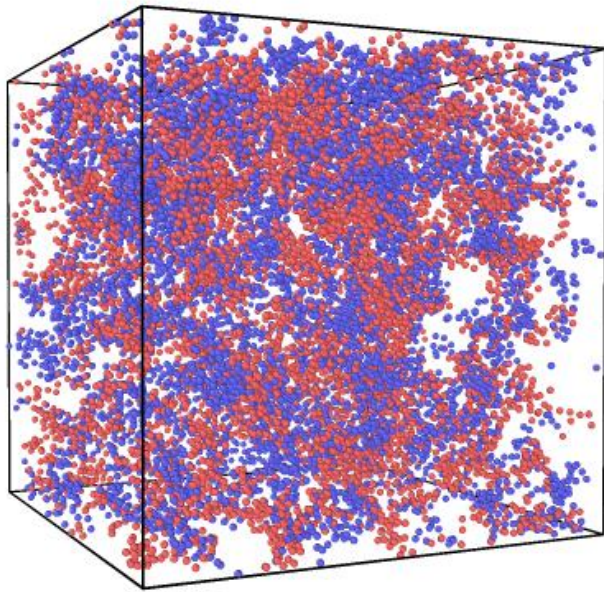
		SCD	κ
sv10		-2.10	0.08
sv15		-4.35	0.14
sv20		-7.37	0.27
sv25		-12.77	0.53
sv30		-27.84	1.00



James Mc Carthy

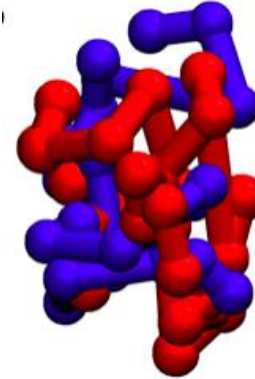


Particle Based Simulations

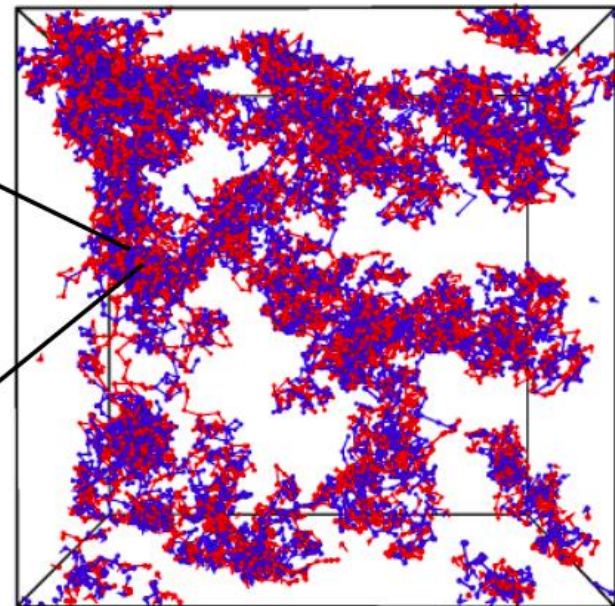
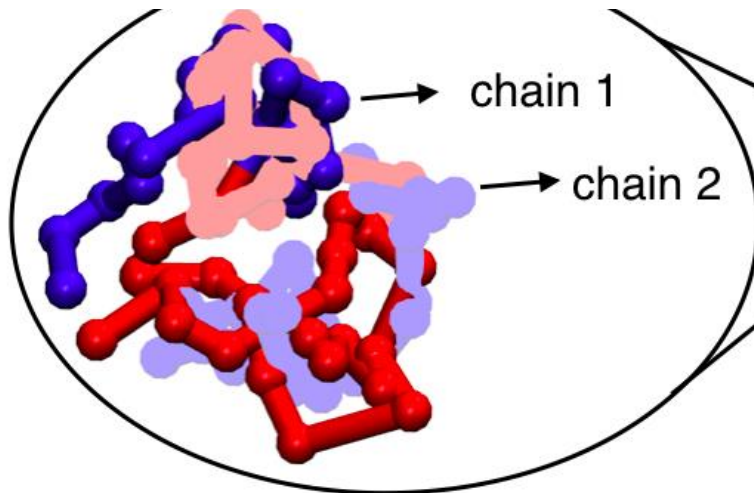


$$n = 300$$

$$N = 50$$



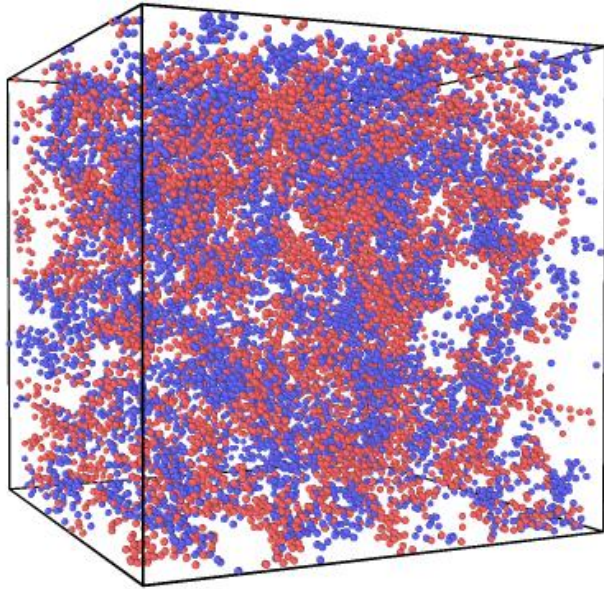
Single Chain



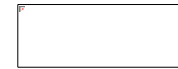
Particle Based versus Field Theoretic Simulations

$n = 300$

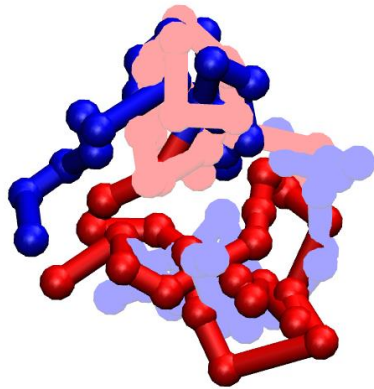
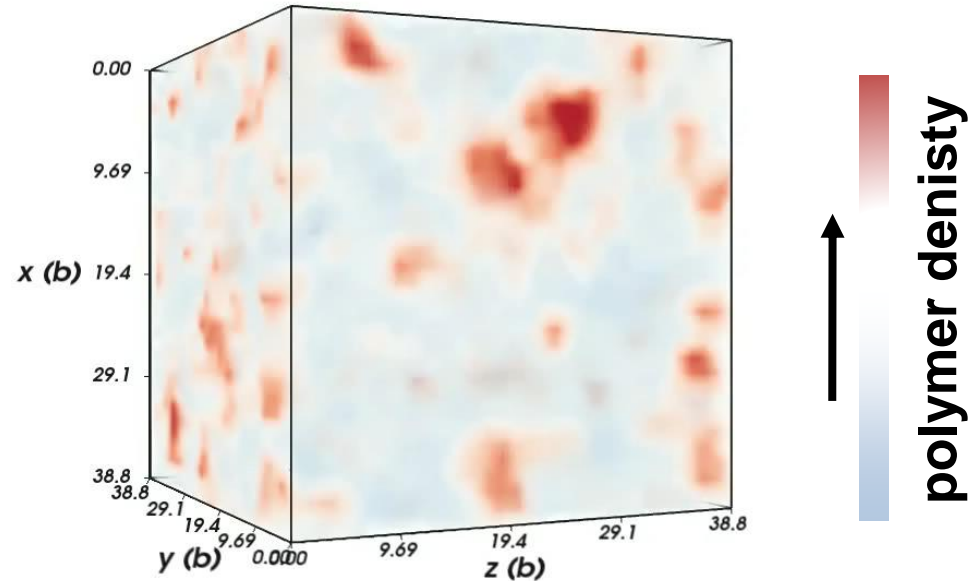
$N = 50$



$C = 0.015$

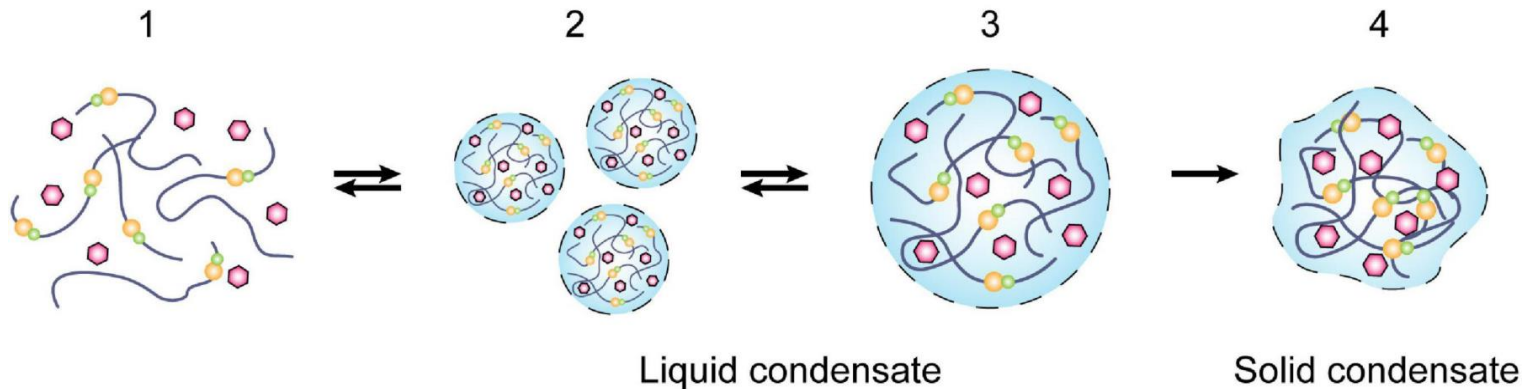
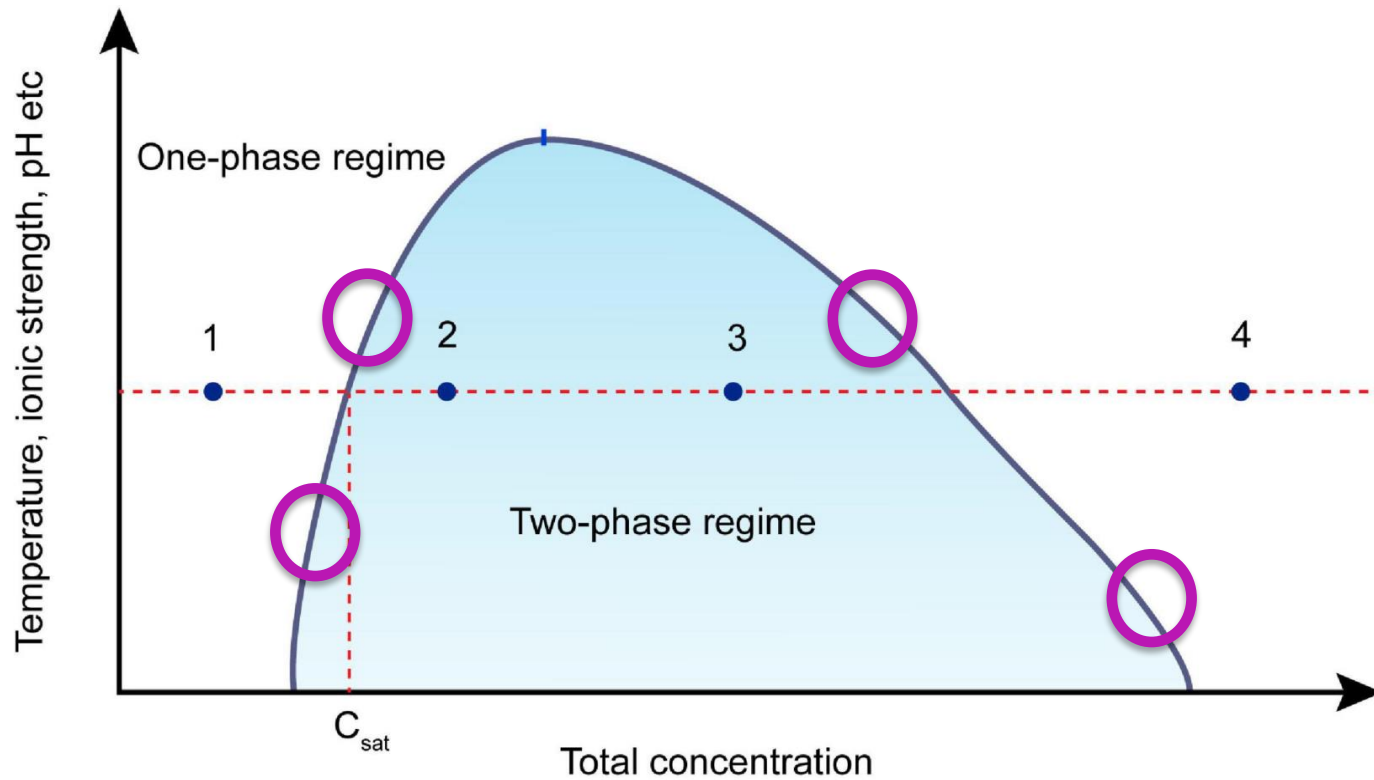


$B = 0.1$

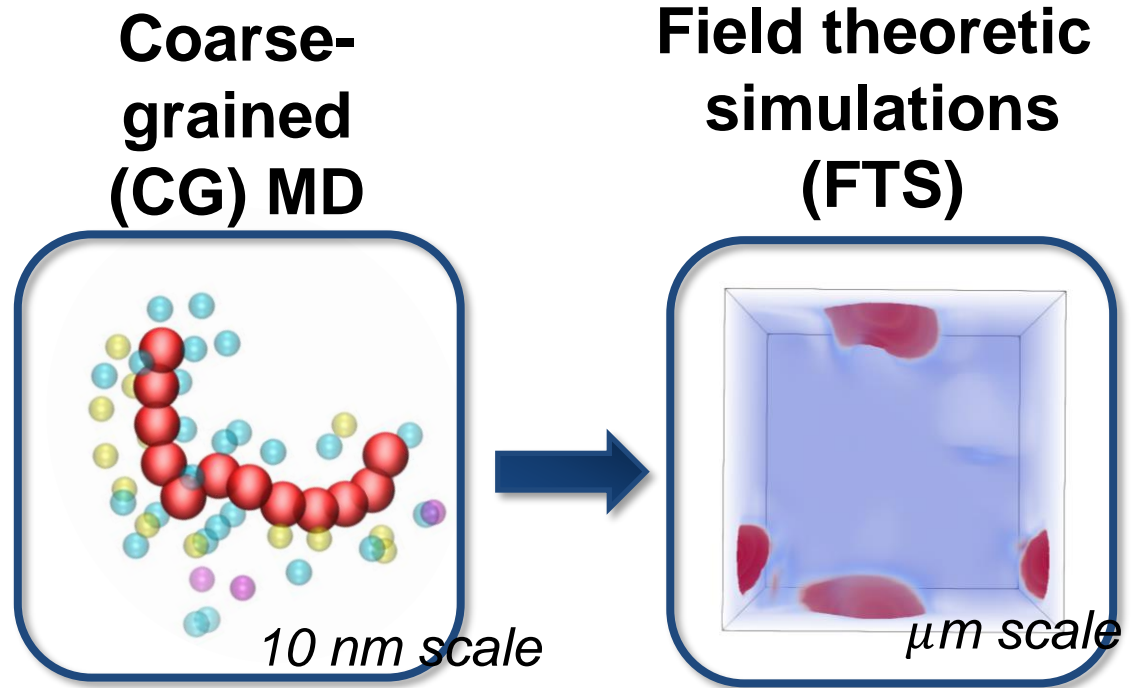


Get a Phase Diagram

We map the boundaries of the phase diagram



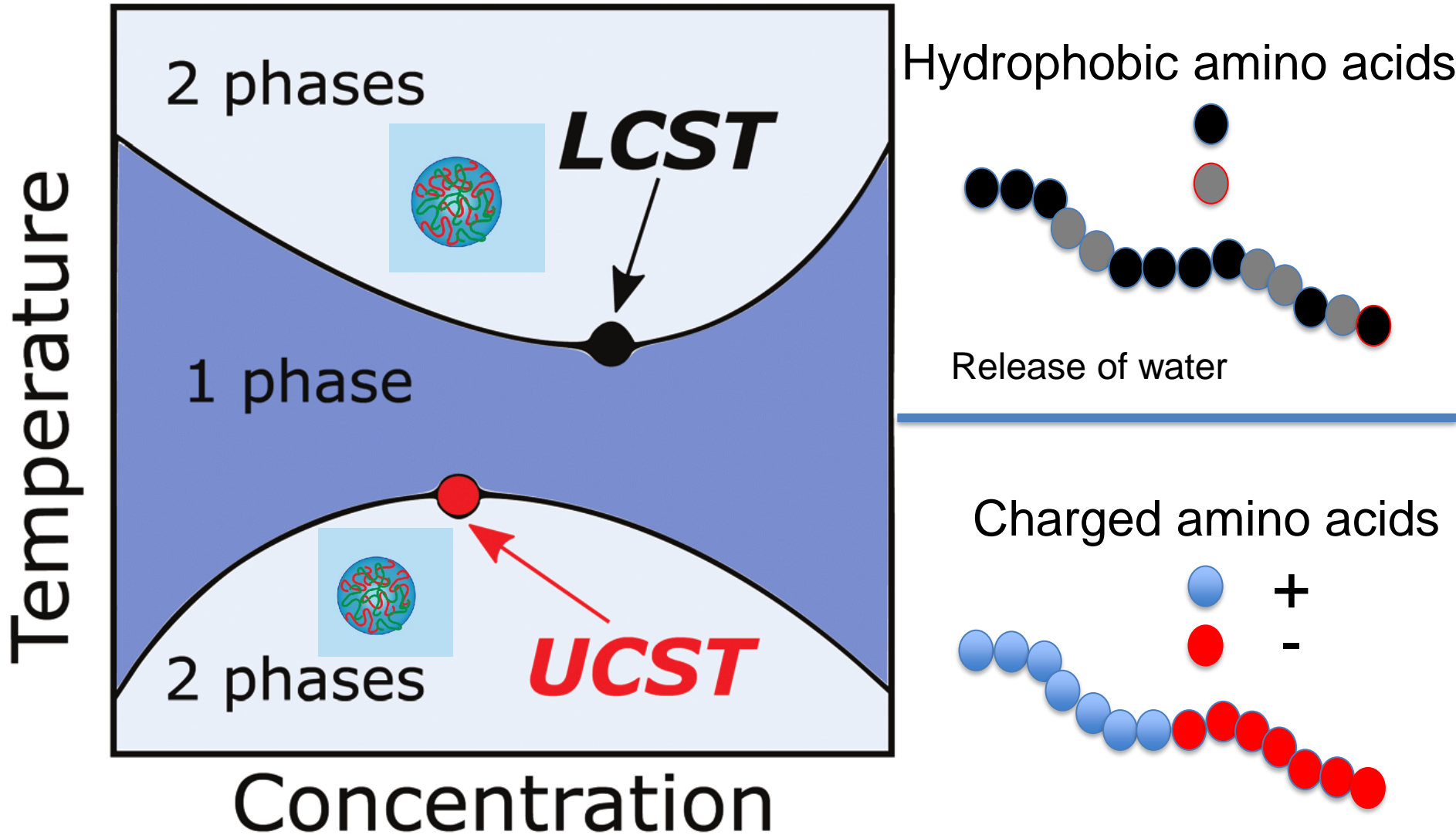
Computational Approach



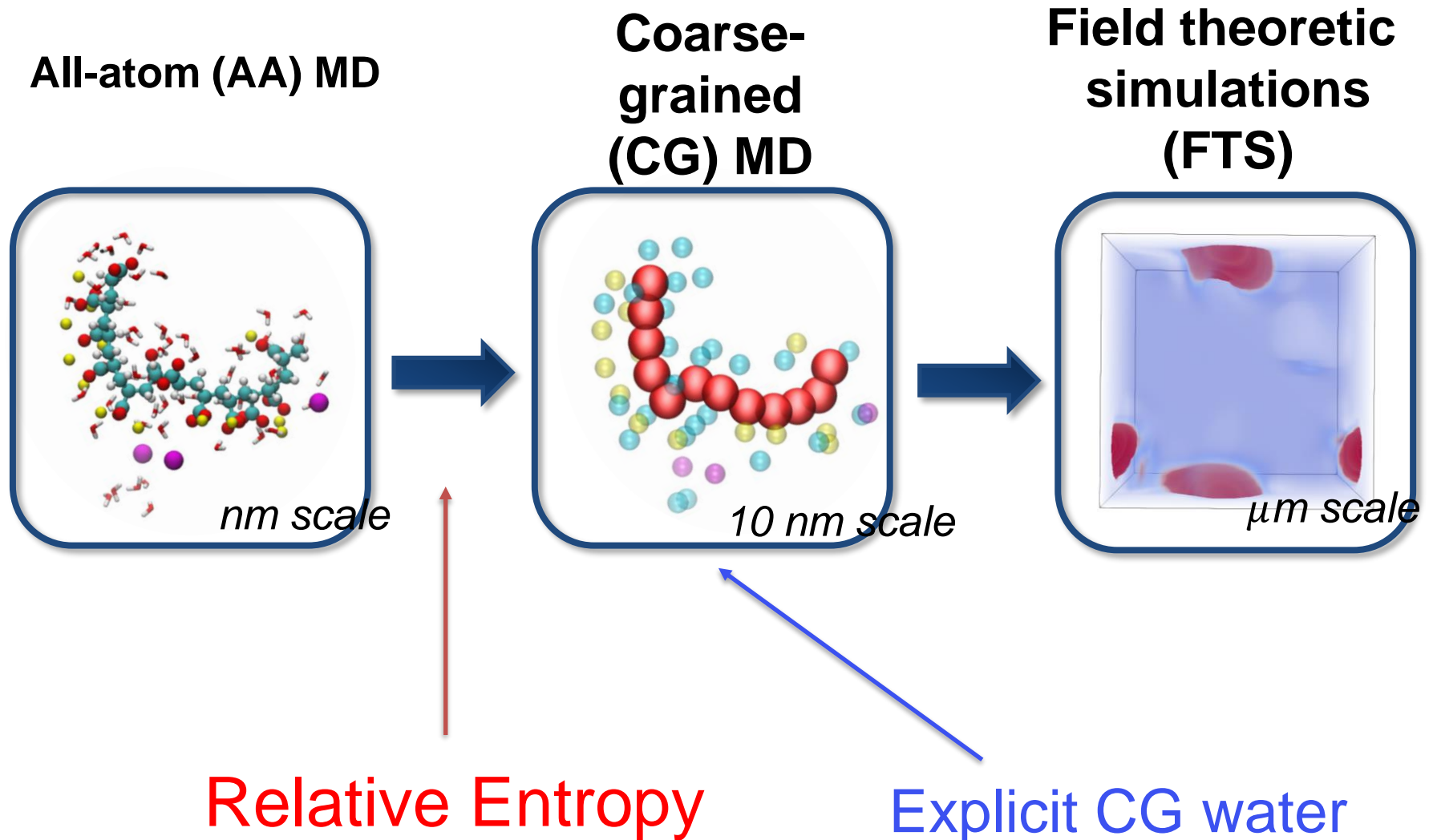
Limitations

- No amino acid specificity
- Implicit solvent

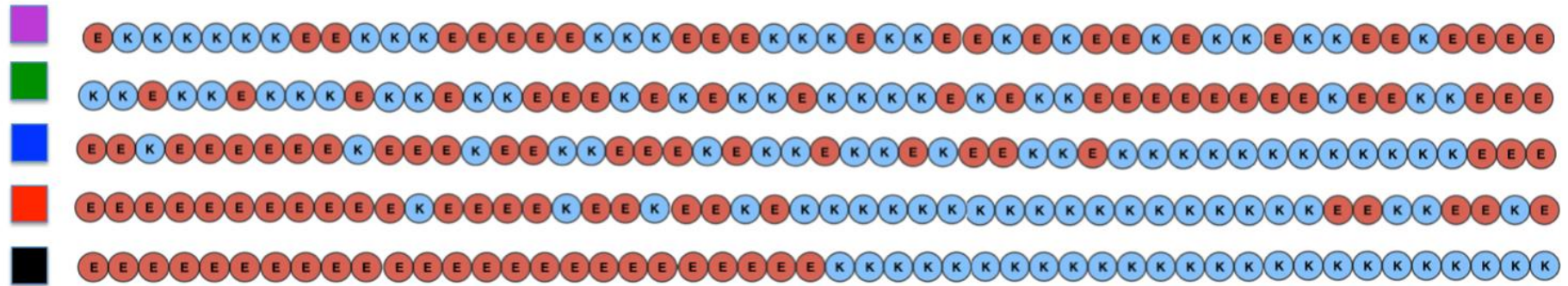
Upper (UCST) and Lower (LCST) critical solution temperature



Computational Approach



OLD: Model System: **KE** (Lys/Glu)sequence



NEW: Model System: **RE** (Arg/Glu)sequence

RE1: Poly-Arg/Glu 

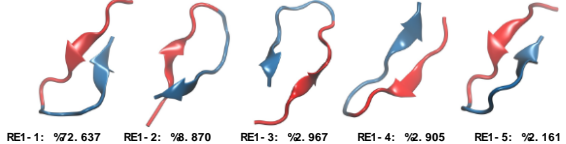
RE2: Poly-Arg/Glu 

RE3: Poly-Arg/Glu 

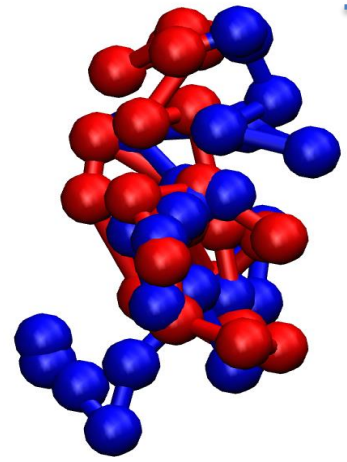
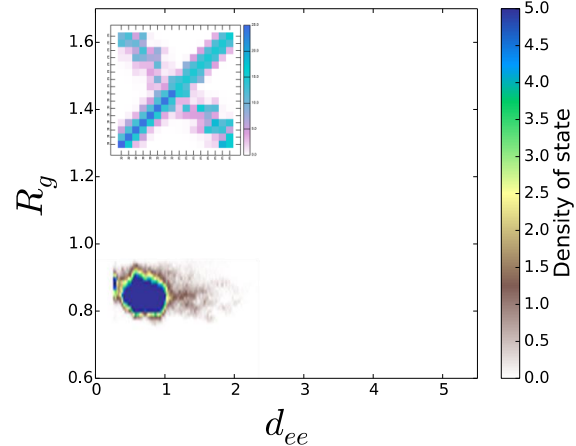
RE4: Poly-Arg/Glu 

All atom replica exchange MD reference simulations

a) RE1: Poly-Arg/Glu ●●●●●●●● ●●●●●●●●

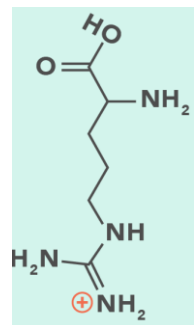


RE1-1: %2.637 RE1-2: %8.870 RE1-3: %2.967 RE1-4: %2.905 RE1-5: %2.161

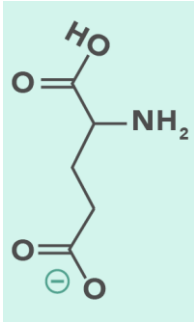


Original
CG

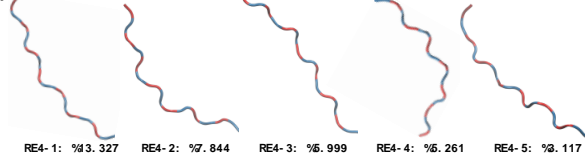
Arg



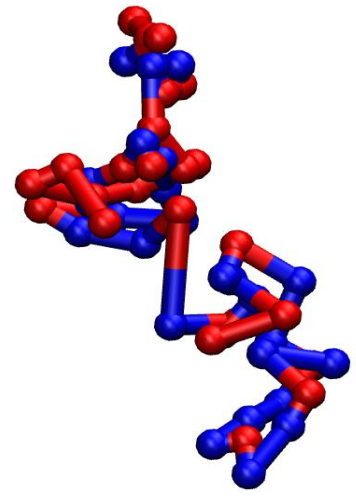
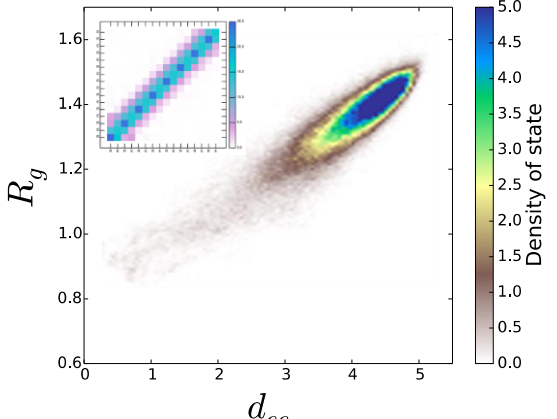
Glu



d) RE4: Poly-Arg/Glu ●●●●●●●● ●●●●●●●●



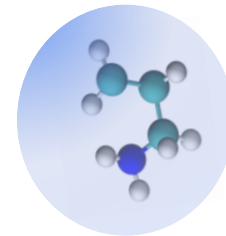
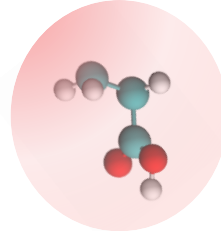
RE4-1: %3.327 RE4-2: %7.844 RE4-3: %6.999 RE4-4: %6.261 RE4-5: %8.117



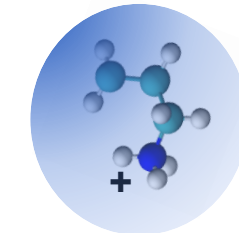
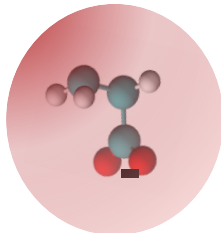
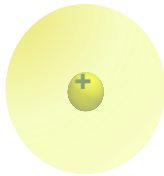
Relative Entropy Coarse-graining

Minimizing the relative entropy:

$$S_{rel} = \int \int \rho_{AA}(\mathbf{r}) \ln \left(\frac{\rho_{AA}(\mathbf{r})}{\rho_{CG}(\mathbf{R})} \right) \delta(\mathbf{M}(\mathbf{r}) - \mathbf{R}) d\mathbf{r} d\mathbf{R}$$



Scott Shell

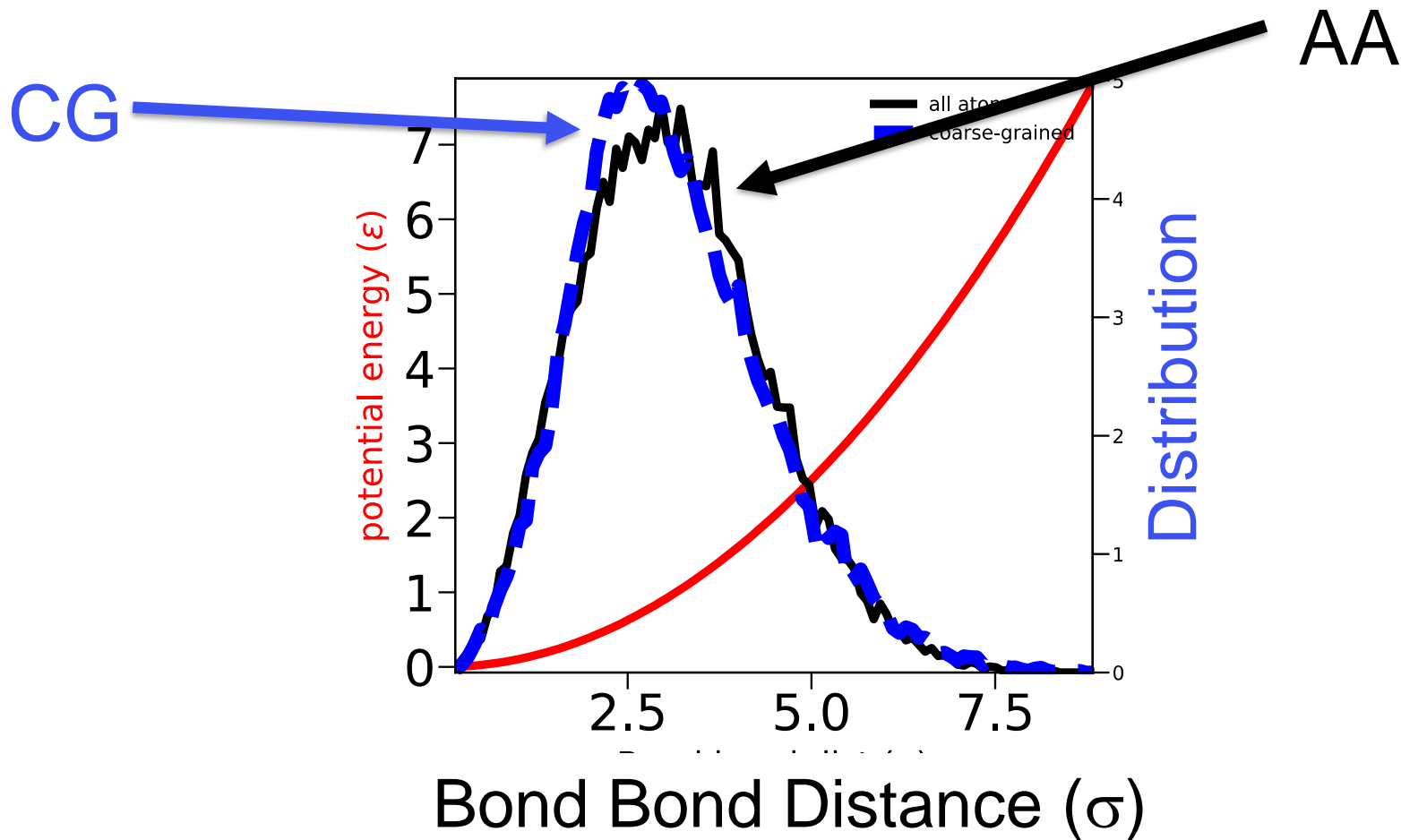


Water

ions

Amino acids

Relative Entropy Parameterization



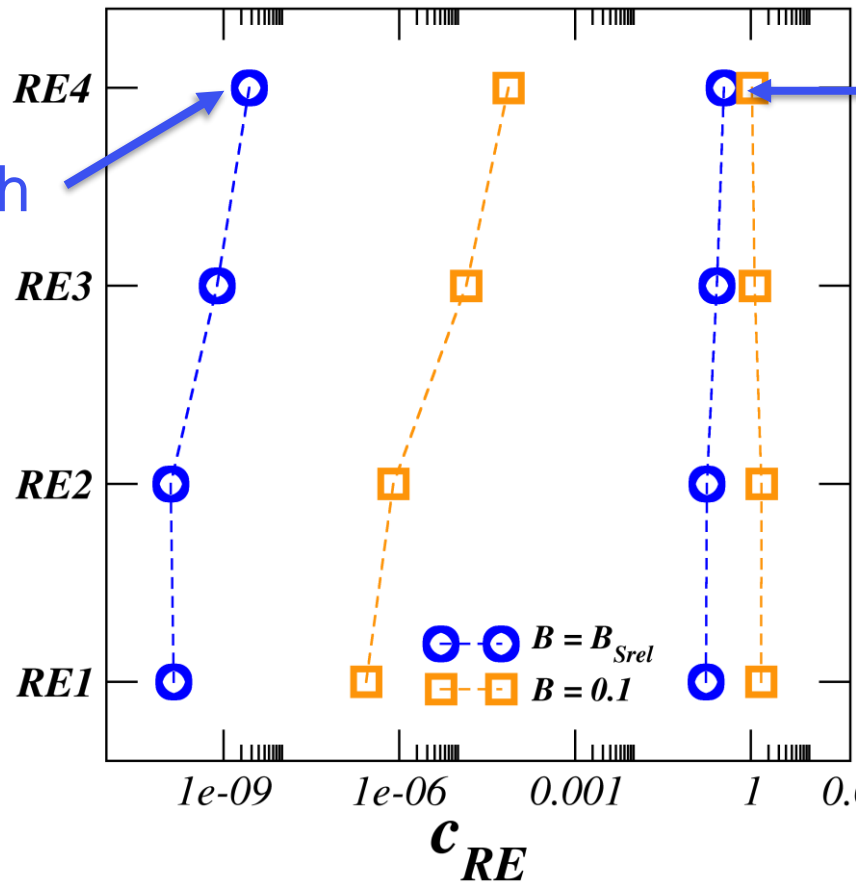
RE peptides phase behavior

RE1: Poly-Arg/Glu ●●●●●●●● ●●●●●●●●

RE2: Poly-Arg/Glu ●●●●●●●● ●●●●●●●●

RE3: Poly-Arg/Glu ●●●●●●●● ●●●●●●●●

RE4: Poly-Arg/Glu ●●●●●●●● ●●●●●●●●



Dense Branch

Dilute Branch

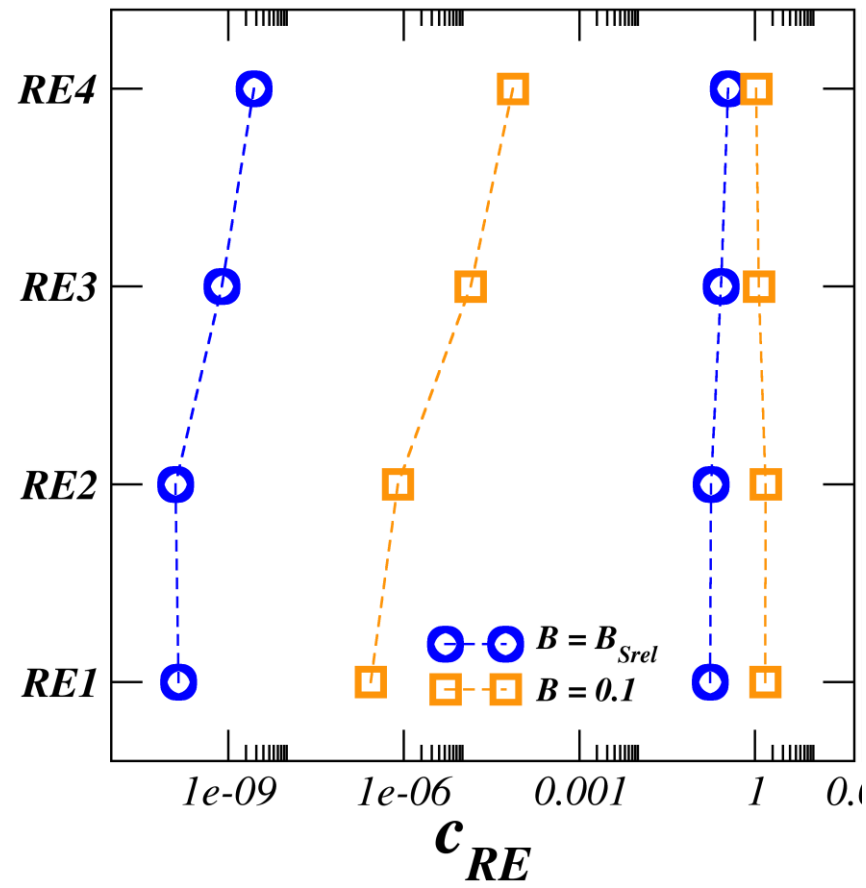
RE peptides phase behavior

RE1: Poly-Arg/Glu ●●●●●●●● ●●●●●●●●

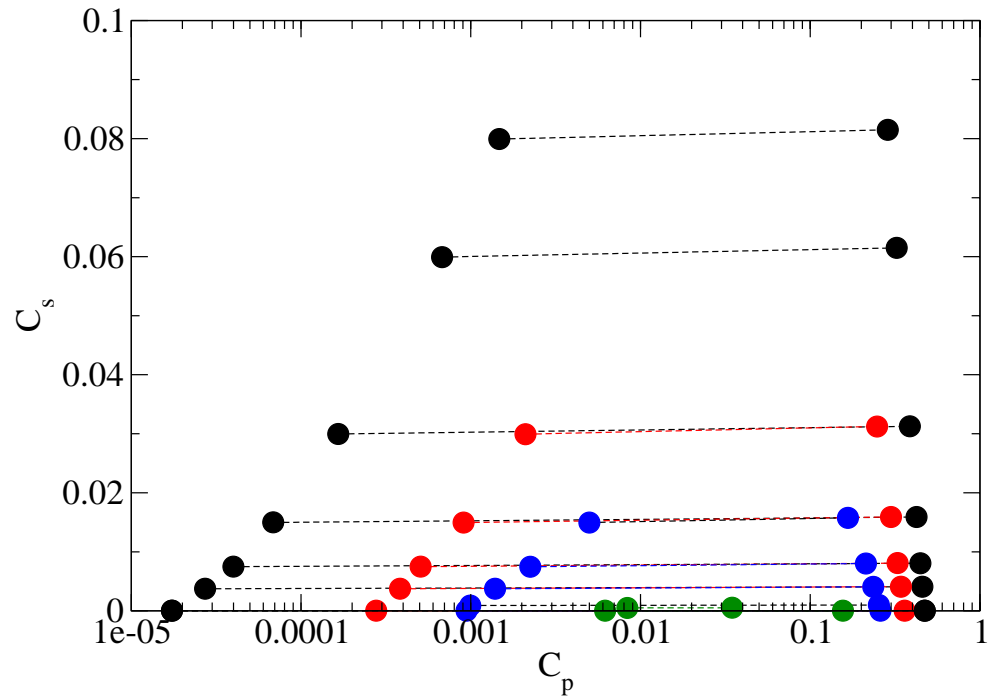
RE2: Poly-Arg/Glu ●●●●●●●● ●●●●●●●●

RE3: Poly-Arg/Glu ●●●●●●●● ●●●●●●●●

RE4: Poly-Arg/Glu ●●●●●●●● ●●●●●●●●



“OLD” FTS

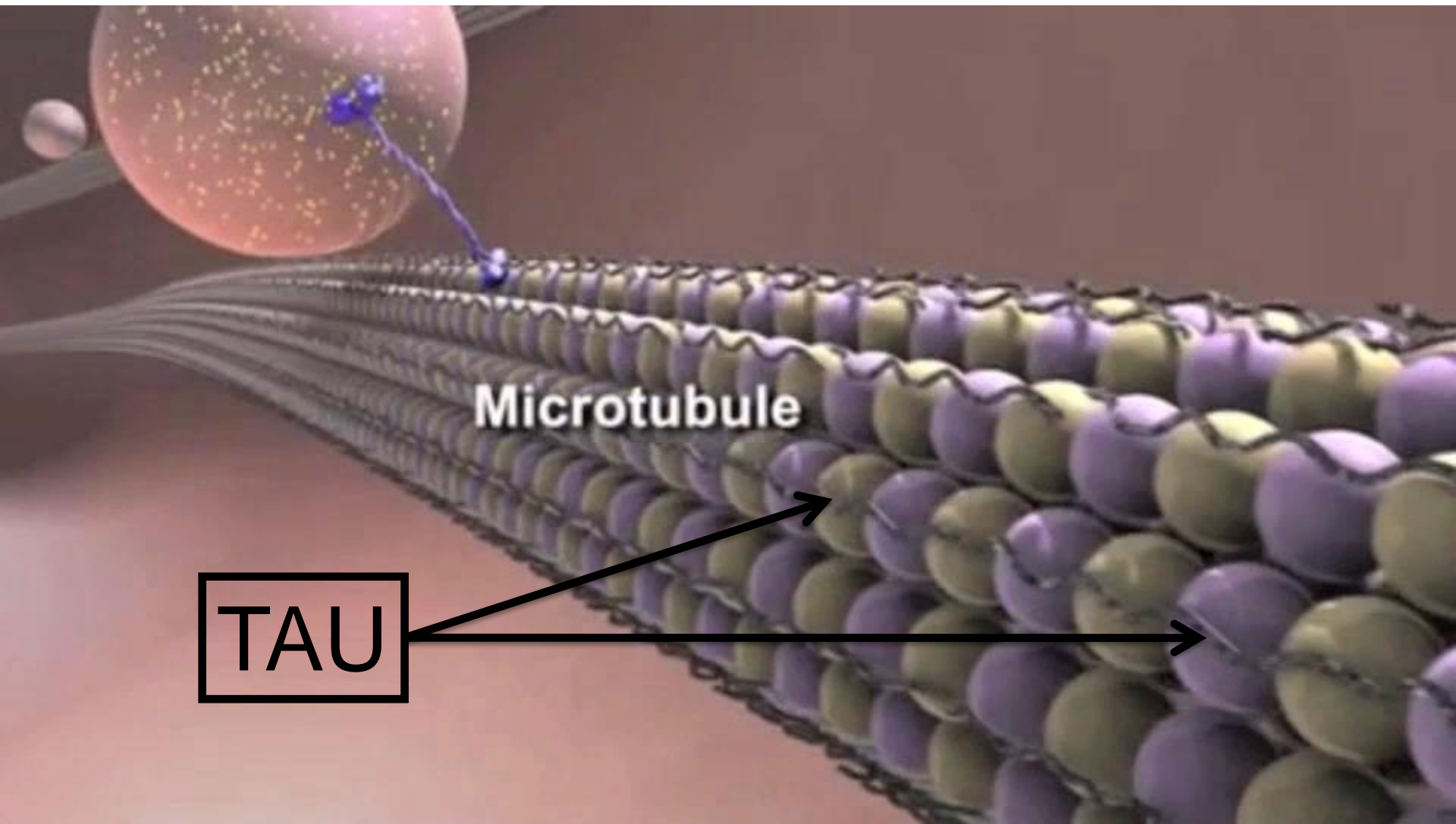


Tau Protein

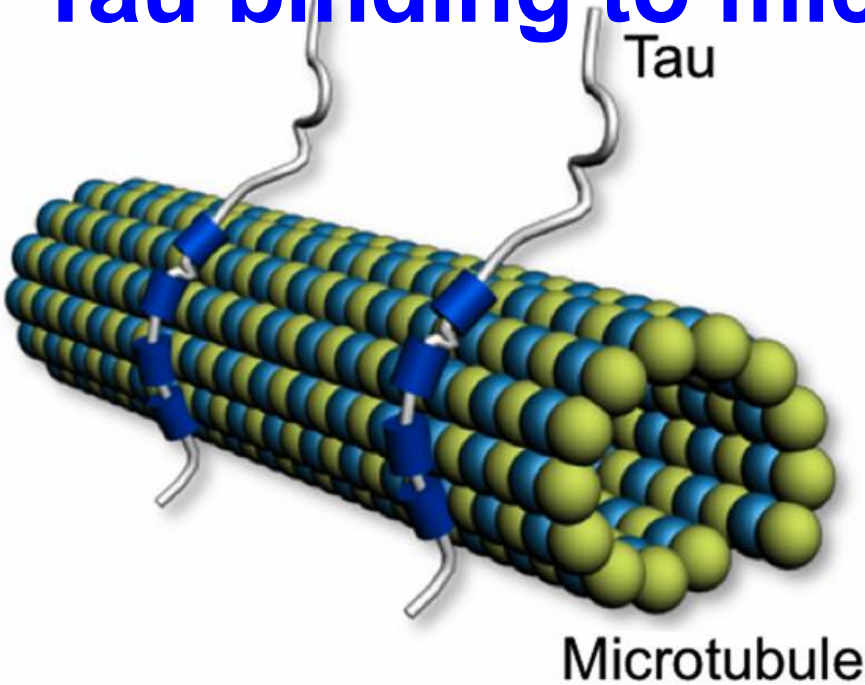
Liquid Liquid Phase Separation and Fibrillization



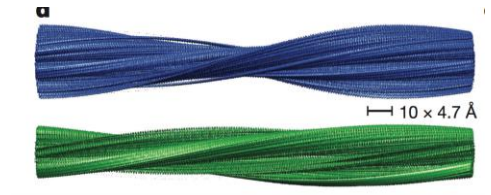
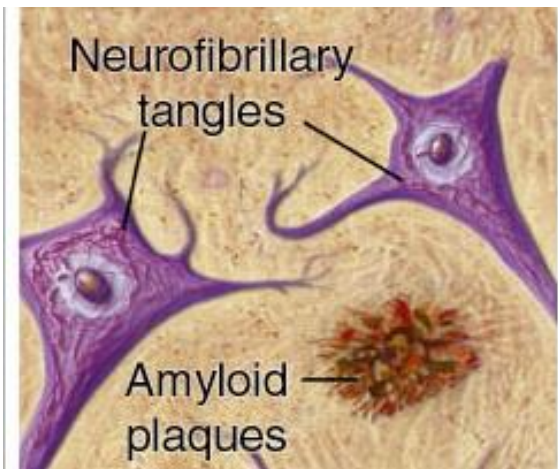
MICROTUBULES ARE STABILIZED BY TAU PROTEINS



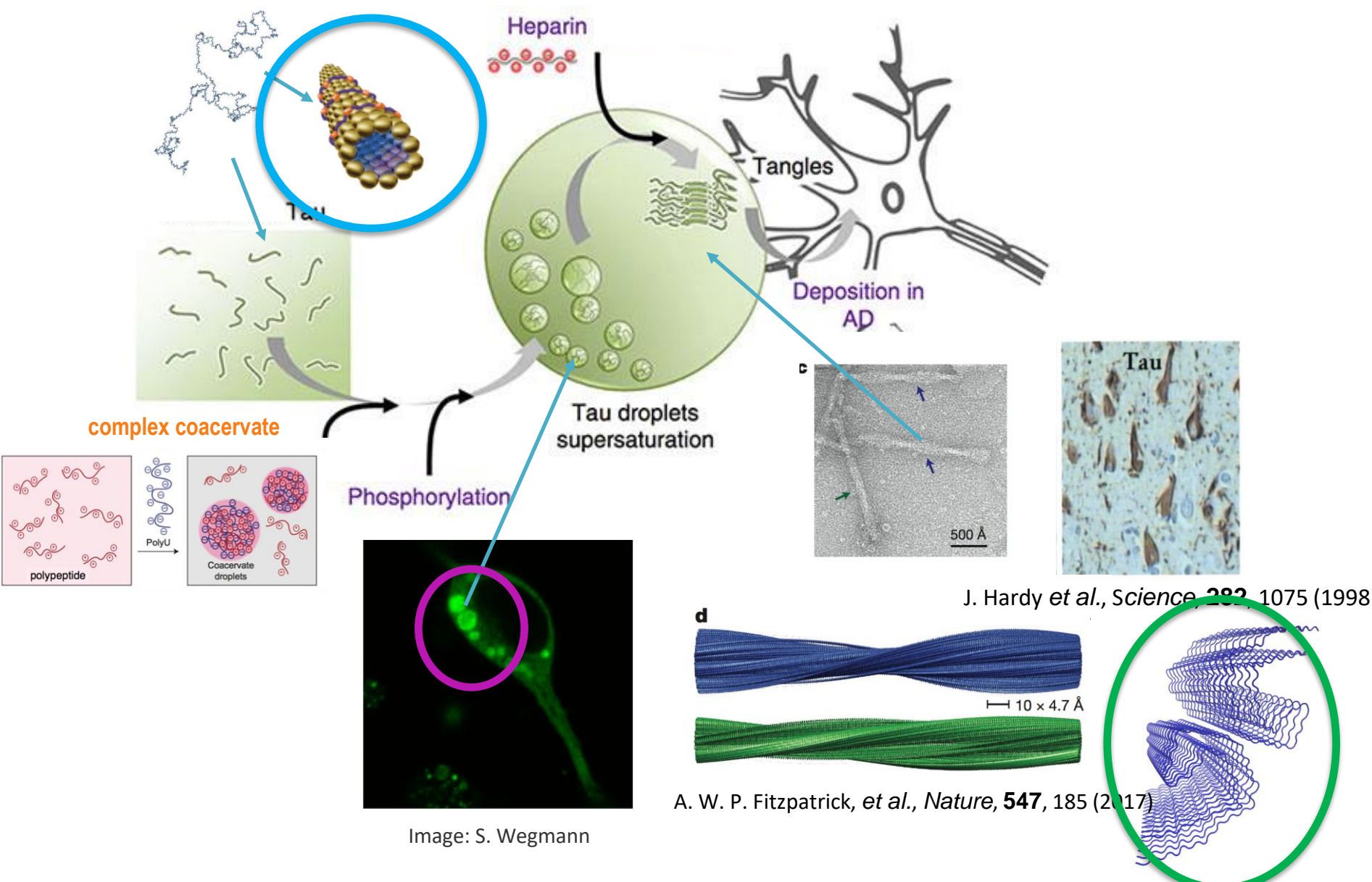
Function: Tau binding to microtubule



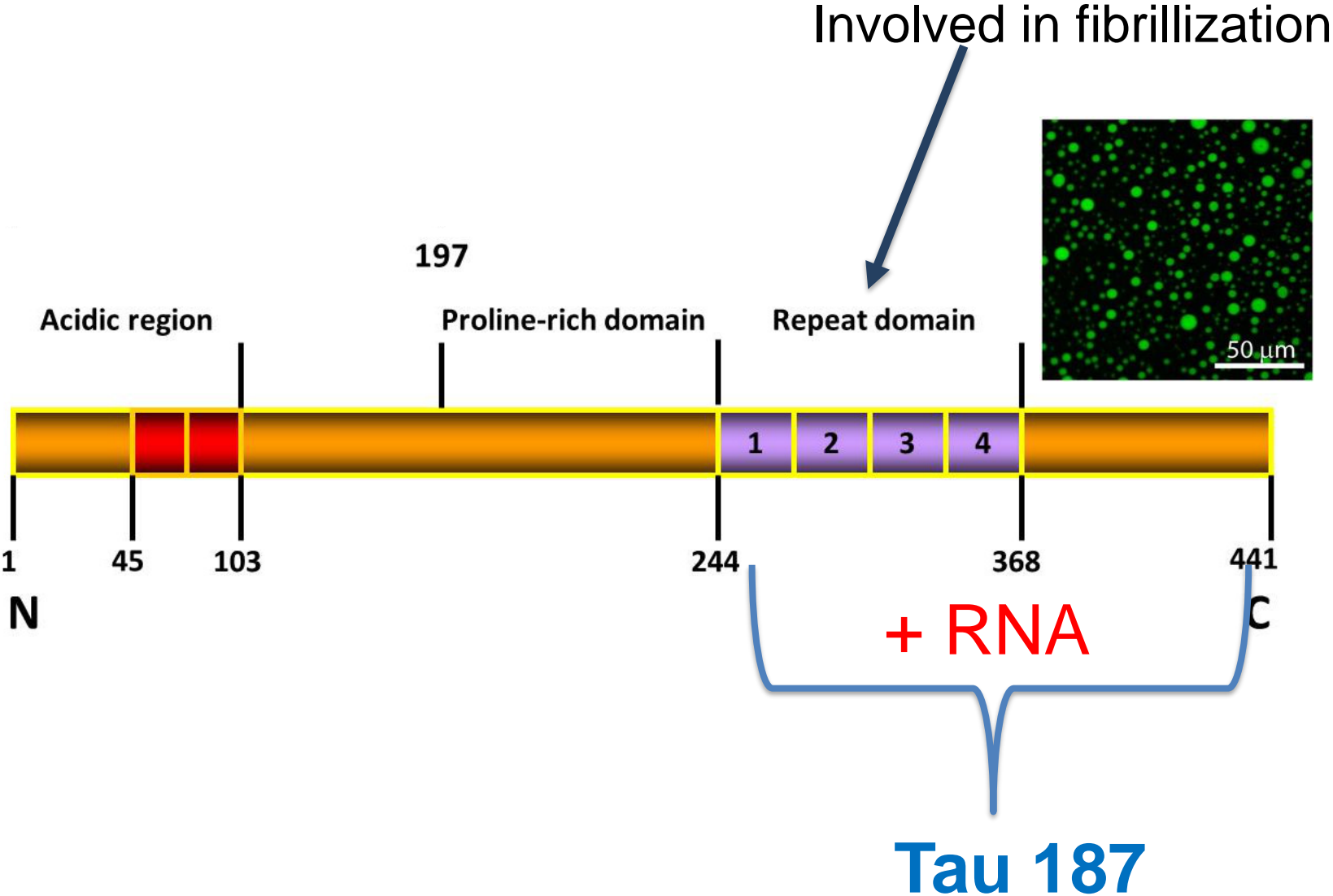
Pathology: Tau and Aggregation



Liquid-Liquid Phase Separation of Tau and Fibril Formation



Tau sequence

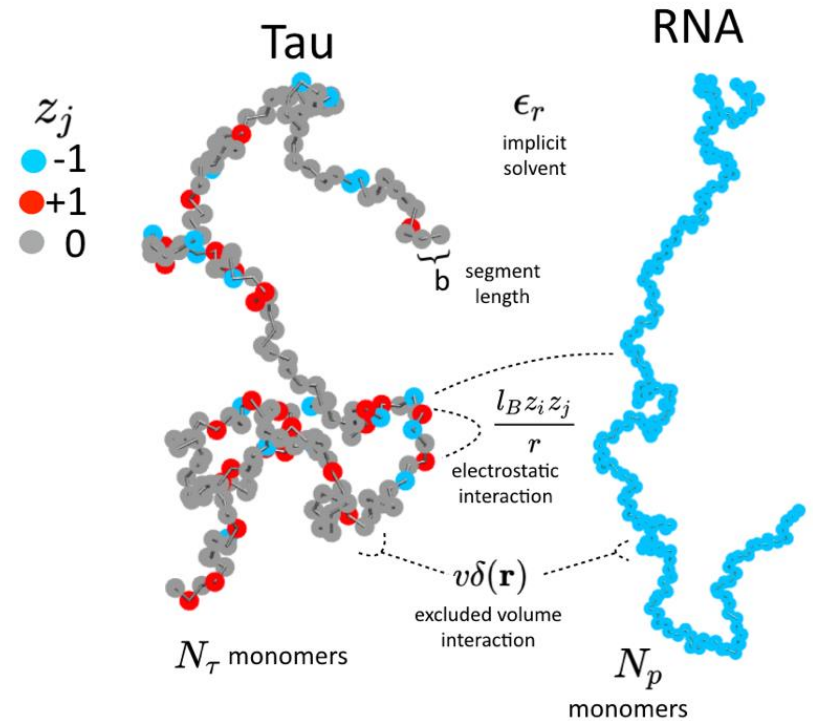


Field Theory Modeling of Tau-RNA complex coacervation

Tau187 primary sequence

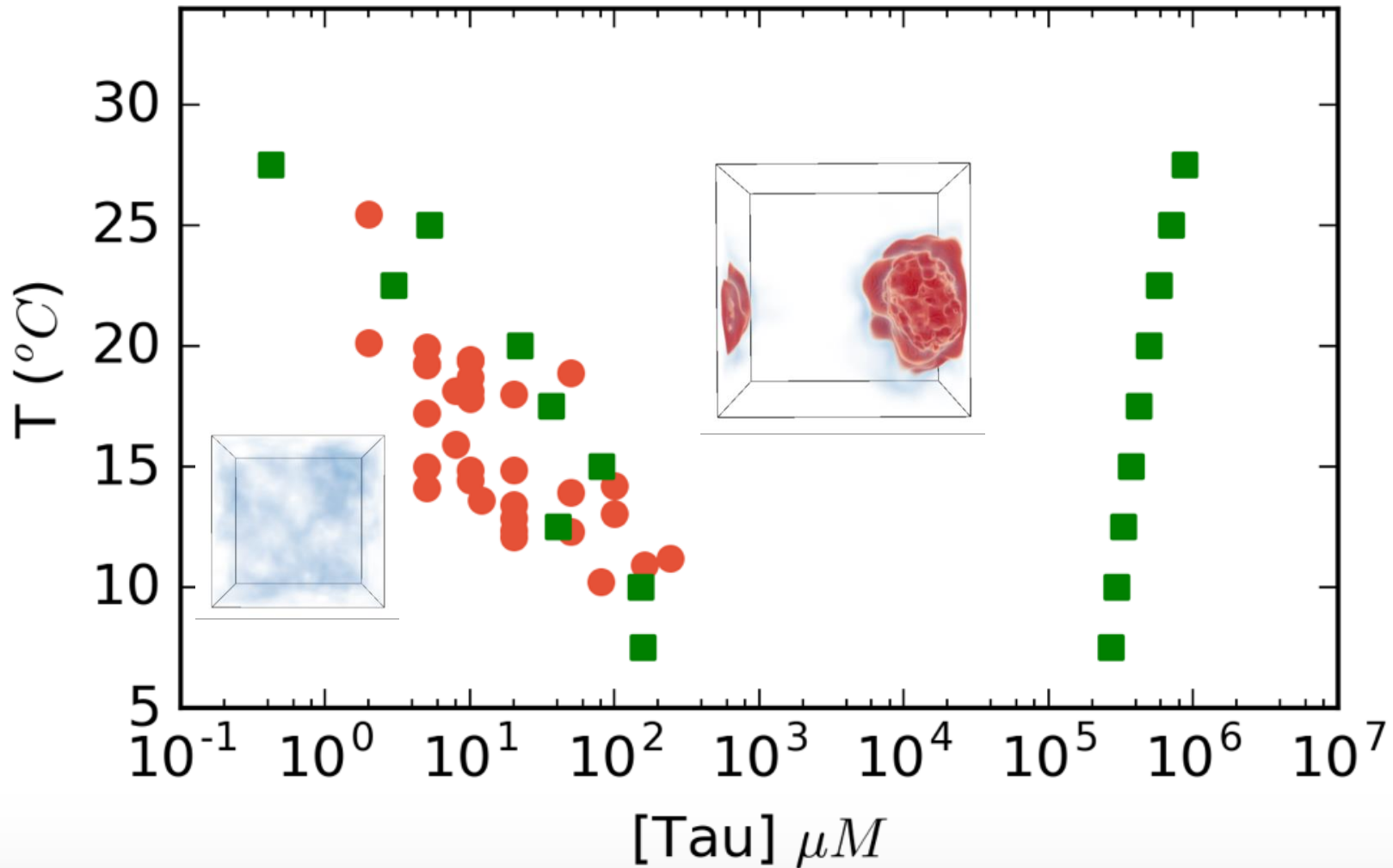


X basic (+)
 X acidic (-)
 X neutral (0)

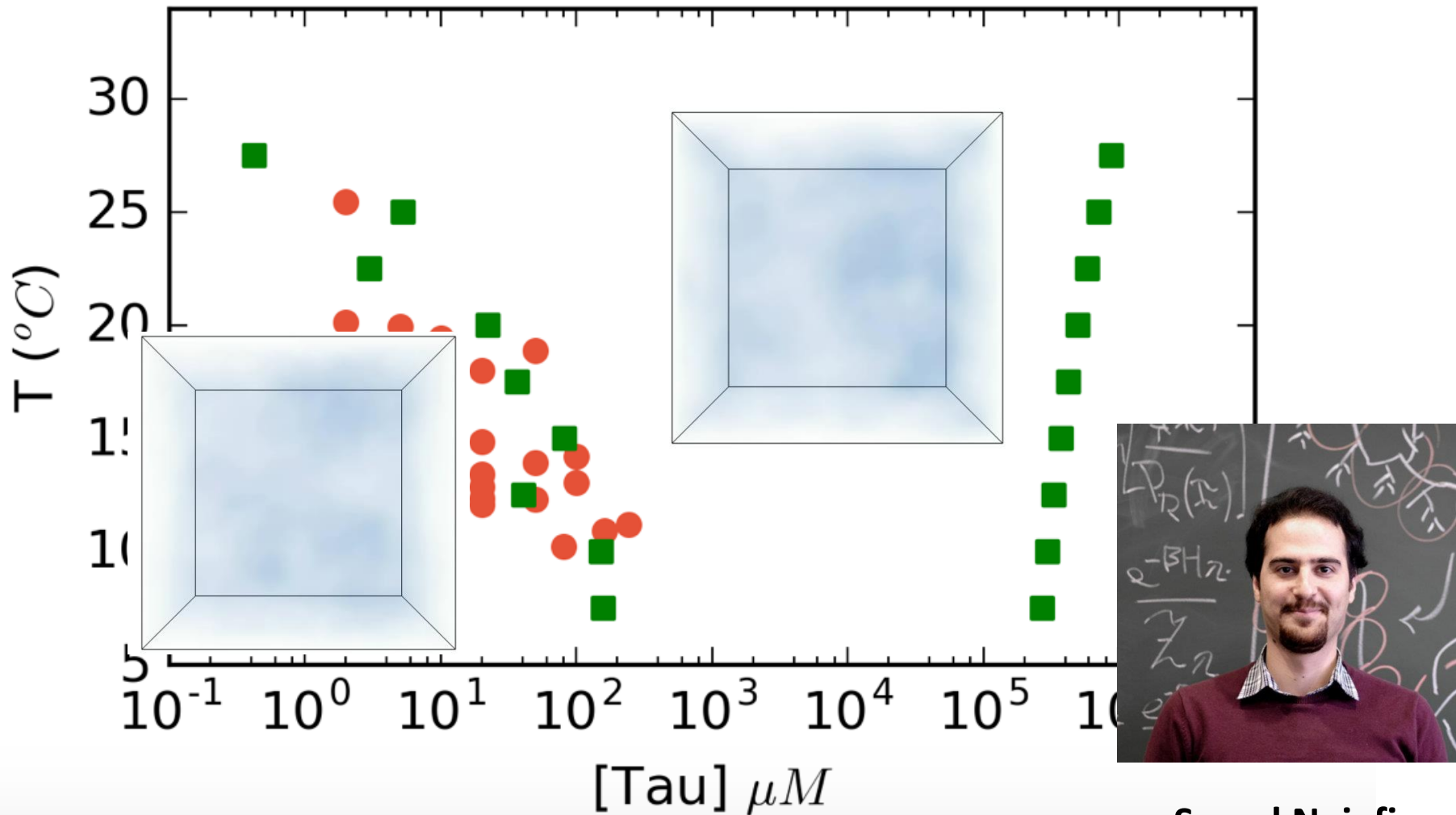


Fit excluded volume (B) and Bjerrum length (E) to experimental values for Tau

Field Theory can map out the entire phase diagram of Tau-RNA Complex Coacervation

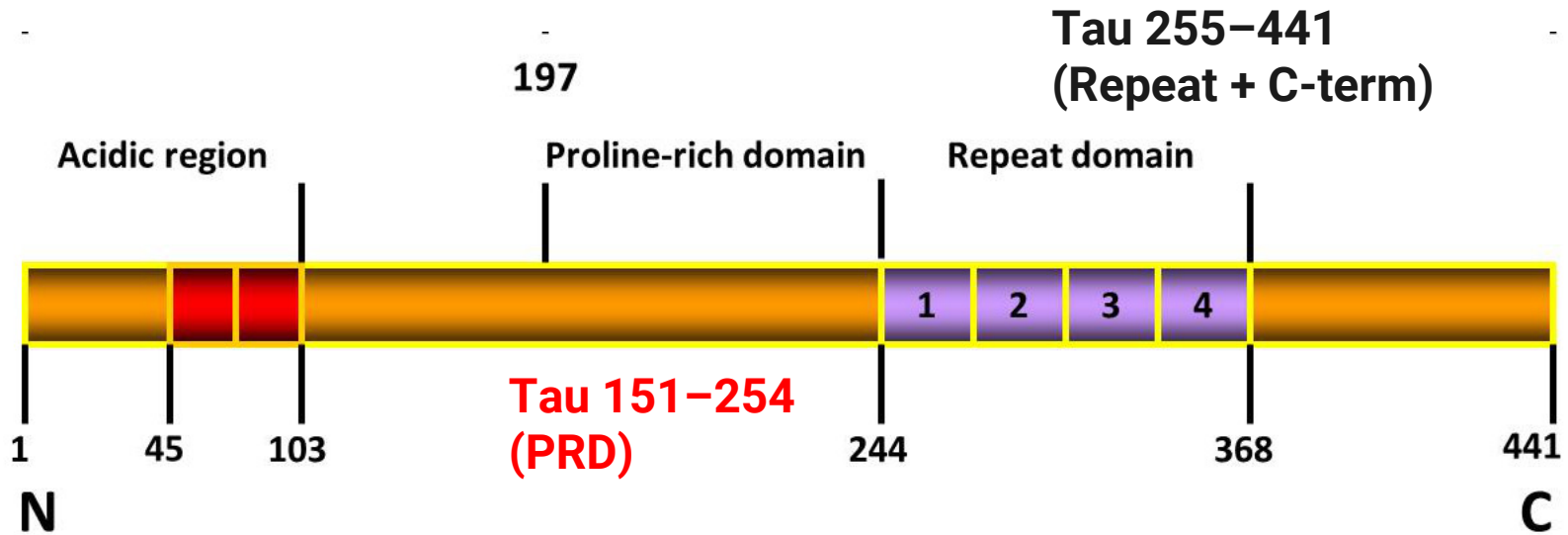


Field Theory can map out the entire phase diagram of Tau-RNA Complex Coacervation



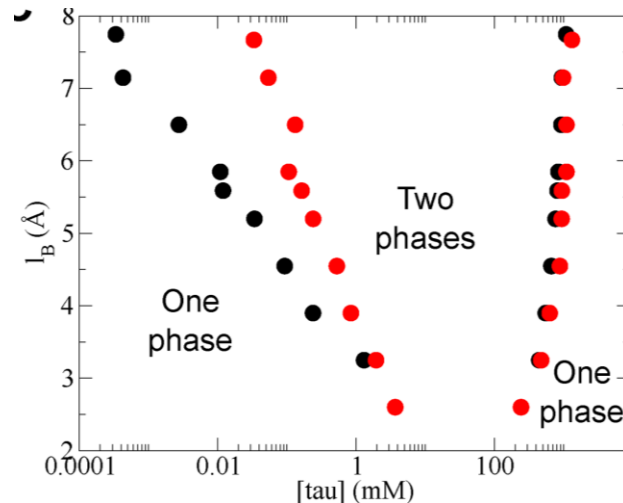
Saeed Najafi

Tau sequence: The Proline-Rich Domain Liquid-Liquid Phase Separates in vitro

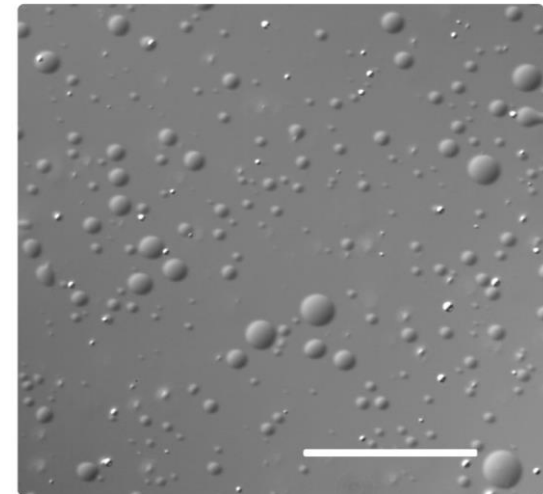


Tau 255-441
(Repeat + C-term)

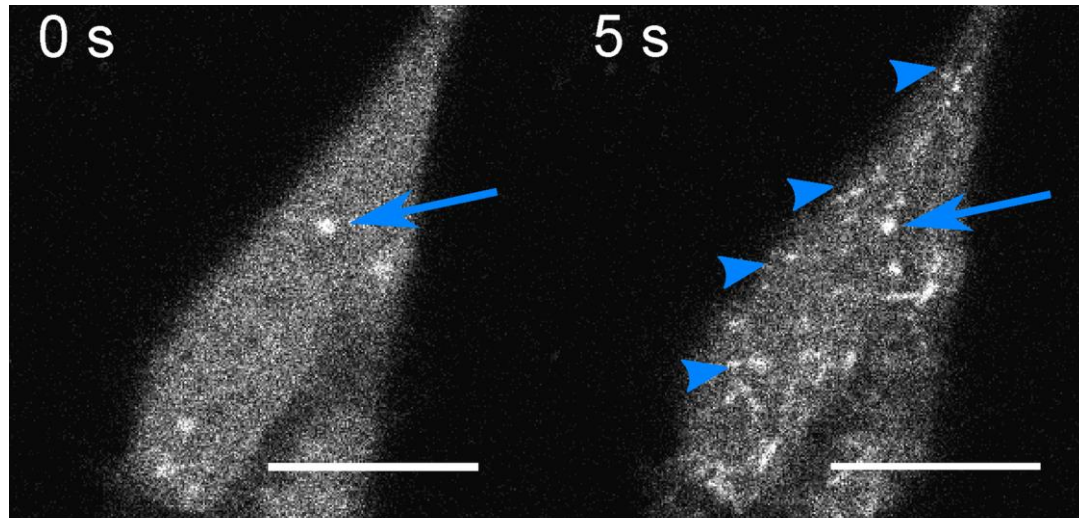
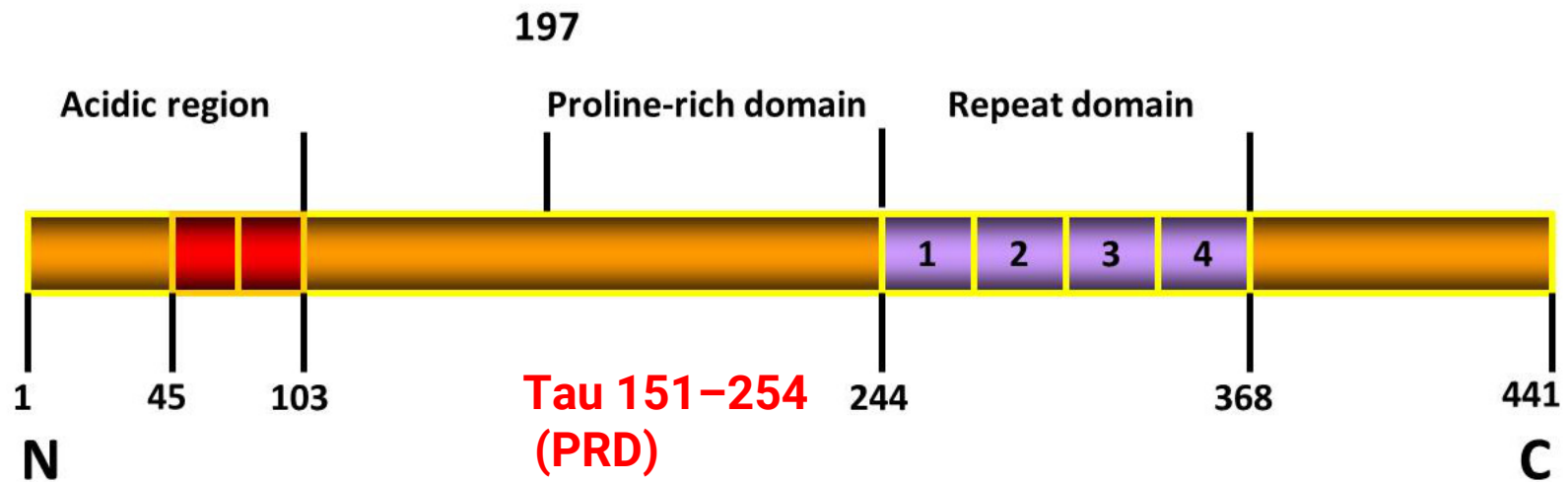
Tau 151-254
(PRD)



In Vitro

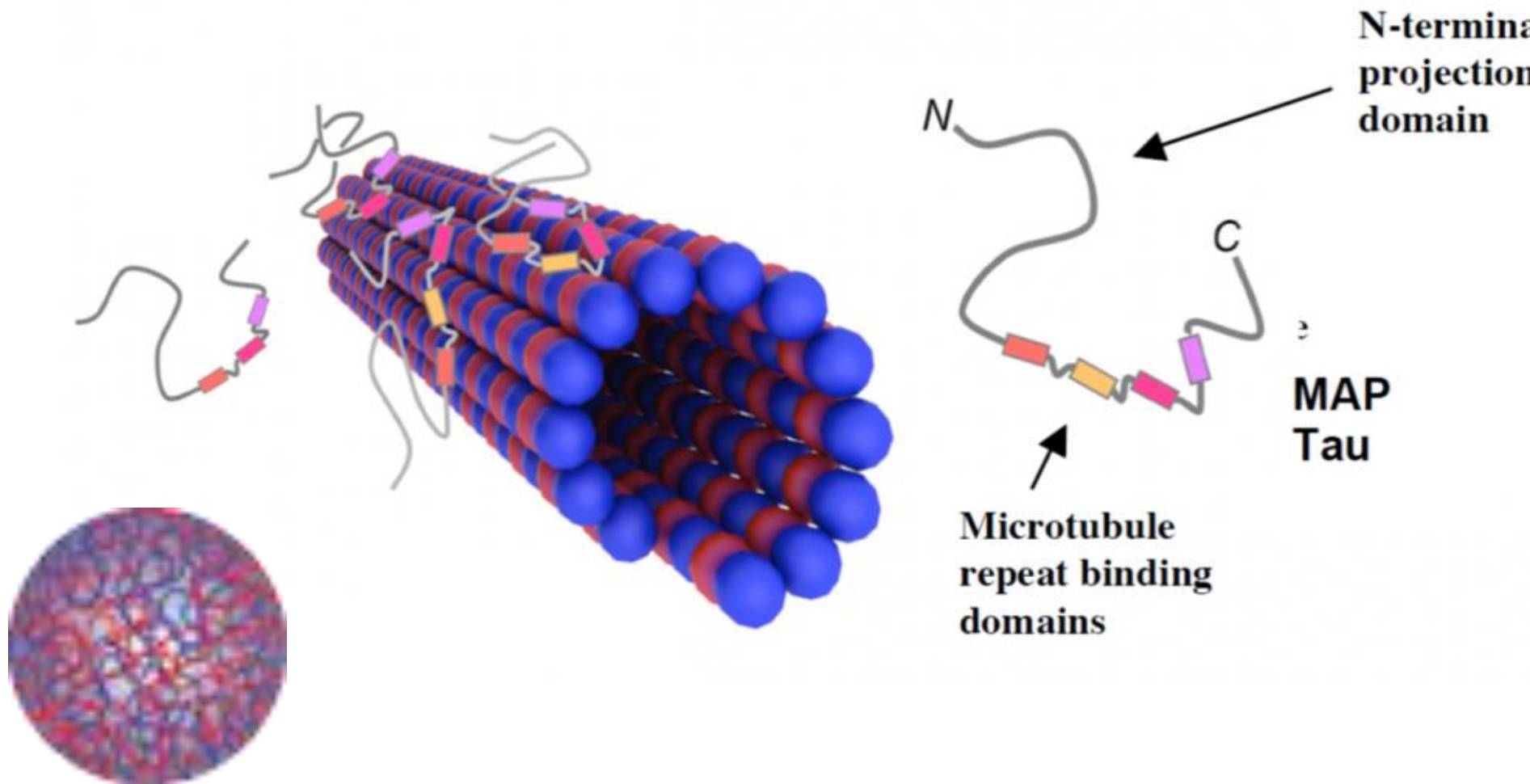


The Proline-Rich Domain Condensates promote Tau association with MTs



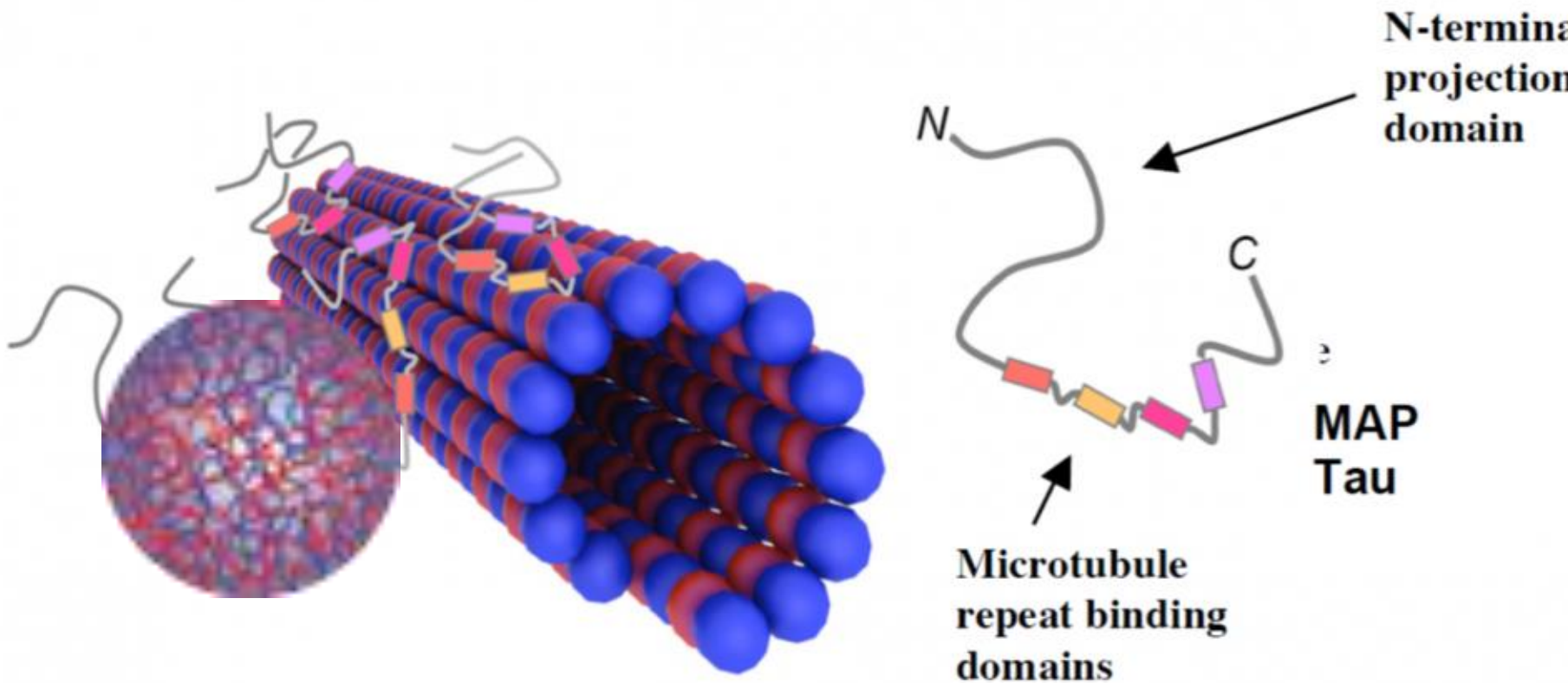
PRD
condensates
align along
the MTs

MICROTUBULES ARE STABILIZED BY TAU PROTEINS



LLPS CONCENTRATES TAU AND FACILITATES BINDING

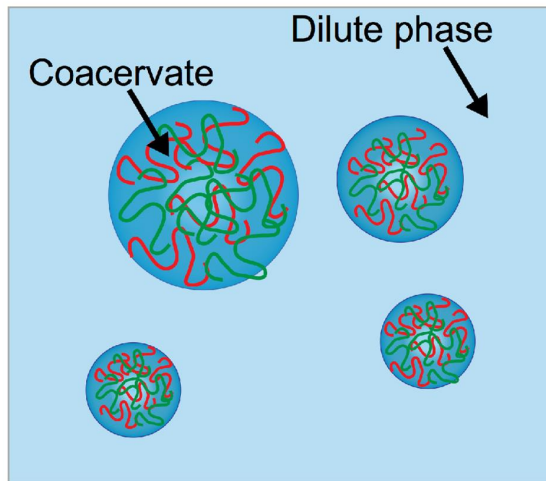
MICROTUBULES ARE STABILIZED BY TAU PROTEINS



LLPS CONCENTRATES TAU AND FACILITATES BINDING

Proteins can assemble in different ways

“Liquid”

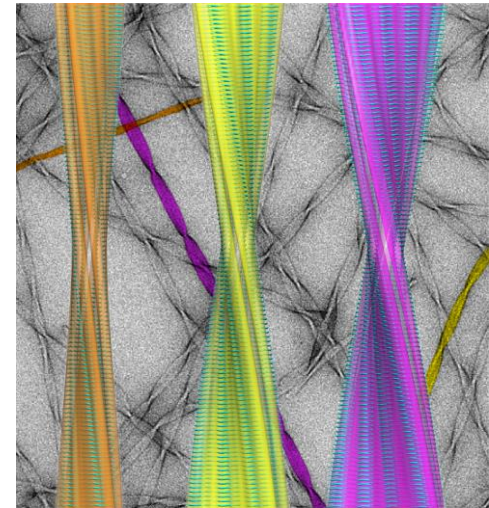


Droplets
Biomolecular condensates
Coacervates

“Solid”

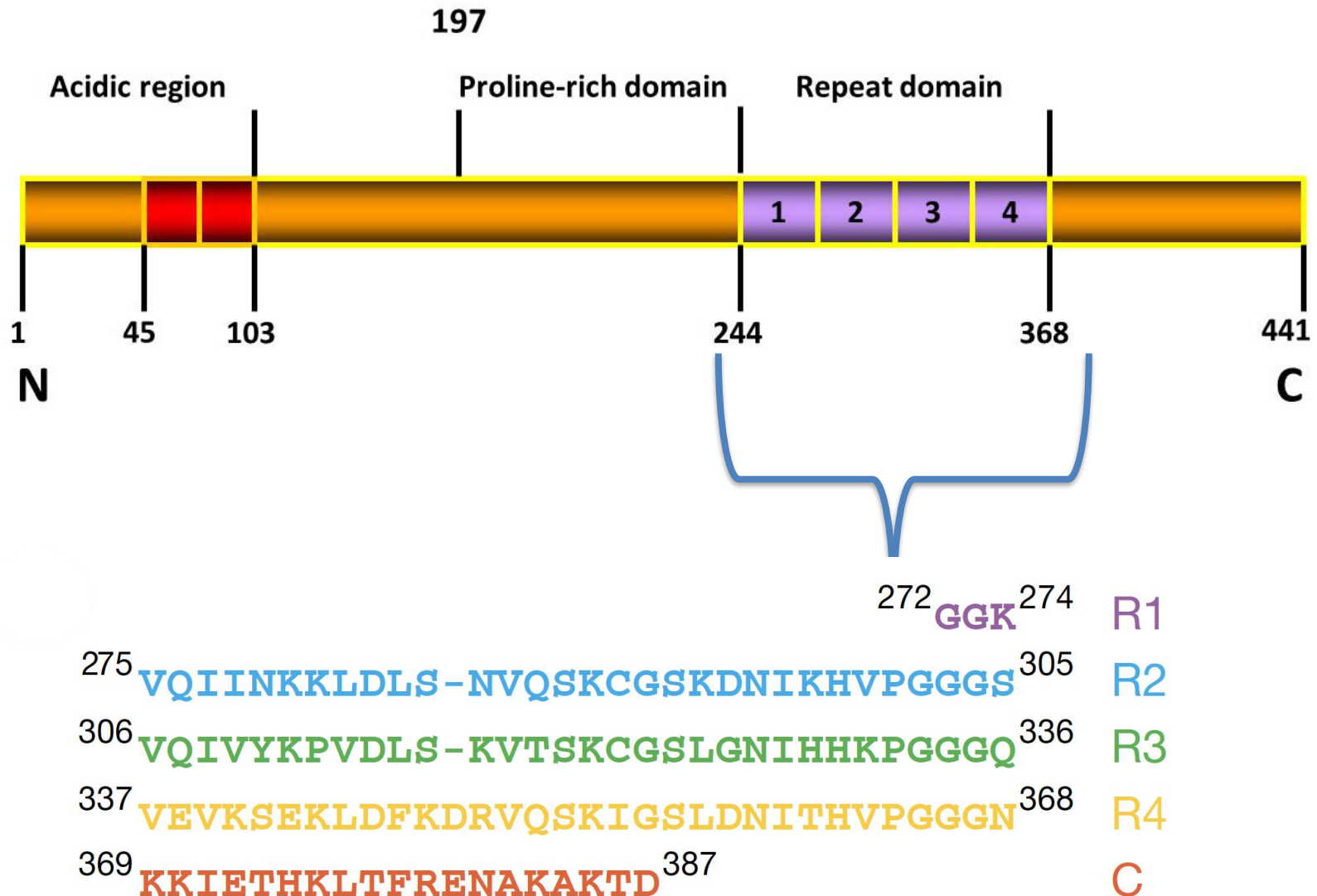
Aging

A black arrow pointing from the liquid phase diagram to the solid phase image, indicating the process of aging.

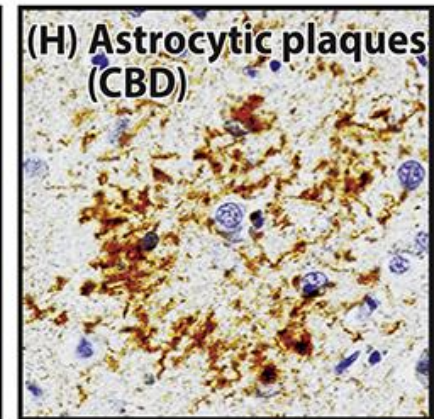
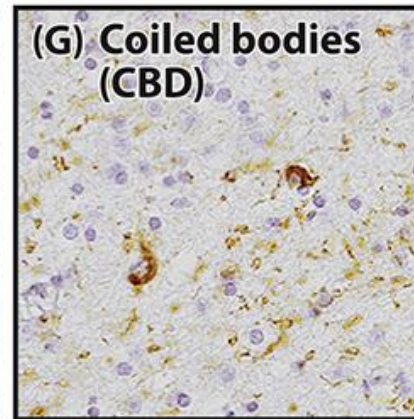
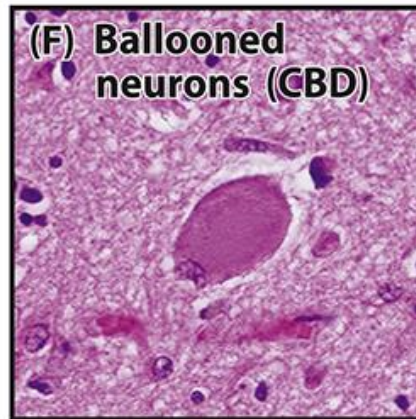
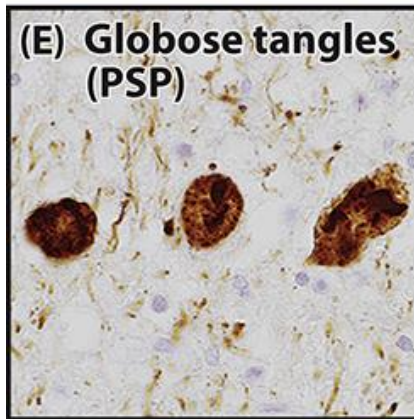
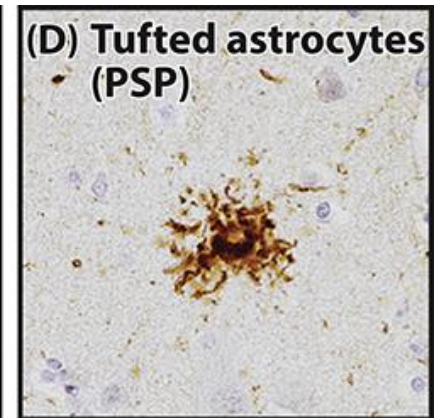
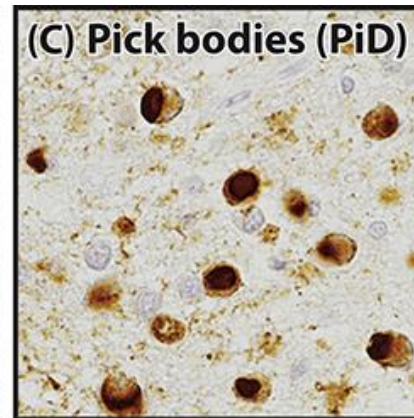
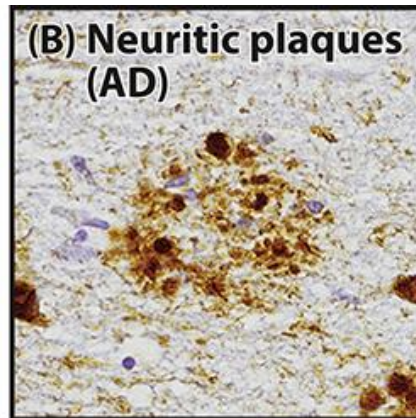
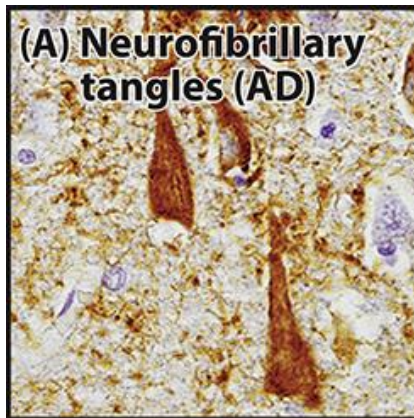


Amyloid Fibrils

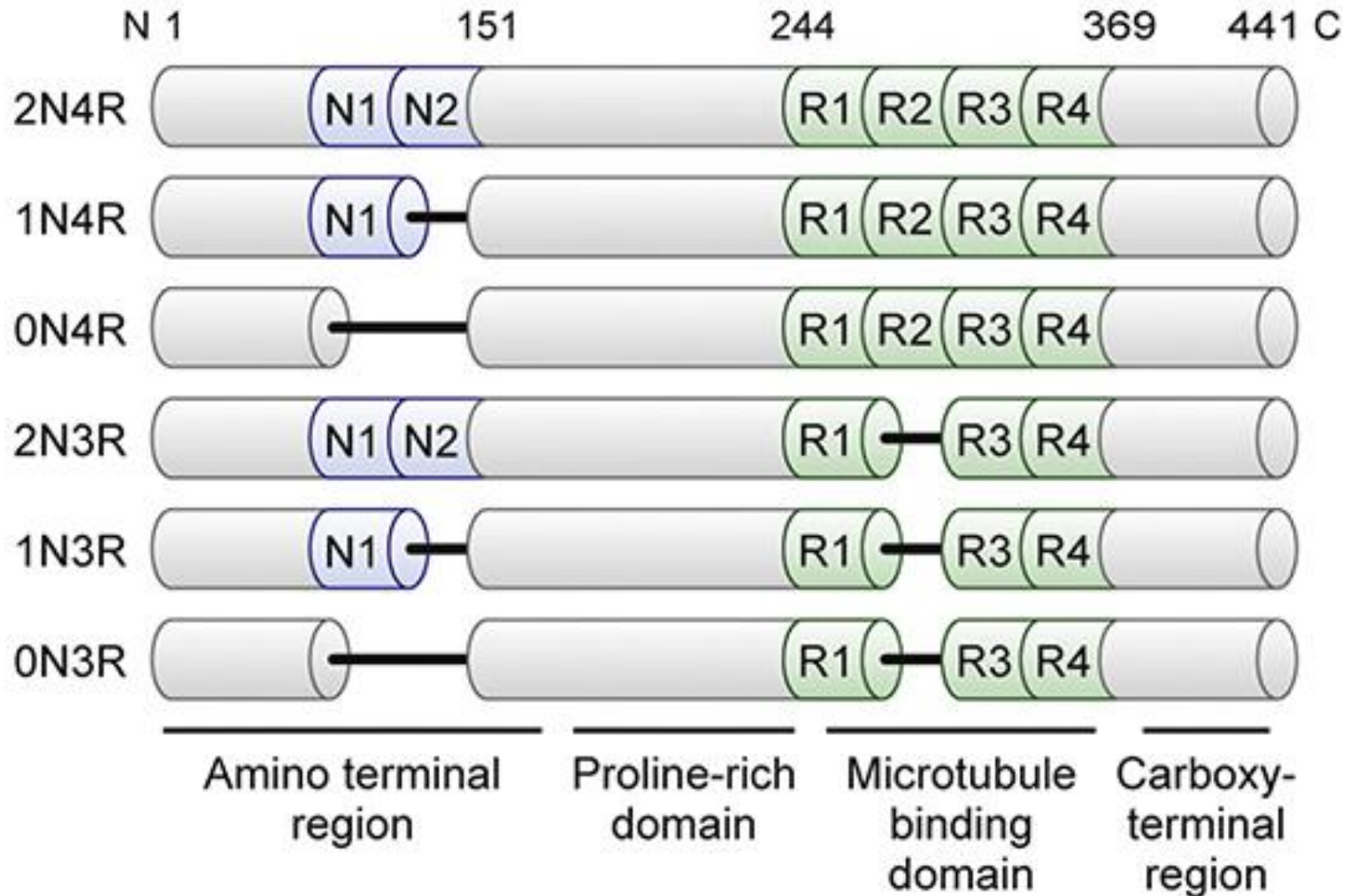
Tau Aggregation: Repeat Domain makes up the core of Tau Fibrils



There are many neurodegenerative diseases associated with Tau

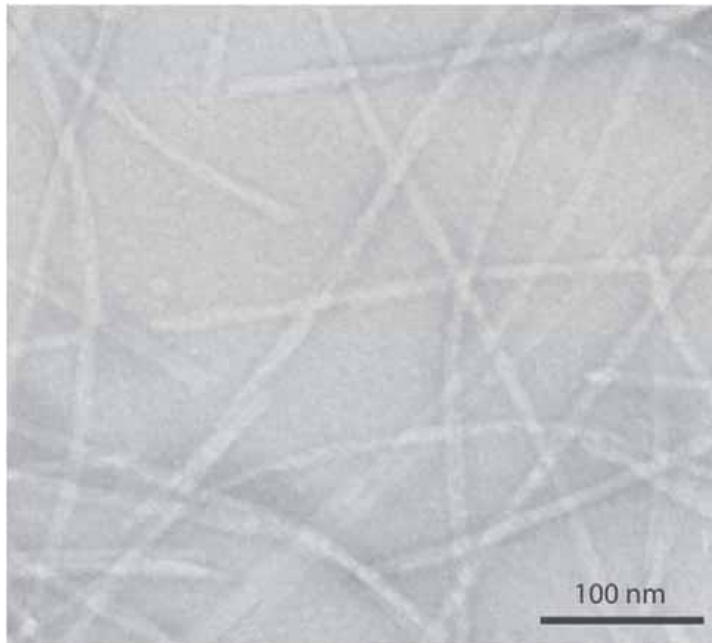


There are many forms of Tau



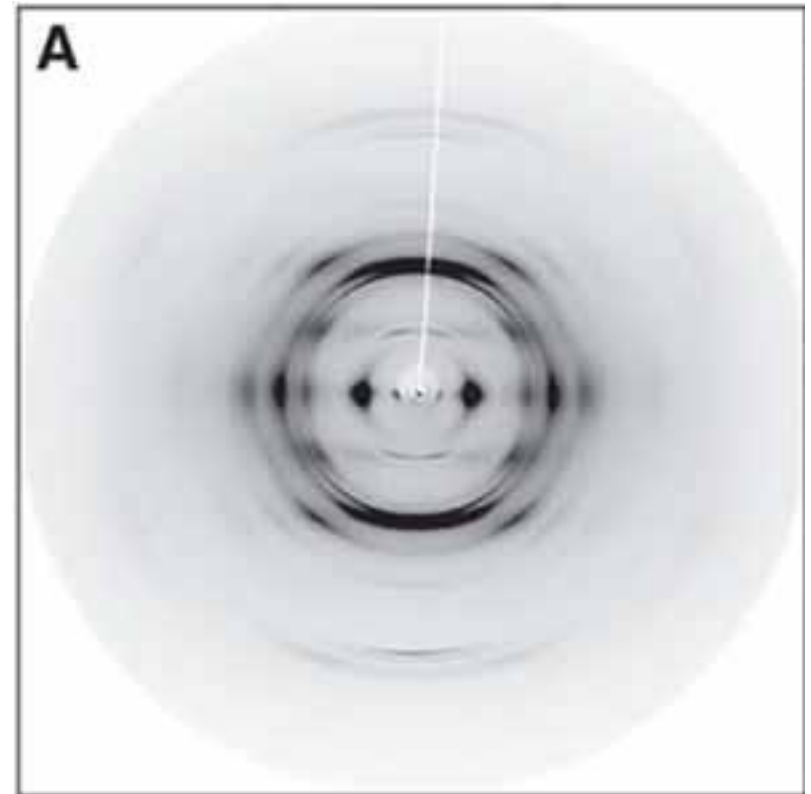
At first glance they all look the same

Transmission Emission
Microscopy (TEM)



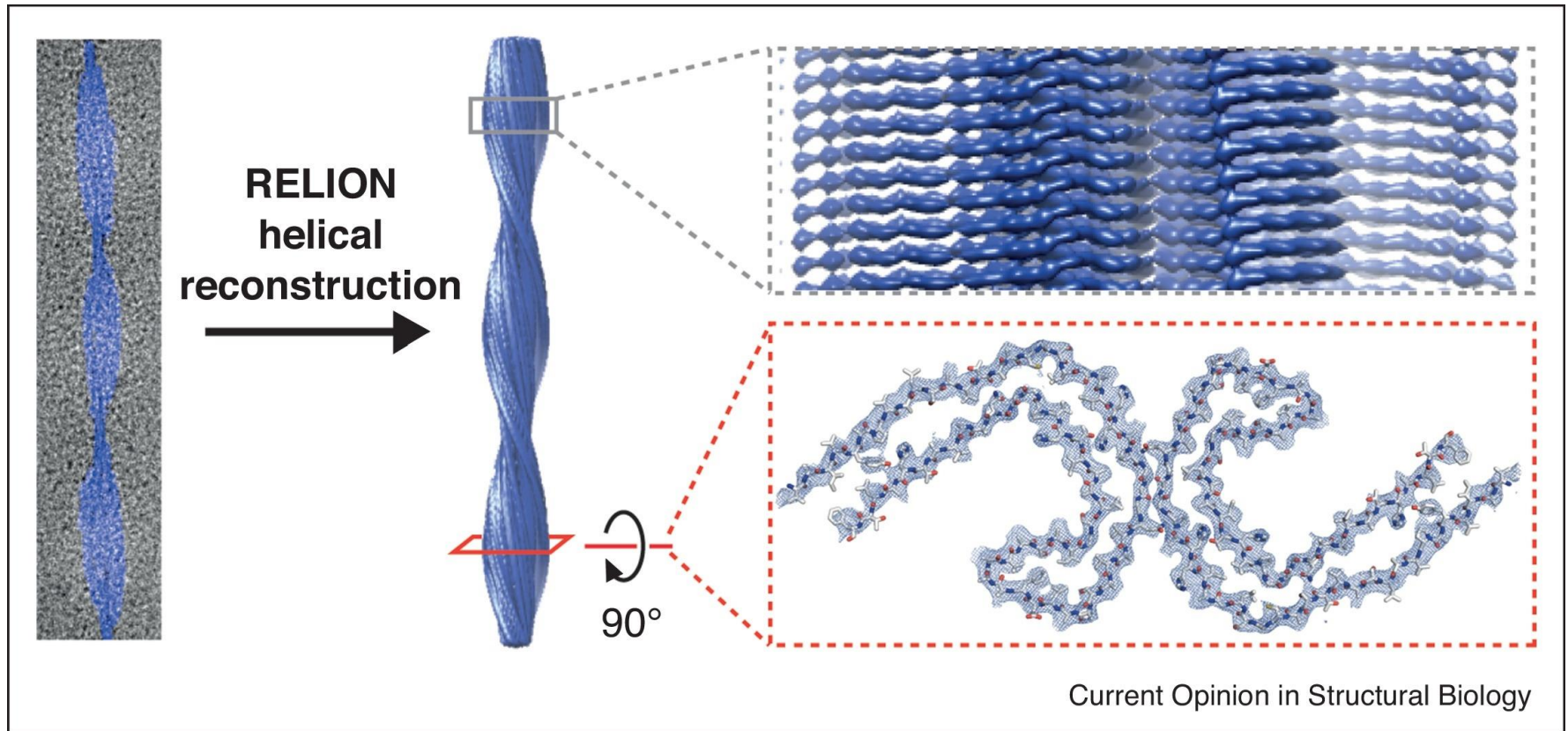
Fibrils

X-Ray diffraction



Cross-beta structure

But Cryo-EM shows (subtle) differences



The specific fibril shape is a signature of a specific disease



CBD



AGD
ARTAG
+3 or +16



PSP



GGT-I
GGT-II



GPT

COMMON STRAND-LOOP-STRAND MOTIF



CBD



AGD



Created: 19 Amino-acid Peptide



WILD TYPE: jR2R3

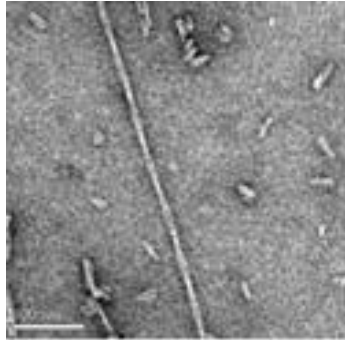


MUTANT: jR2R3-P301L

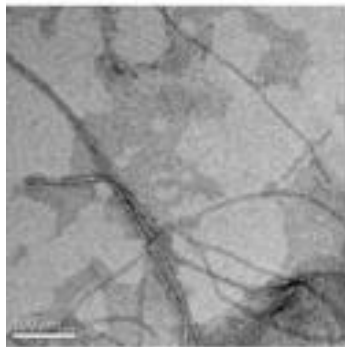


jR2R3-P301L mutant aggregates faster than jR2R3 and shows more fibril morphologies

jR2R3

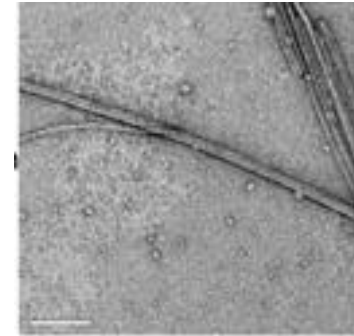
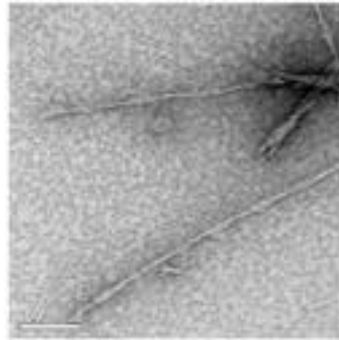


PHF

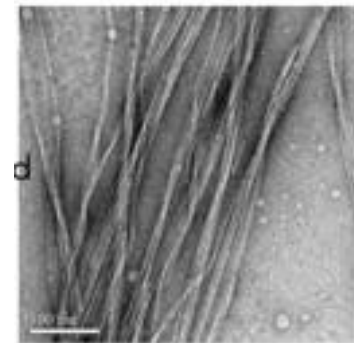
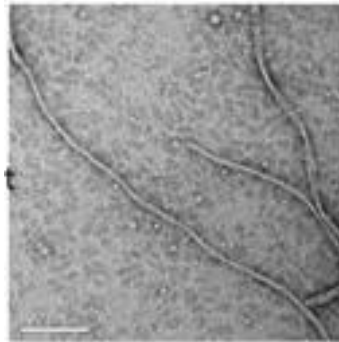


Straight

jR2R3-P301L



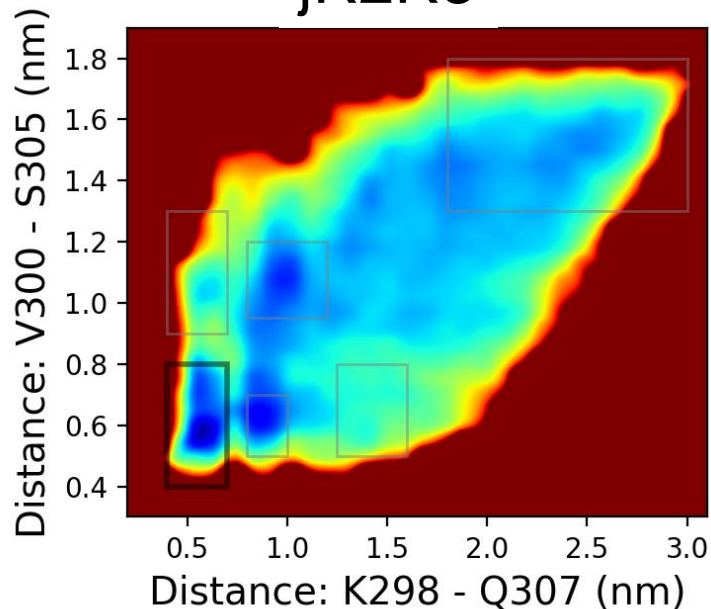
Ribbon



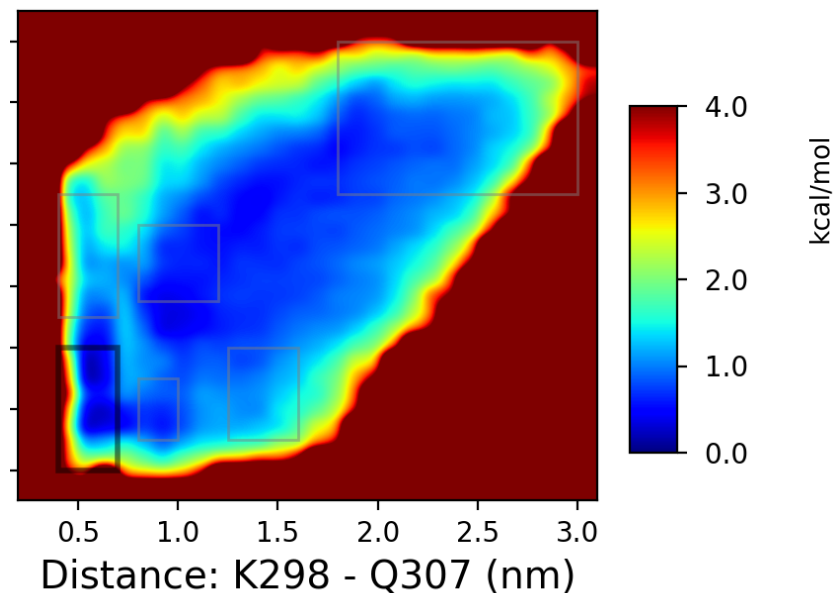
Bundle

jR2R3-P301L can explore more conformational space

jR2R3

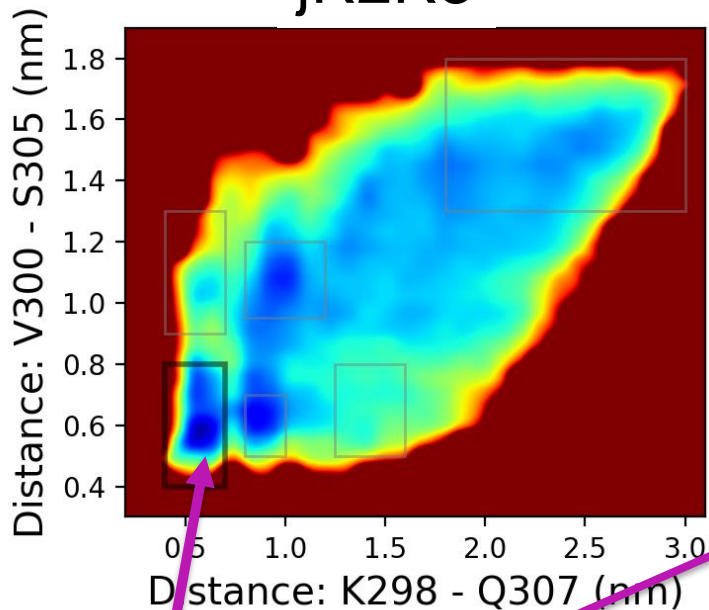


jR2R3-P301L (mutant)

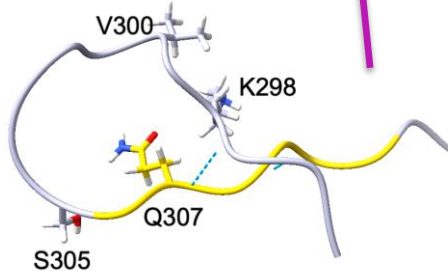
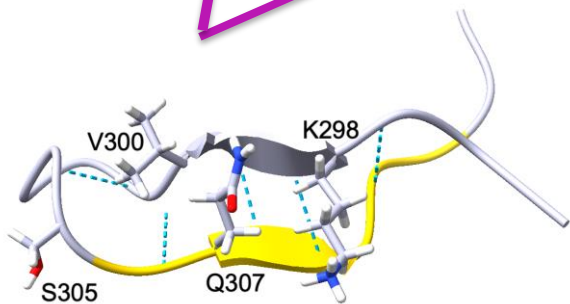
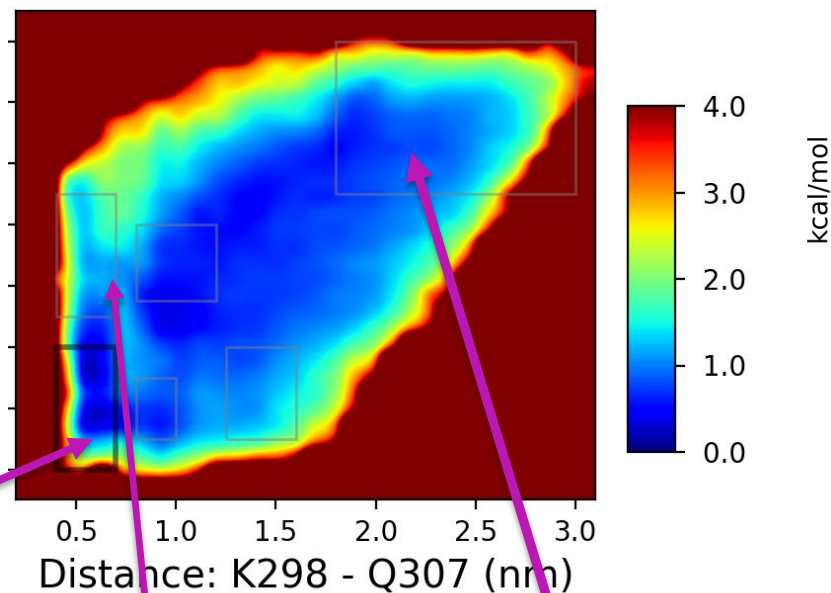


jR2R3-P301L can get out of a "fibril protective" hairpin

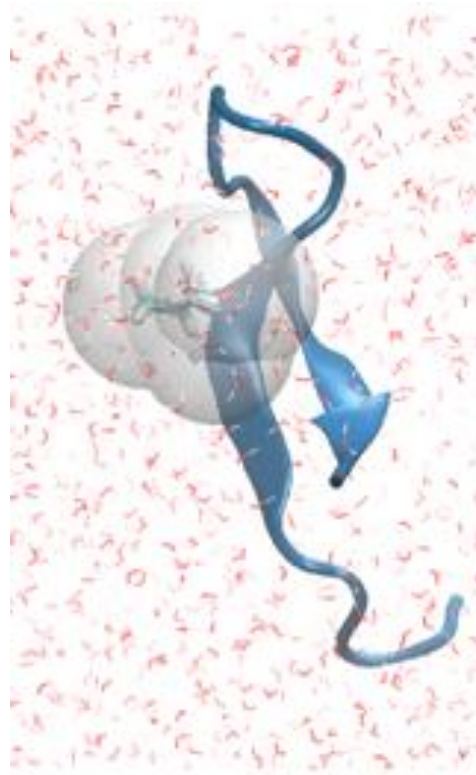
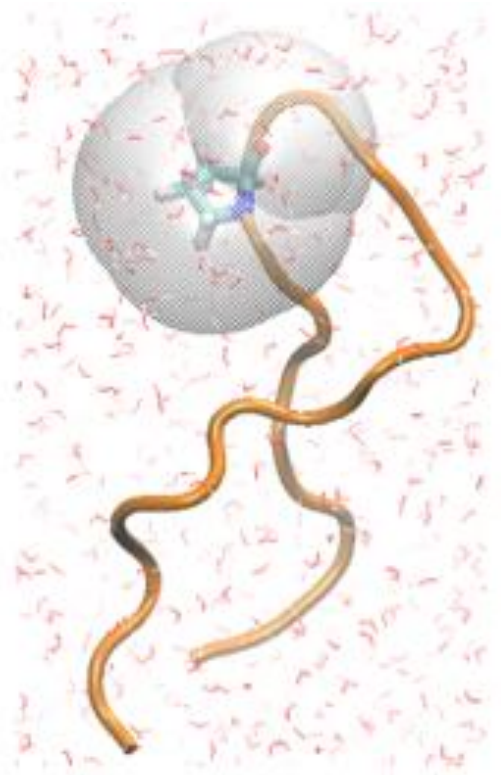
jR2R3



jR2R3-P301L (mutant)



Overhauser Dynamic Nuclear Polarization (ODNP) experiments show a reduction in hydration water dynamics around 301 site for the P→L mutant (jR2R3-P301L)



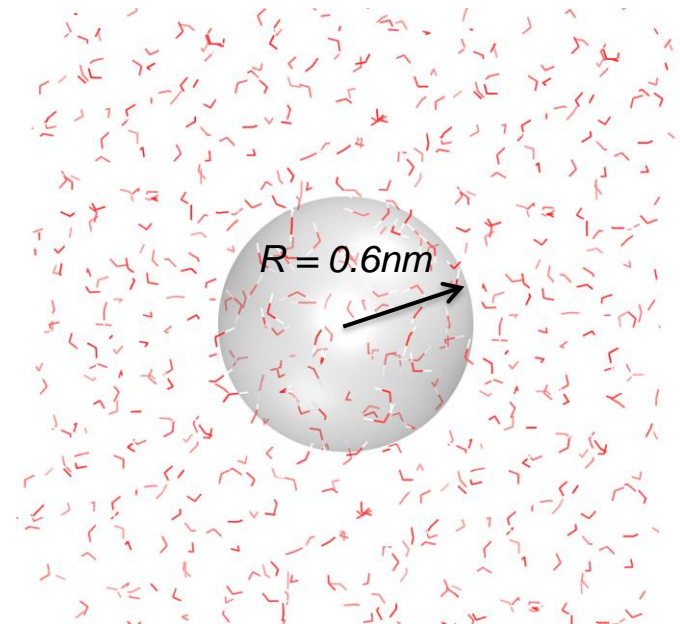
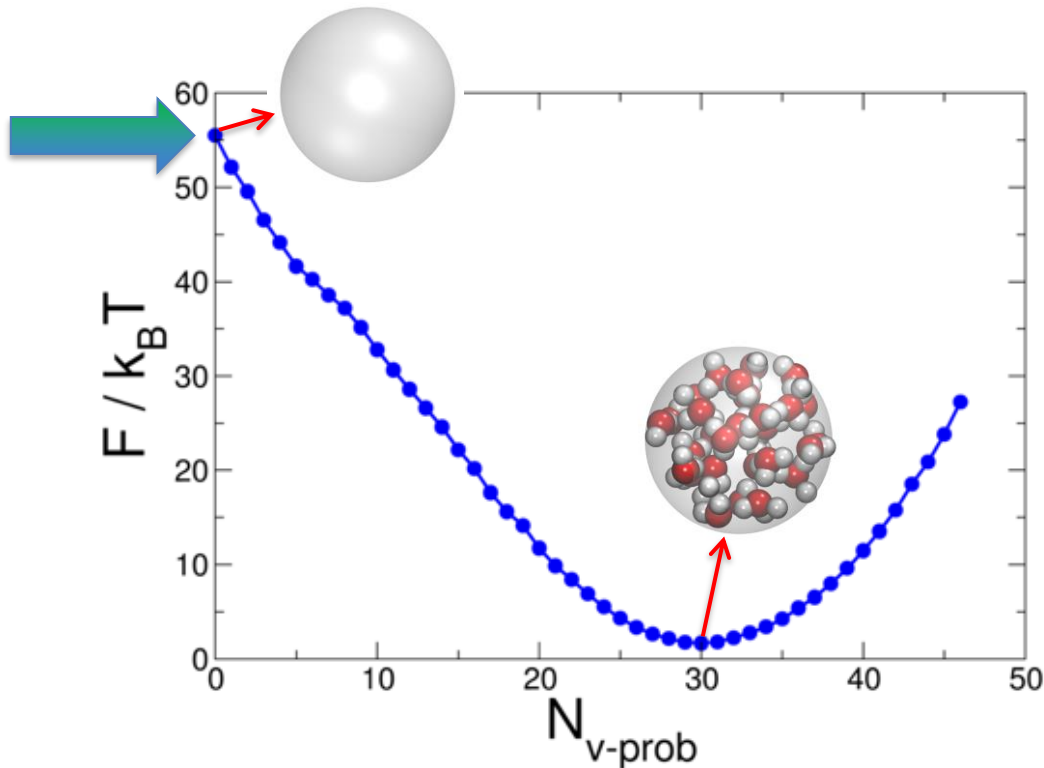
Increased ordering of water around mutation site

→ locally more hydrophobic

Probing Hydrophobicity Computationally through Umbrella Sampling (INDUS)

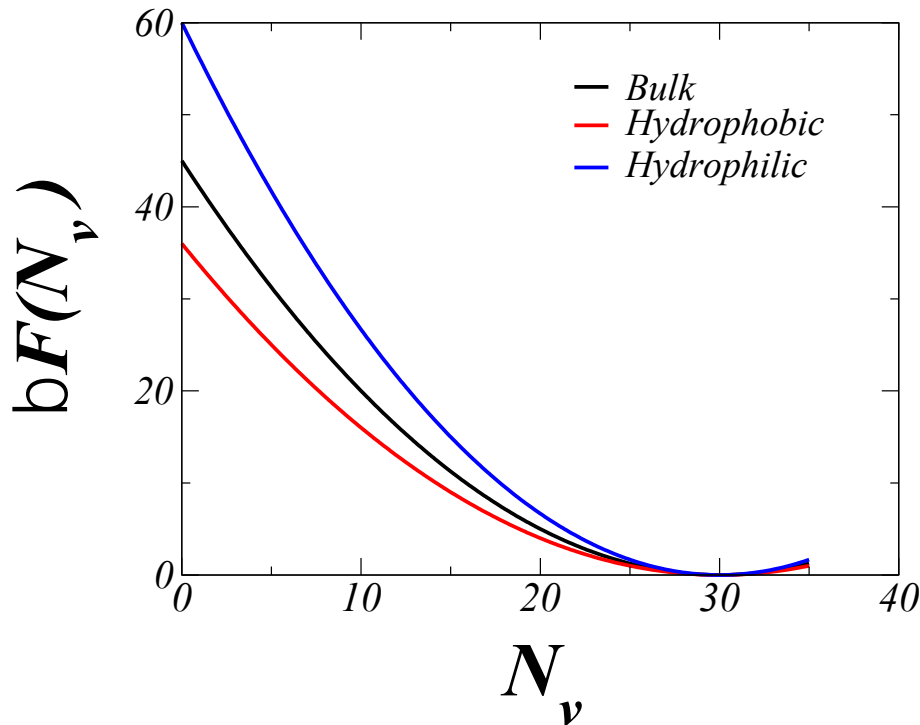
Free energy of dewetting a spherical volume in bulk

$$\mu_{\text{ex}} = \mathbf{F}(\mathbf{0}) = -\ln \mathbf{P}_{\mathbf{v}}(\mathbf{0})$$

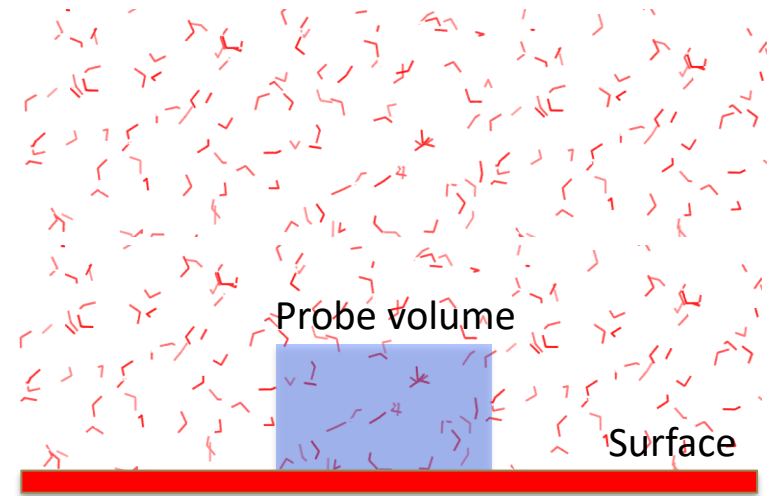


Free energy of dewetting the probe volume in vicinity of a surface

Excess chemical potential is an indication of hydrophilicity or hydrophobicity of the surface

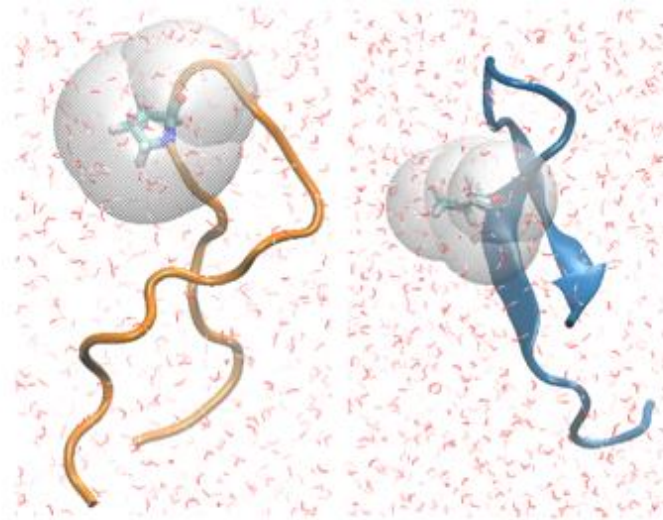


$$\mu_{\text{ex}}^{\text{phil}} > \mu_{\text{ex}}^{\text{bulk}} > \mu_{\text{ex}}^{\text{phob}}$$



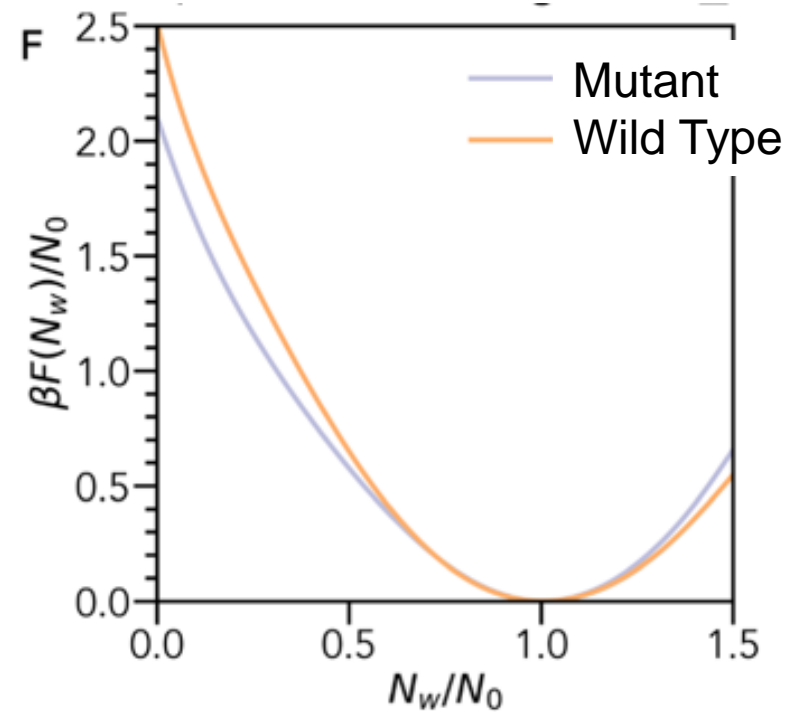
$$\mu_{\text{ex}} = \mathbf{F}(0) = -\ln P_v(0)$$

Free energy of dewetting lower for jR2R3-P301L: an additional factor favoring association of jR2R3-P301L

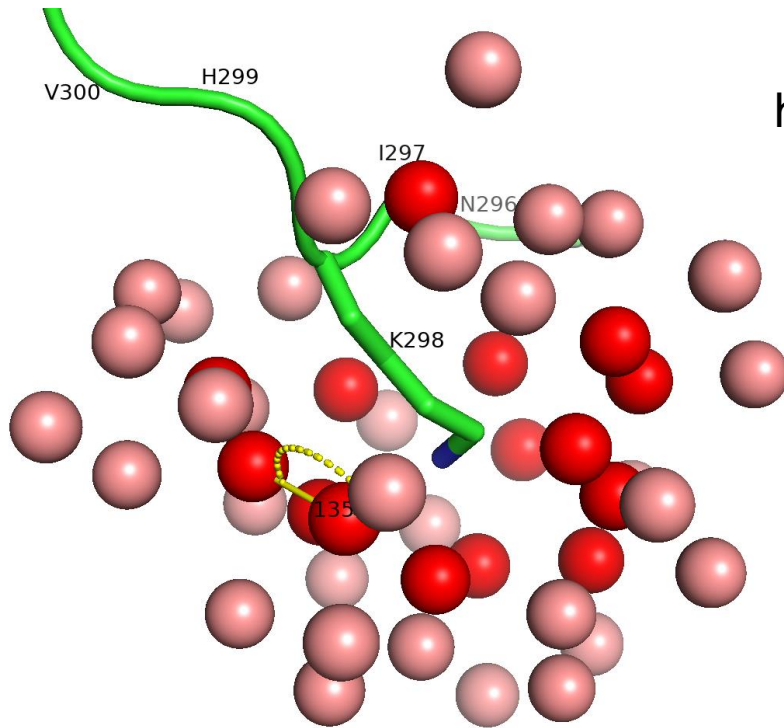


Wild Type

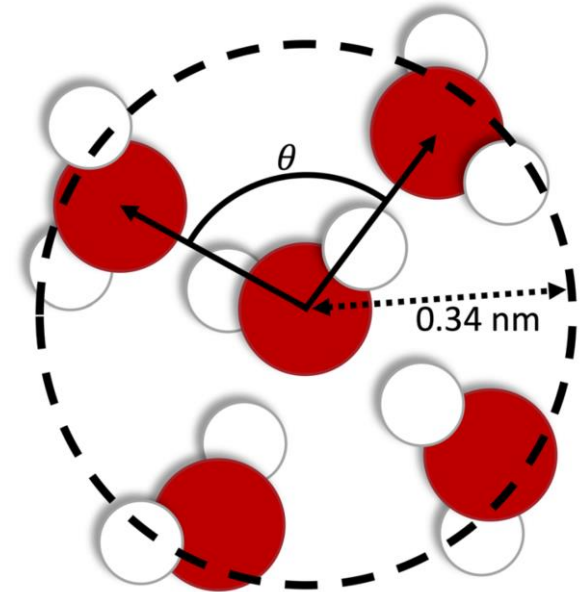
Mutant



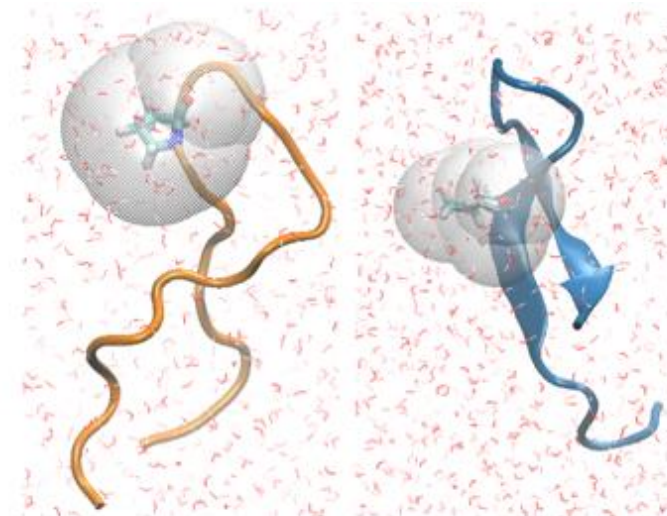
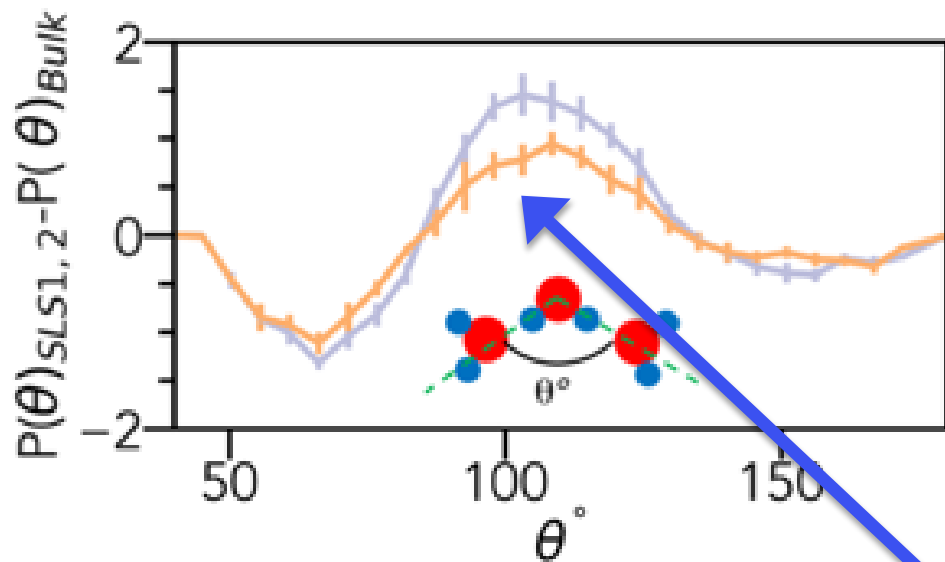
Quantifying Water Structure: *water triplet distribution*



histogram
the
angles



Increased tetrahedral ordering of hydration waters near the L301 (mutant) compared to P301 (wild type)

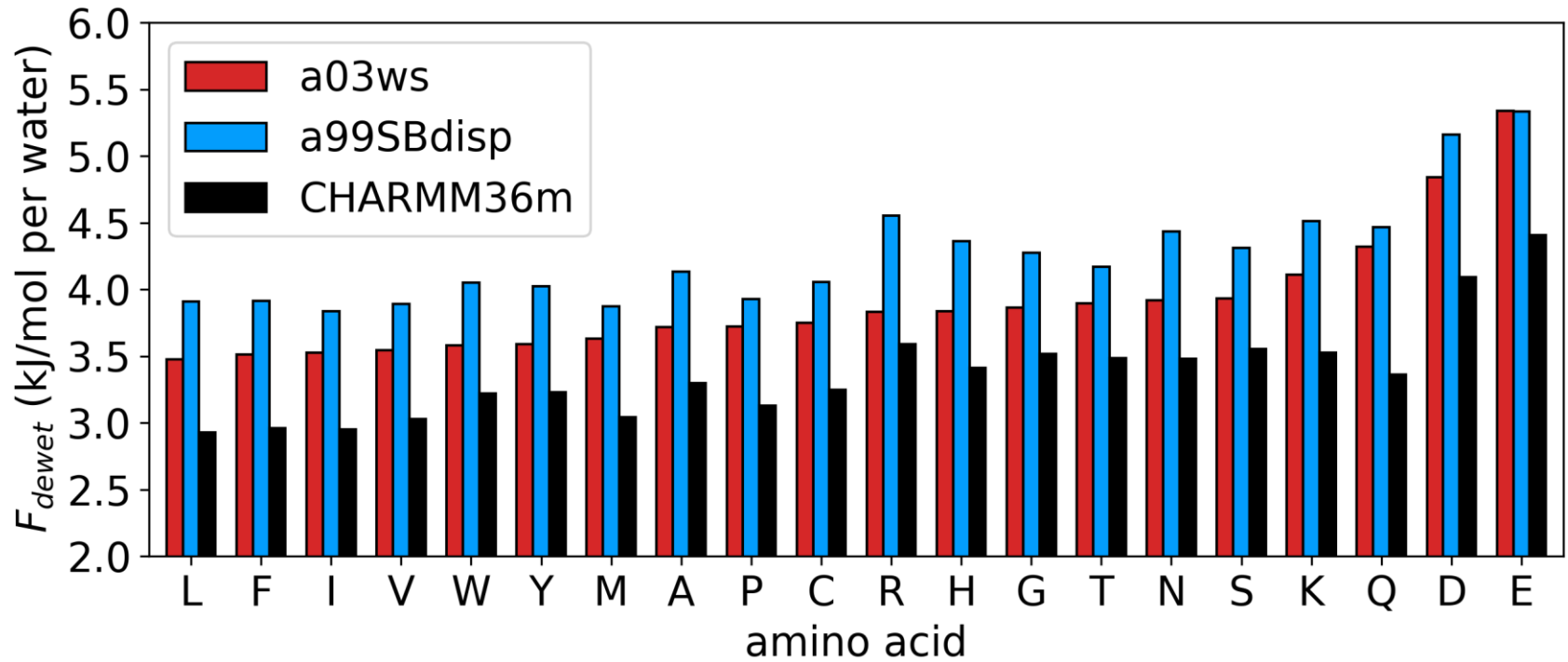


Wild Type

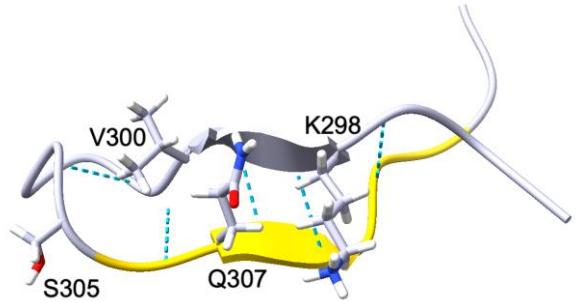
Mutant

TETRAHEDRAL
“hydrophobic”

Different Force Fields Show Different Hydrophobicity



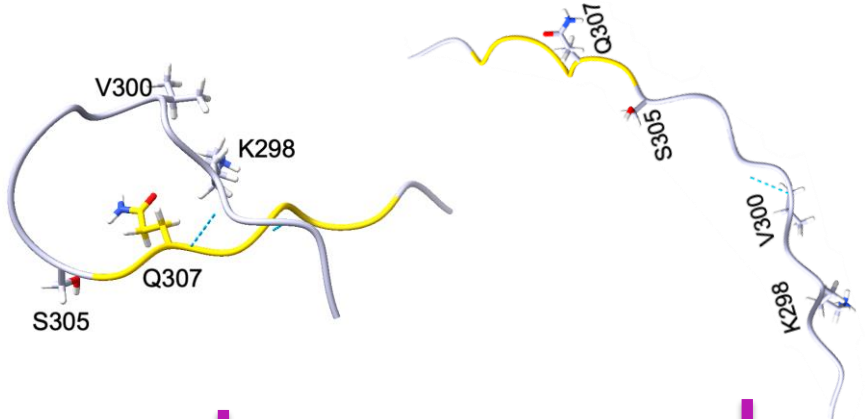
”fibril protective structure”



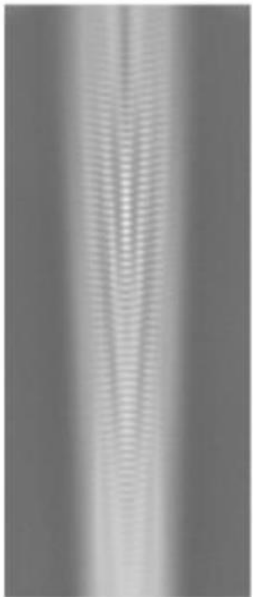
Dead End



”fibril inducing structure”



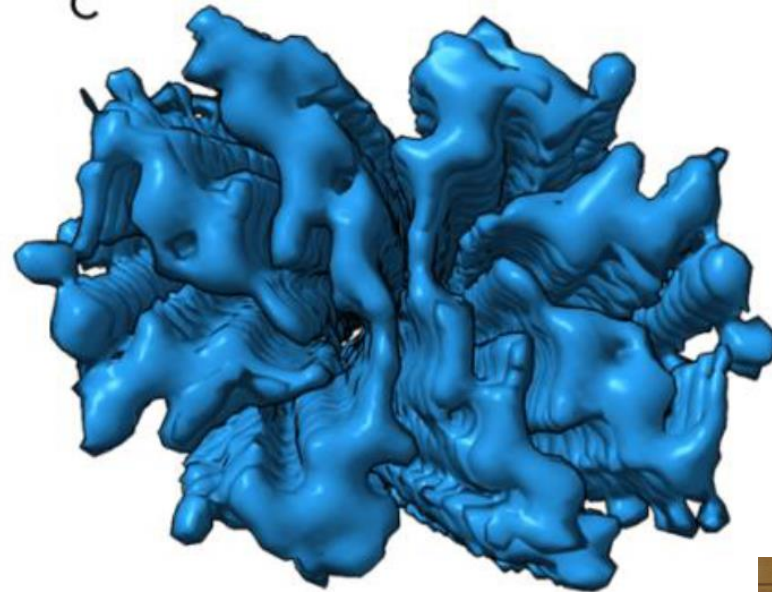
Recent CryoEM structure of jR2R3-P301L



B



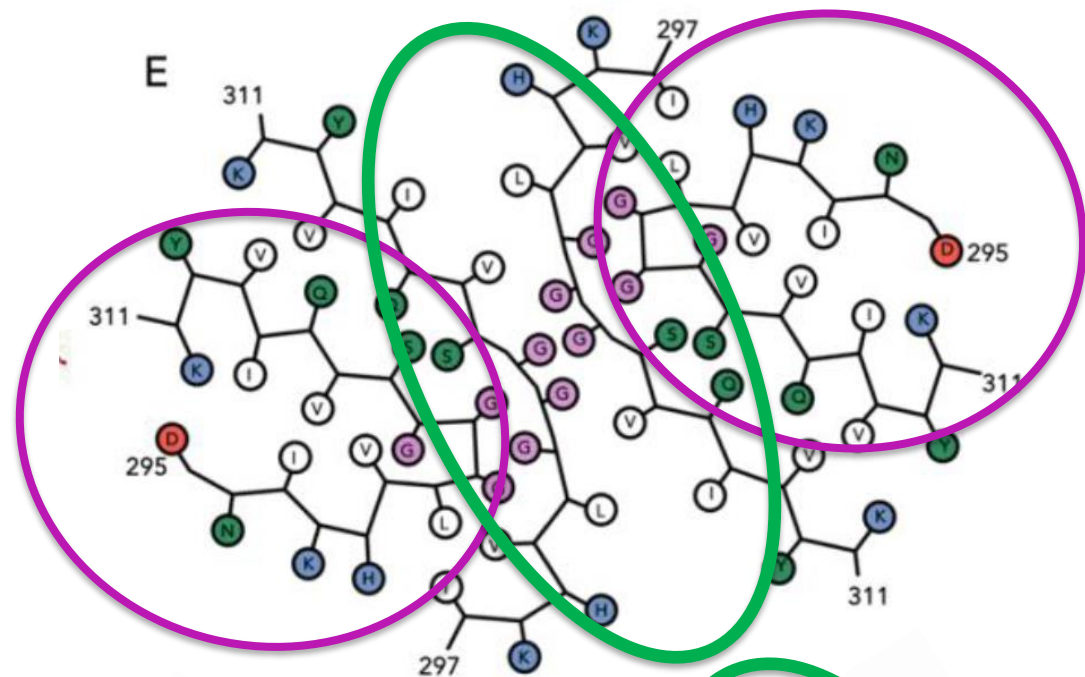
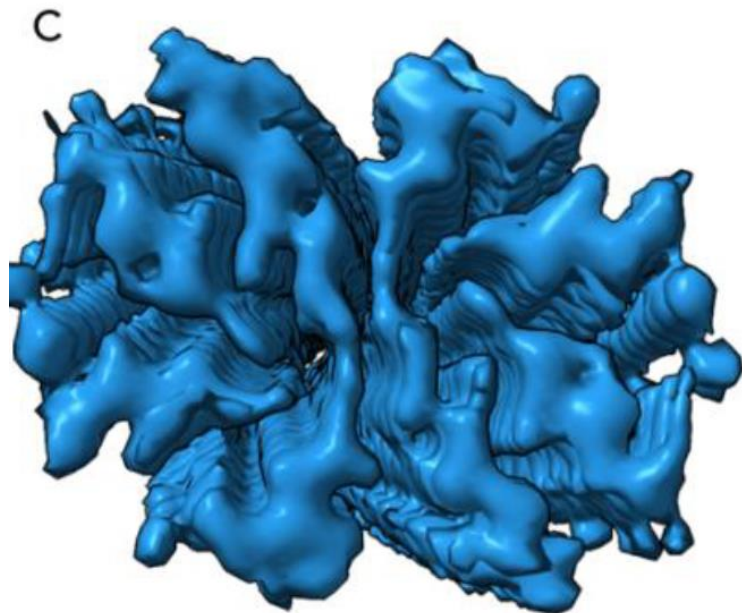
C



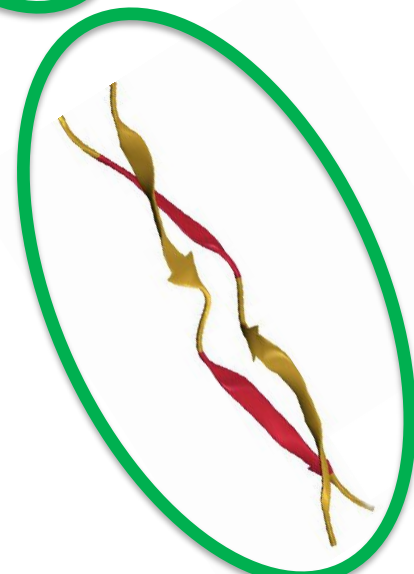
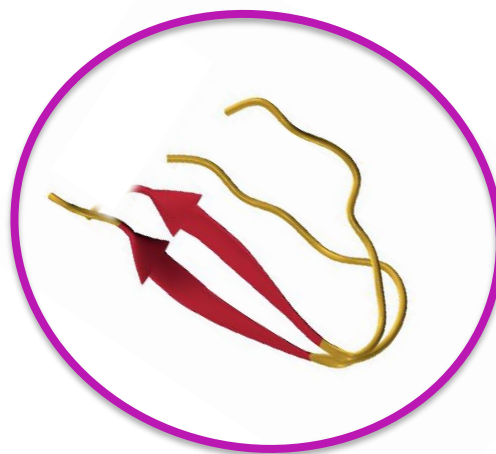
Professor Songi Han
UCSB/
Northwestern University



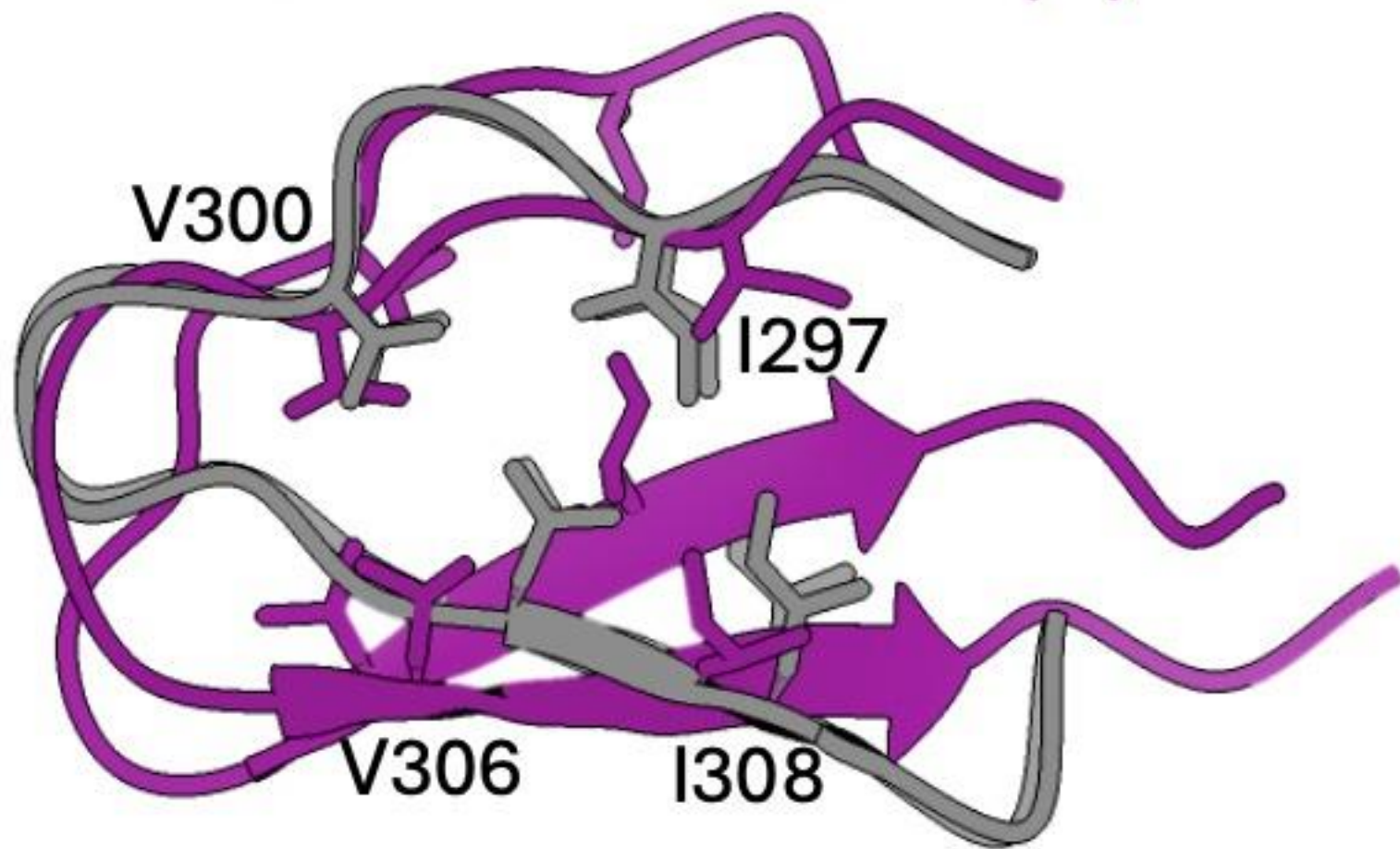
CryoEM structure of jR2R3-P301L



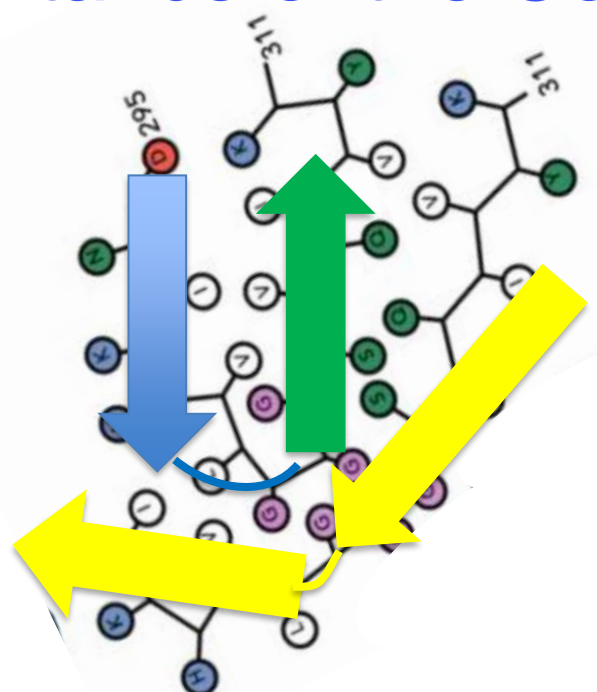
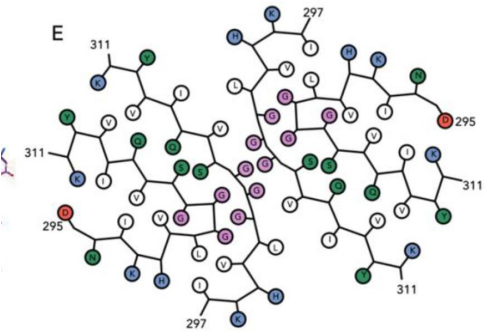
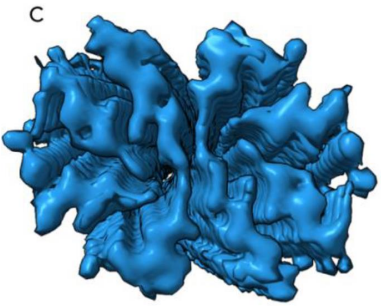
Simulation



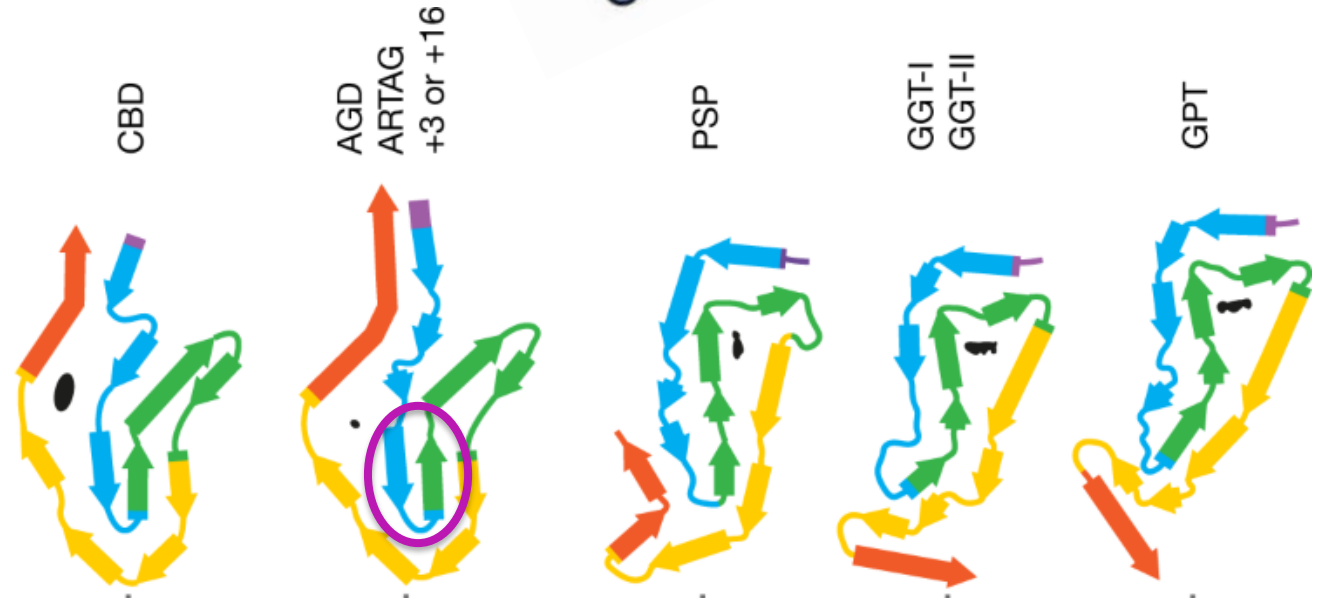
cryo-EM structure
from CHARMM36m (iv)



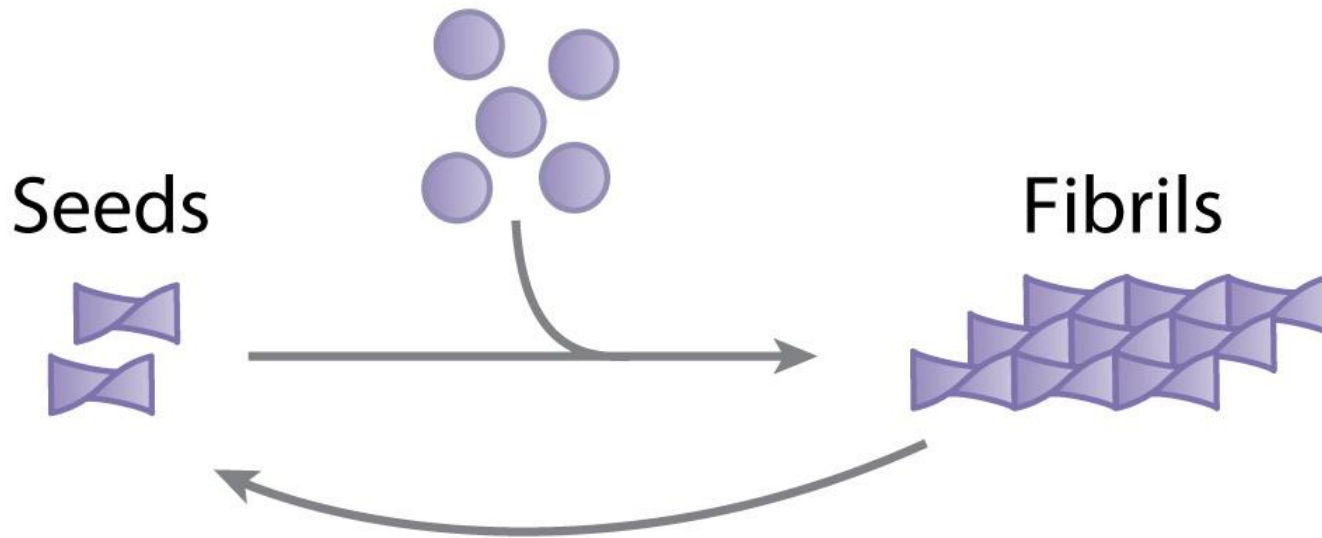
Importance of the Counter-Strand



jR2R3-P301L

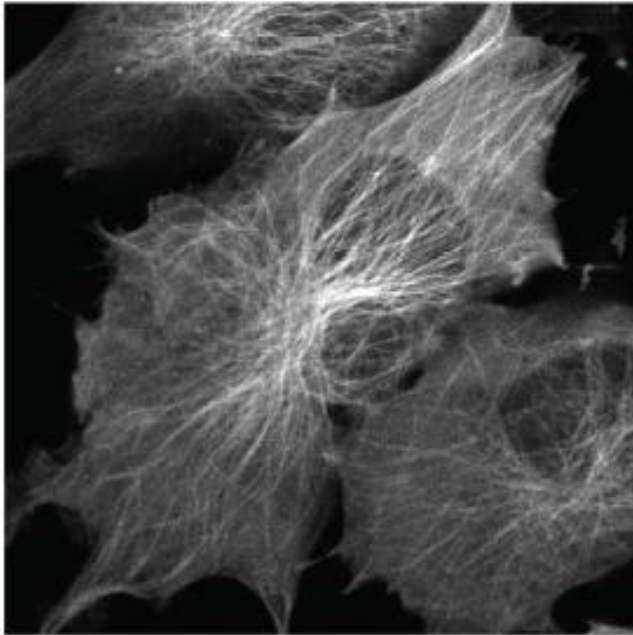


jR2R3-P301L can seed the fibrillization of full length Tau in Vivo

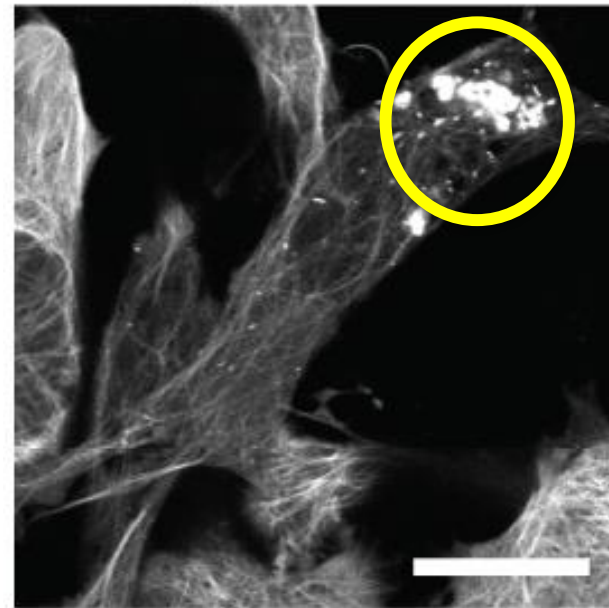


jR2R3-P301L can seed the fibrillization of full length Tau in Vivo

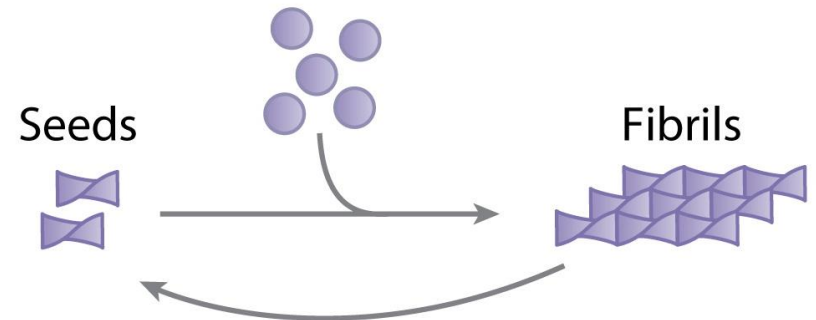
Before jR2R3 P301L



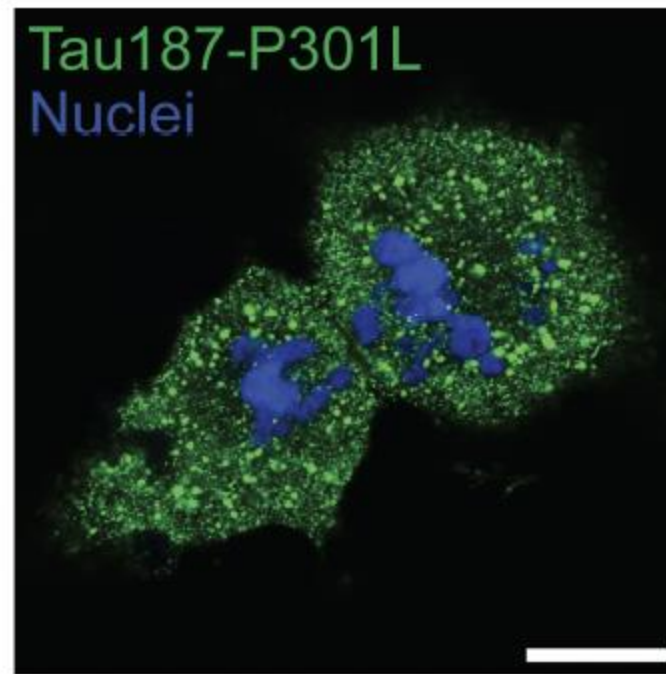
After jR2R3 P301L



Prof. Ken
Kosik, UCSB



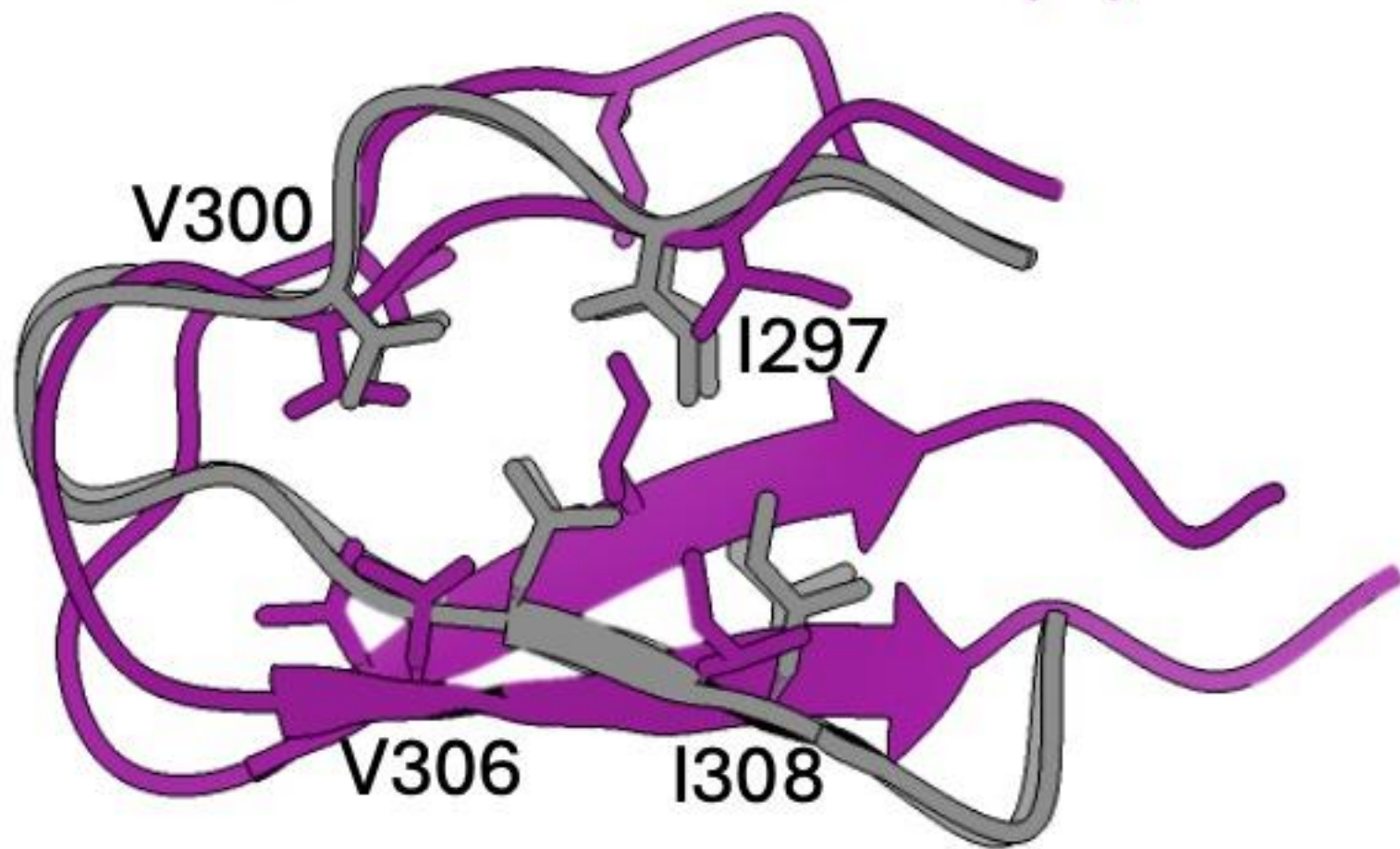
jR2R3-P301L acts as a prion: propagates the strain



PNAS (2024)
121 (15) e2320456121

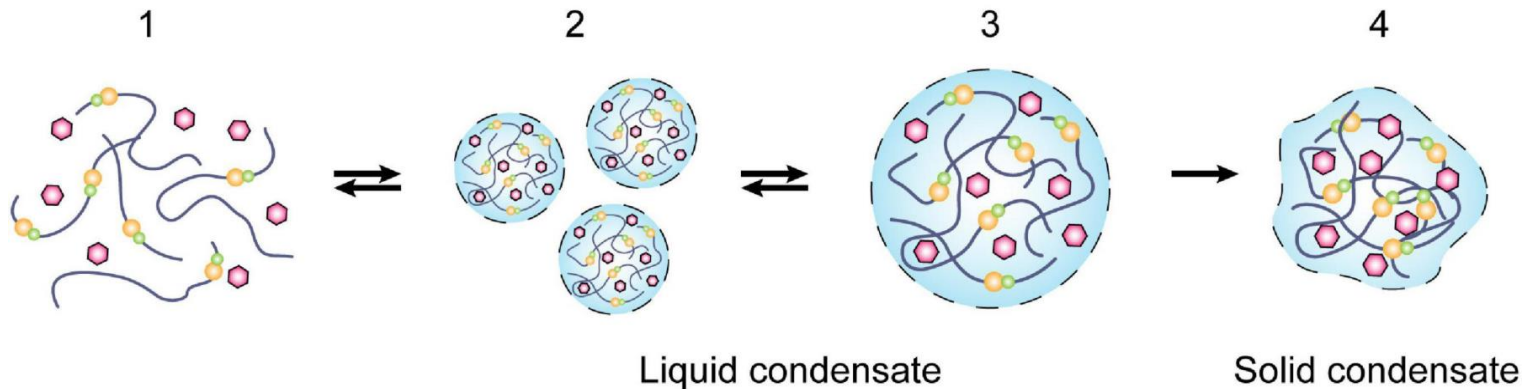
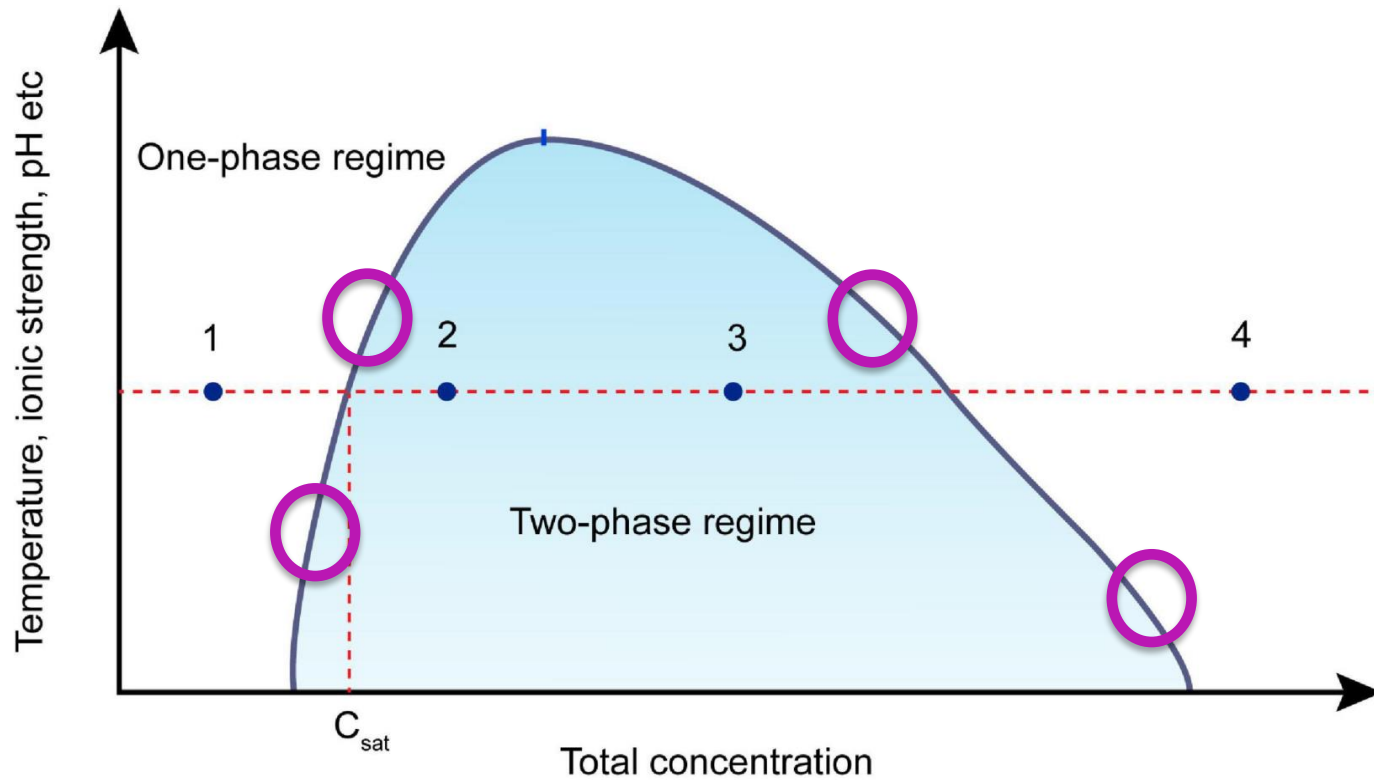
Cells seeded with jR2R3-P301L fibrils undergo division and propagate aggregates to daughter cells

cryo-EM structure
from CHARMM36m (iv)



Back-up Slides

We map the boundaries of the phase diagram



Field Theoretic Model

Partition function for a system of charged Gaussian chains and salt in implicit solvent

$$Z = Z_0 \int Dw \int D\psi e^{-H[w,\psi]}$$

Excluded volume interactions

Electrostatic interactions

$$H[w, \psi] = \frac{1}{2B} \int d\mathbf{r} w(\mathbf{r})^2 + \frac{1}{2E} \int d\mathbf{r} |\nabla\psi|^2 - \sum_l \frac{CV\bar{\phi}_l}{N_l} \ln Q_l$$

Fluctuating chemical potential field

Fluctuating electrostatic potential field

Single chain partition function for polymers and salt ions (complex valued)

B: dimensionless excluded volume parameter

E: dimensionless Bjerrum length

C: dimensionless monomer density

Field Theoretic Simulations

Complex Langevin equations of motion

$$\frac{\partial w(r, t)}{\partial t} = -\lambda_w \frac{\delta H[w, \psi]}{\delta w(r, t)} + \eta_w(r, t)$$
$$\frac{\partial \psi(r, t)}{\partial t} = -\lambda_\psi \frac{\delta H[w, \psi]}{\delta \psi(r, t)} + \eta_\psi(r, t)$$

← real Gaussian white noise

Ensemble averages over the field configurations

$$\langle O \rangle = \frac{\int Dw \int D\psi O e^{-H[w, \psi]}}{\int Dw \int D\psi e^{-H[w, \psi]}}$$

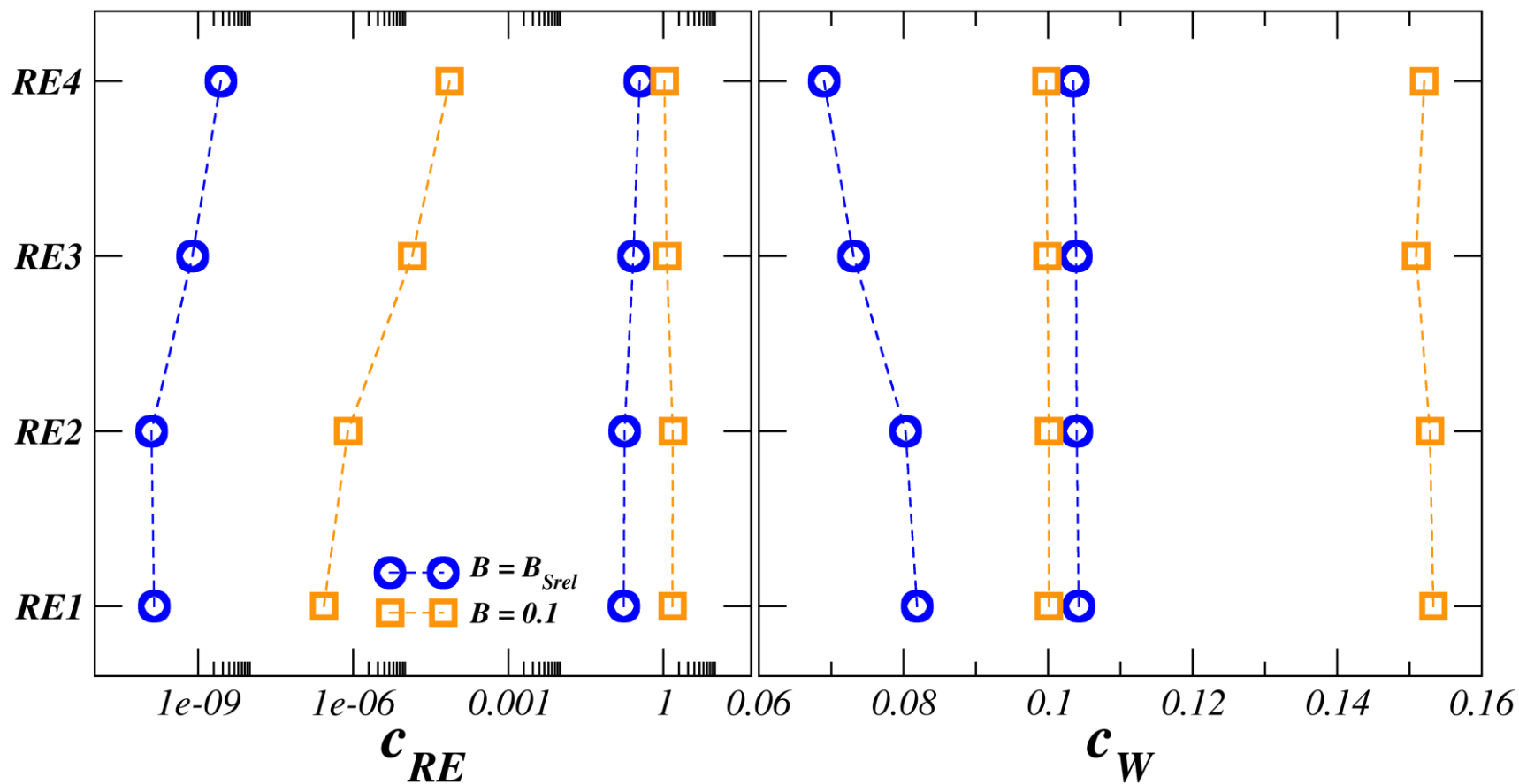
RE peptides phase behavior

RE1: Poly-Arg/Glu ●●●●●●●● ●●●●●●●●

RE2: Poly-Arg/Glu ●●●●●●●● ●●●●●●●●

RE3: Poly-Arg/Glu ●●●●●●●● ●●●●●●●●

RE4: Poly-Arg/Glu ●●●●●●●● ●●●●●●●●



Discrete Gaussian chain polyelectrolyte model

dimensionless monomer density

$$\boxed{C} \sim \rho b^3$$

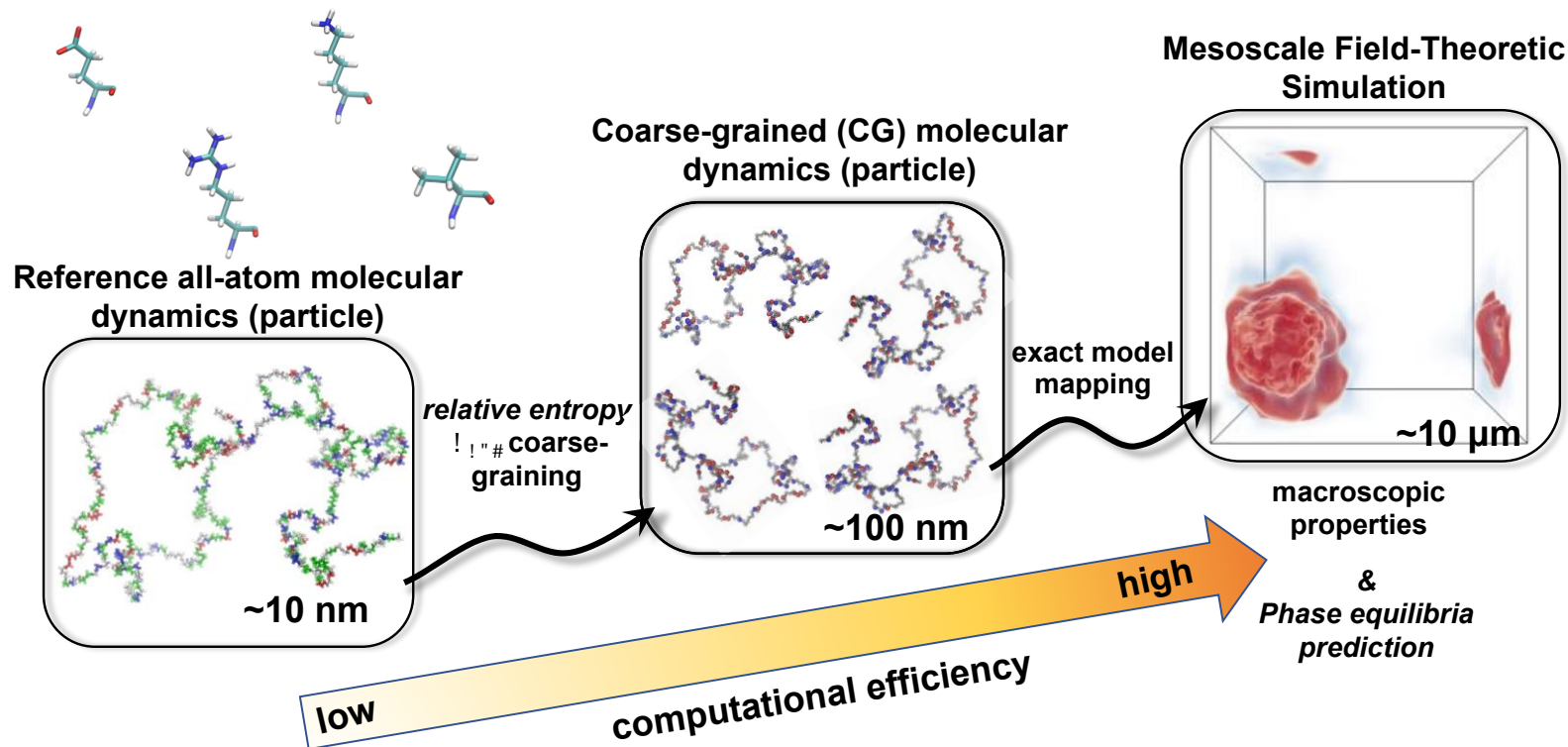
dimensionless excluded volume parameter

$$\beta U = \frac{v}{2} \int d\mathbf{r} \bar{\rho}^2(\mathbf{r}) \quad \boxed{B} \sim \frac{v}{b^3}$$

dimensionless Bjerrum length

$$\beta U = \frac{l_B}{2} \int d\mathbf{r} \int d\mathbf{r}' \frac{\bar{\rho}_e(\mathbf{r}) \bar{\rho}_e(\mathbf{r}')}{|\mathbf{r} - \mathbf{r}'|} \quad \boxed{E} \sim \frac{l_B}{b}$$

Coarse graining through minimizing S_{rel} (Information Loss)



Chemical Detail & transferability

Minimizing the relative entropy (information-loss):

$$S_{rel} = \int \int \rho_{AA}(\mathbf{r}) \ln \left(\frac{\rho_{AA}(\mathbf{r})}{\rho_{CG}(\mathbf{R})} \right) \delta(\mathbf{M}(\mathbf{r}) - \mathbf{R}) d\mathbf{r} d\mathbf{R}$$

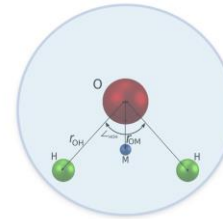
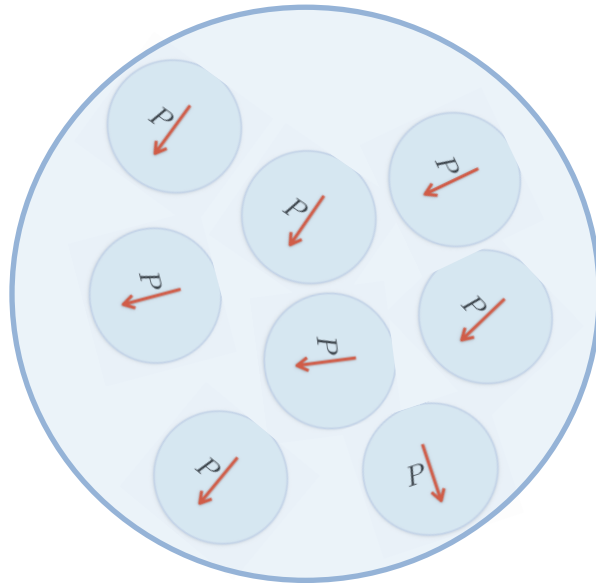
Shell Adv.
Chem. Phys.
2016



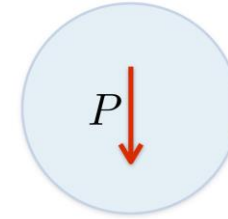
Field theoretic simulation water model

FTS simulation in NVT ensemble

8 AA waters → 1 CG water



Atomistic model

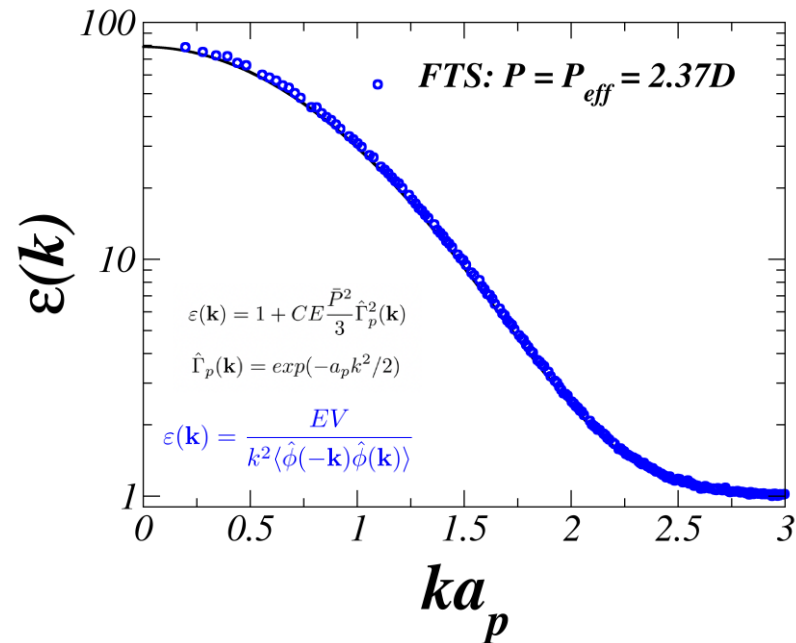


Dimer model

$$\beta\bar{U}[\mathbf{r}] = \frac{\nu}{2} \int d\mathbf{r} \bar{\rho}^2(\mathbf{r}) + \frac{l_B}{2} \iint d\mathbf{r} d\mathbf{r}' \frac{\bar{\rho}_e(\mathbf{r})\bar{\rho}_e(\mathbf{r}')}{|\mathbf{r} - \mathbf{r}'|}$$

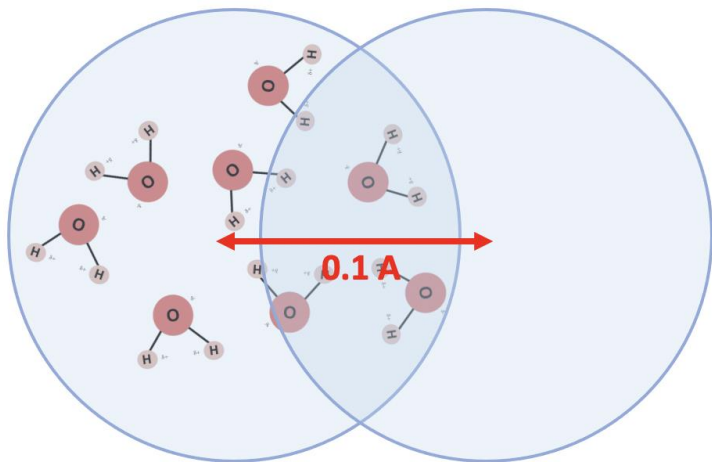
$$\bar{\rho}(\mathbf{r}) = \int d\mathbf{r}' \Gamma(|\mathbf{r} - \mathbf{r}'|) \hat{\rho}(\mathbf{r}')$$

$$\Gamma(r) = \left(\frac{1}{2\pi a^2} \right)^{3/2} \exp(-r^2/2a^2)$$



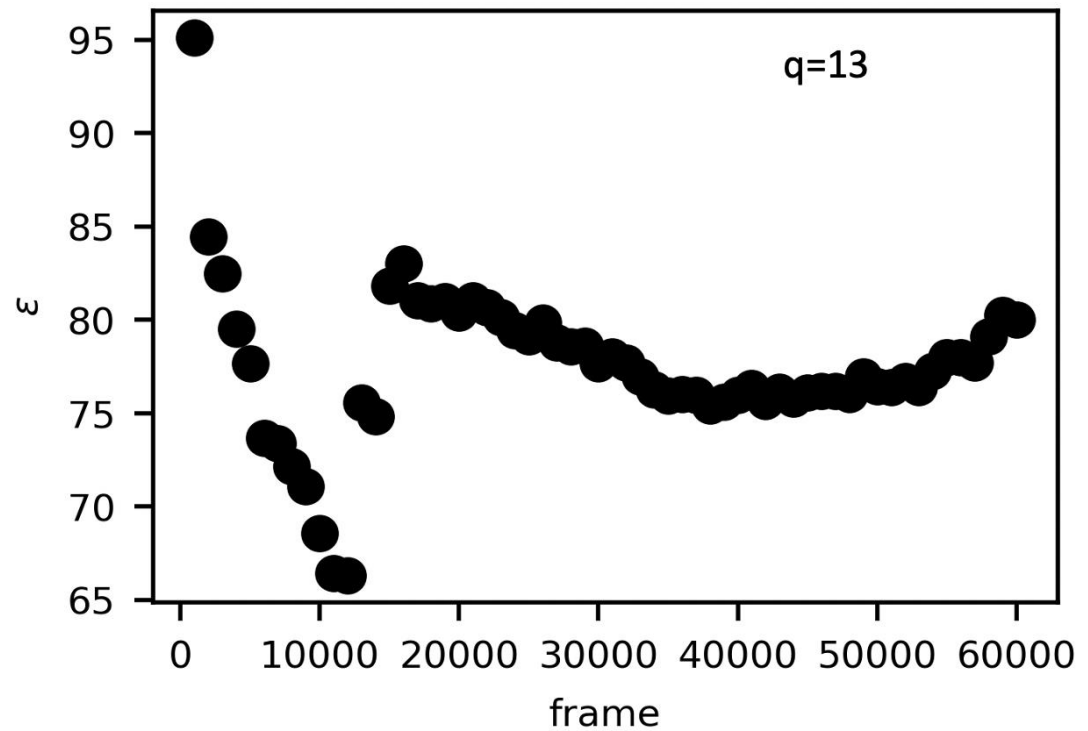
MD coarse-grained water model

8 AA waters \rightarrow 1 CG water



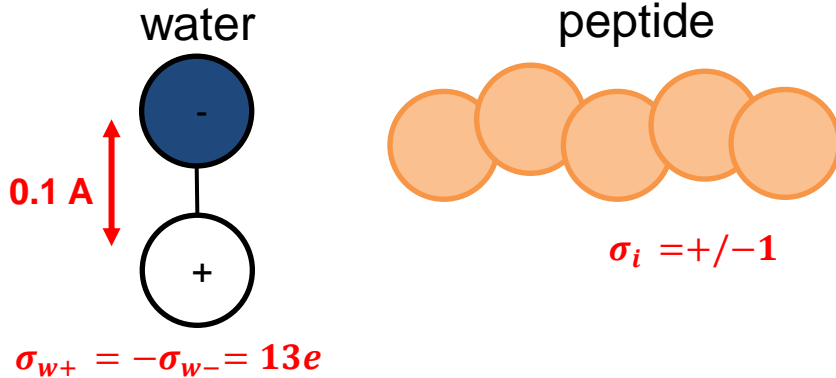
$$\sigma_{w+} = -\sigma_{w-} = 13 e$$

Match $\epsilon = 80$ at 300 K



Relative entropy parametrization of peptide and water interaction

RE1: Poly-Arg/Glu 



$$\sigma = a_i = R_w = 0.158 \text{ nm}$$

- $\beta U_{bond,water}$: stiff harmonic with $b = 0.01 \text{ nm}$
- $\beta U_{bond,residue}$: harmonic with $b = \sqrt{6} \sigma$
- Electrostatics: $\beta U_{el,W-,W+}, \beta U_{el,W+,W+}, \beta U_{el,W-,W-}$

- Excluded volumes:

- $u_{W-,W-} = u_{Lys,Lys} = u_{Cl,Cl} = u_{W-,Cl} = u_{Lys,Cl} = 0.1 \text{ kT } \sigma^3$
- $u_{W-,residue} = [B^{Srel} (4\pi\sigma^2)^{\frac{3}{2}} \sigma^3] N_{ref}^2 \sigma^{-3} = B_{W-,residue}^{Srel} (4\pi)^{3/2} \sigma^3$

Coarse-grain interactions

$$U_{CG} = \sum_{bonds} U_{bond} + \sum_i^{N_T-1} \sum_{j=i+1}^{N_T} U_{ev}(r_{ij}) + U_{el}(r_{ij})$$

$$\beta U_{bond}(r_{ij}) = \frac{3}{2b^2} (r_{ij} - r_0)^2$$

$$\beta U_{ev}(r_{ij}) = \frac{u_{ij}}{(2\pi(a_i^2 + a_j^2))^{3/2}} e^{-r_{ij}^2/2(a_i^2 + a_j^2)}$$

$$\beta U_{el}(r_{ij}) = \frac{l_B \sigma_i \sigma_j}{r_{ij}} \text{erf} \left(\frac{r_{ij}}{2\sqrt{a_i^2/2 + a_j^2/2}} \right)$$

$a_i = 0.316 \text{ nm}$: bead radius

b : statistical segment length

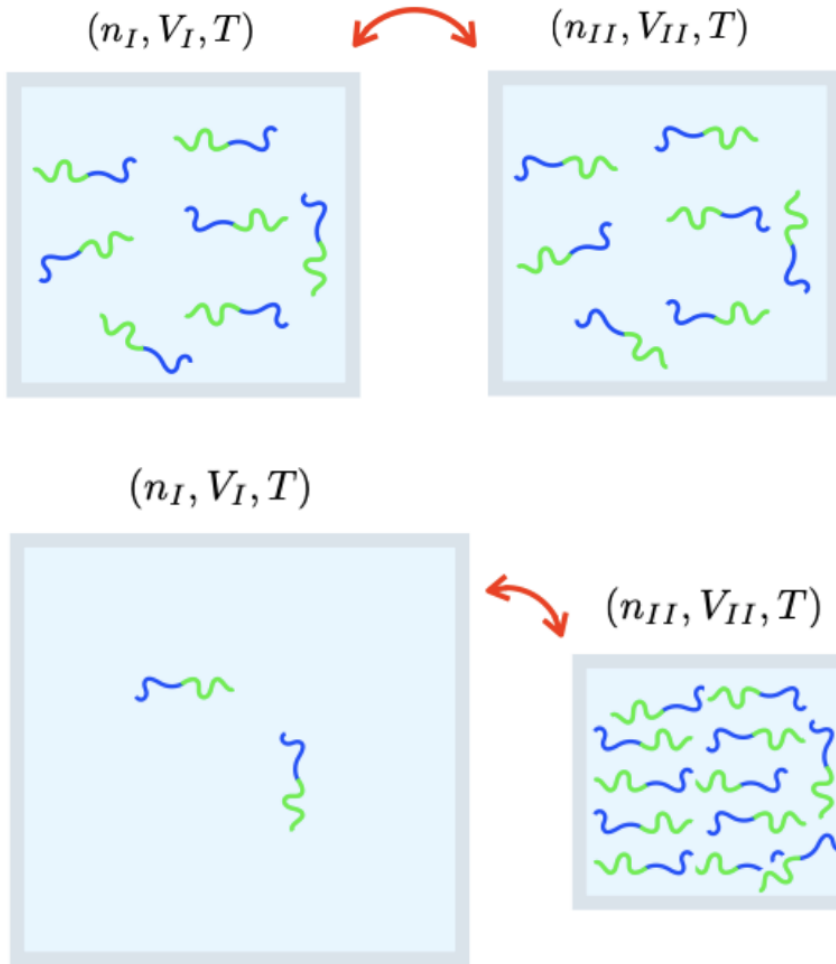
$r_0 = 0$: equilibrium bond distance

u_{ij} : excluded volume

σ_i : charge

$l_B = 561.6 \text{ nm}$: Bjerrum length

Gibbs Ensemble Simulations



$$V_T = V_I + V_{II} \quad n_T = n_I + n_{II}$$

$$F(n, V_T, T) = F_I(n_I, V_I, T) + F_{II}(n_{II}, V_{II}, T)$$

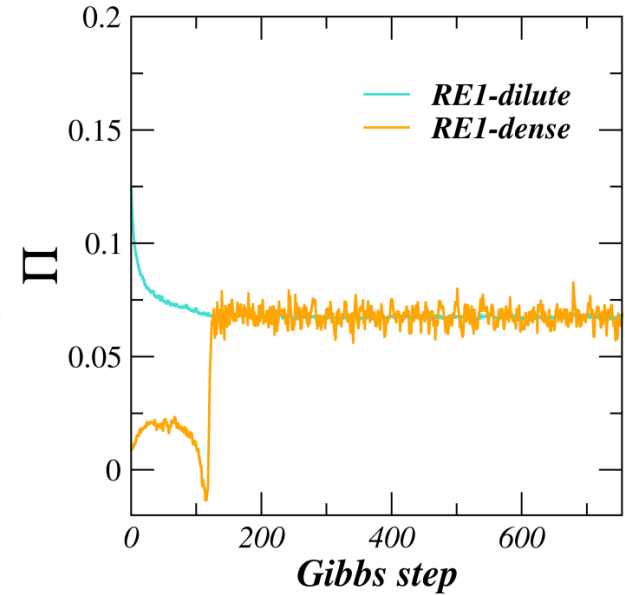
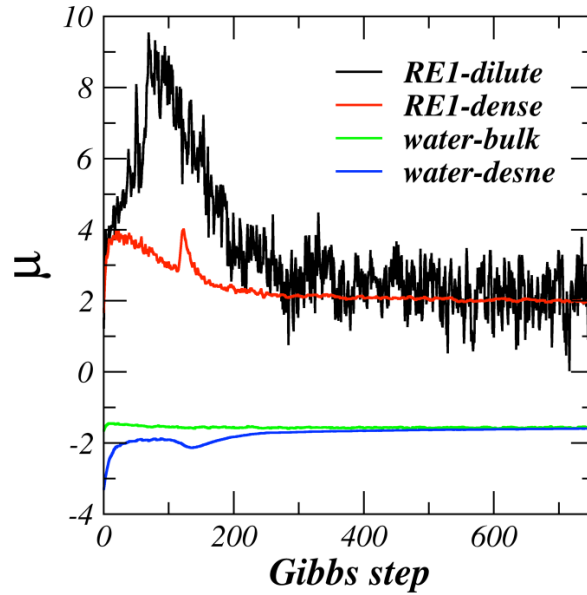
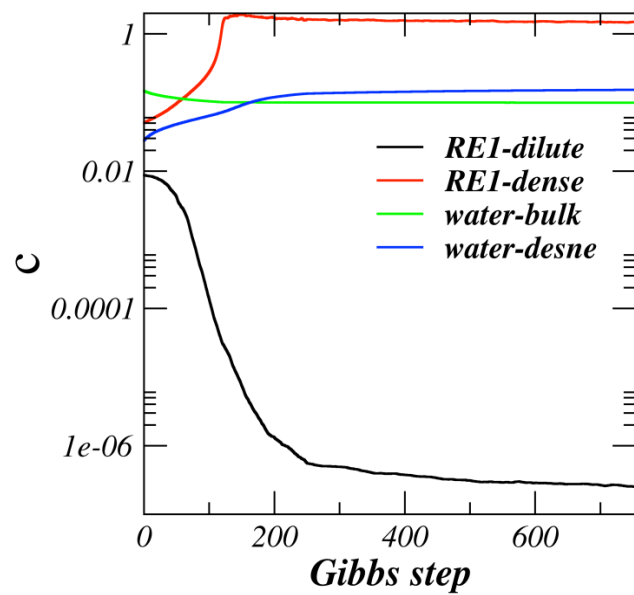
$$\frac{\partial F}{\partial V_I} = -(\Pi_I - \Pi_{II})$$

$$\frac{\partial F}{\partial n_I} = (\mu_I - \mu_{II})$$

$$\frac{\partial F}{\partial V_I} = -(\Pi_I - \Pi_{II}) = 0$$

$$\frac{\partial F}{\partial n_I} = (\mu_I - \mu_{II}) = 0$$

Gibbs Ensemble Field Theory Simulation (FTS) convergence



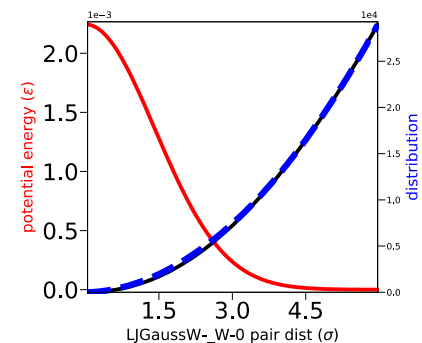
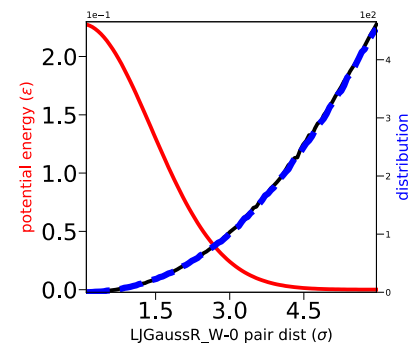
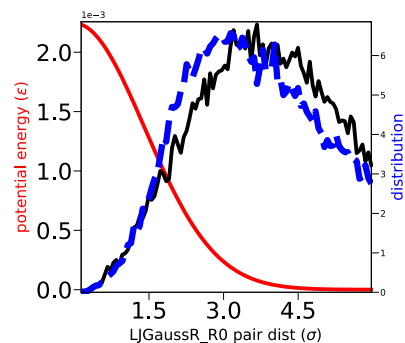
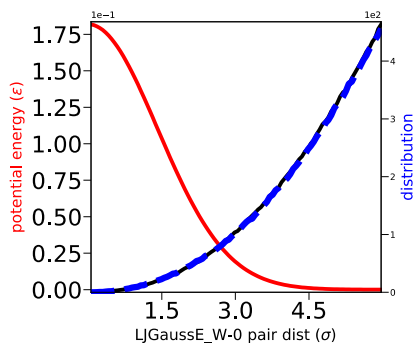
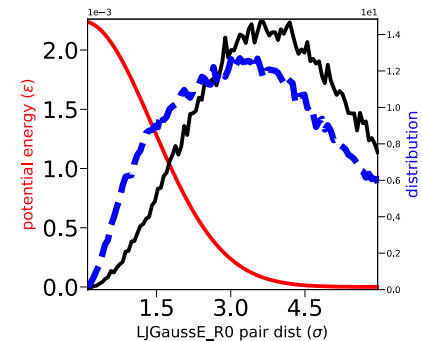
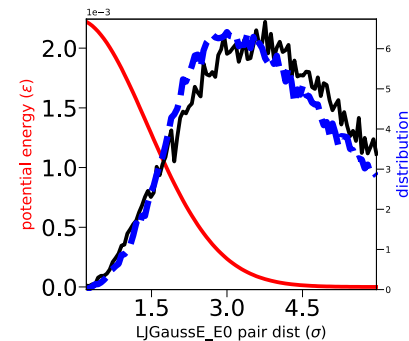
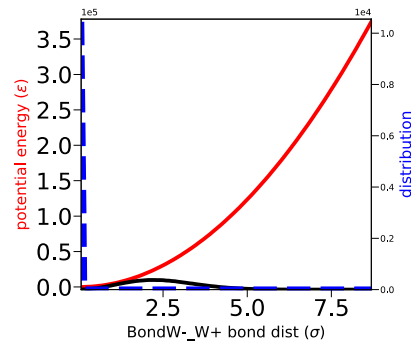
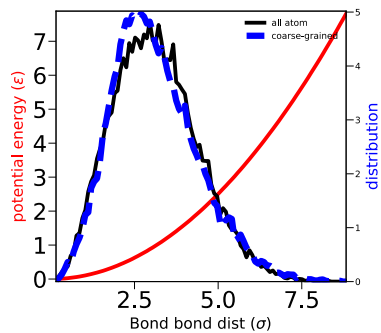
CG parametrization of peptide-water interaction using relative-entropy

Optimized parameters:

Blurring sigma 0.35

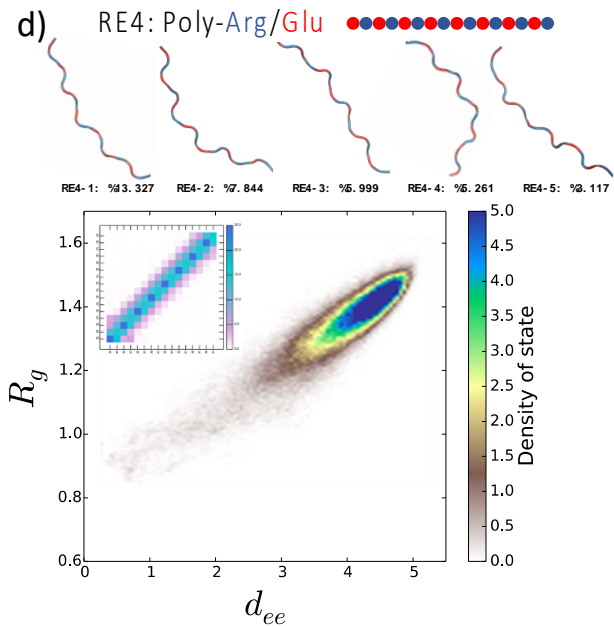
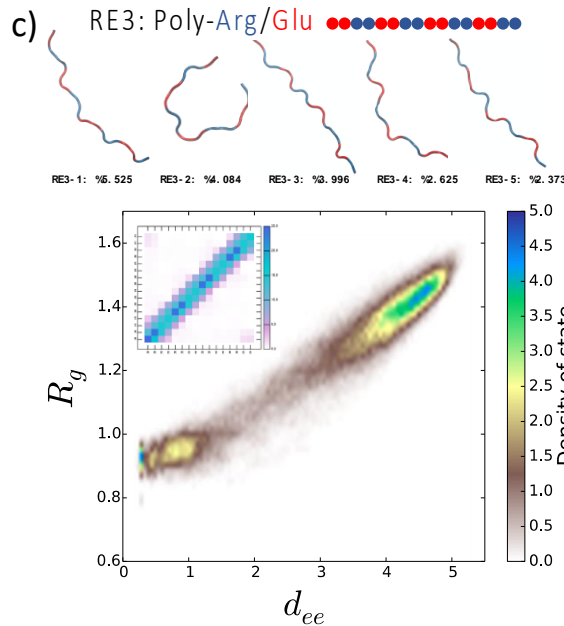
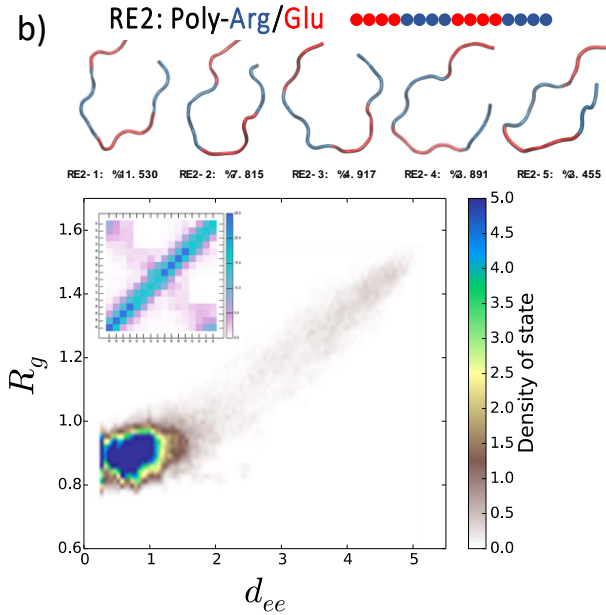
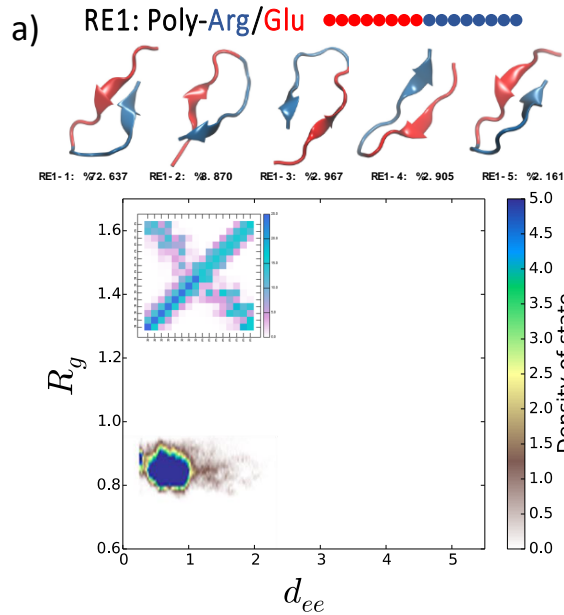
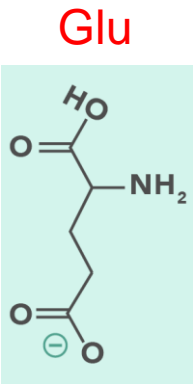
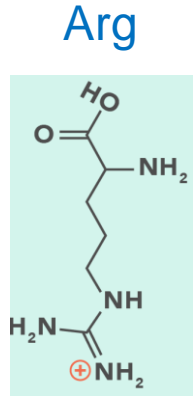
E-W B=0. 182

R-W B=0.228



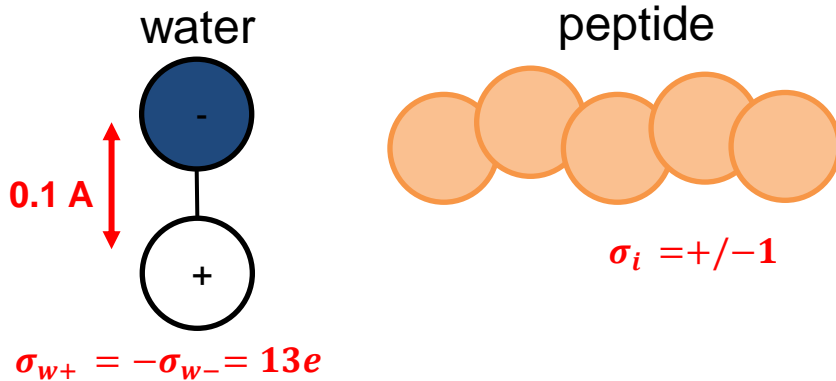
- The implicit solvent model cannot capture the heterogeneous dielectricity that may occur within the peptide-dense phase. In contrast, the explicit solvent model accounts for environment-dependent dielectricity, unlike the uniform dielectricity assumed in the implicit solvent model.
- This explicit solvent model can be parameterized to incorporate the effect of the peptide sequence on the effective interaction between residues and water into the coarse-graining (CG) process. Previous CG methods totally ignore this.
- As a result, the phase diagram derived from accurately transferring chemical details to the CG system is expected to capture any mesoscopic phase transitions and morphological complexities.
-

All atom reference simulations for coarse graining



Relative entropy parametrization of peptide and water interaction

RE1: Poly-Arg/Glu 



$$\sigma = a_i = R_w = 0.158 \text{ nm}$$

- $\beta U_{bond,water}$: stiff harmonic with $b = 0.01 \text{ nm}$
- $\beta U_{bond,residue}$: harmonic with $b = \sqrt{6} \sigma$
- Electrostatics: $\beta U_{el,W-,W+}, \beta U_{el,W+,W+}, \beta U_{el,W-,W-}$

- Excluded volumes:

- $u_{W-,W-} = u_{Lys,Lys} = u_{Cl,Cl} = u_{W-,Cl} = u_{Lys,Cl} = 0.1 \text{ kT } \sigma^3$
- $u_{W-,residue} = [B^{Srel} (4\pi\sigma^2)^{\frac{3}{2}} \sigma^3] N_{ref}^2 \sigma^{-3} = B_{W-,residue}^{Srel} (4\pi)^{3/2} \sigma^3$

Coarse-grain interactions

$$U_{CG} = \sum_{bonds} U_{bond} + \sum_i^{N_T-1} \sum_{j=i+1}^{N_T} U_{ev}(r_{ij}) + U_{el}(r_{ij})$$

$$\beta U_{bond}(r_{ij}) = \frac{3}{2b^2} (r_{ij} - r_0)^2$$

$$\beta U_{ev}(r_{ij}) = \frac{u_{ij}}{(2\pi(a_i^2 + a_j^2))^{3/2}} e^{-r_{ij}^2/2(a_i^2 + a_j^2)}$$

$$\beta U_{el}(r_{ij}) = \frac{l_B \sigma_i \sigma_j}{r_{ij}} \text{erf} \left(\frac{r_{ij}}{2\sqrt{a_i^2/2 + a_j^2/2}} \right)$$

$a_i = 0.316 \text{ nm}$: bead radius

b : statistical segment length

$r_0 = 0$: equilibrium bond distance

u_{ij} : excluded volume

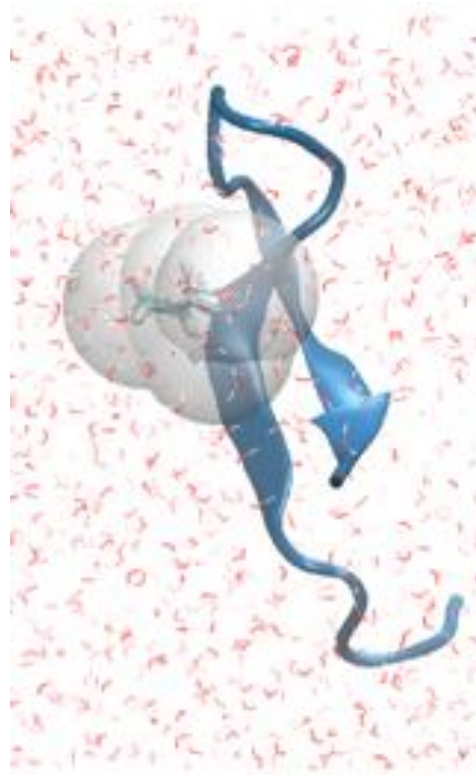
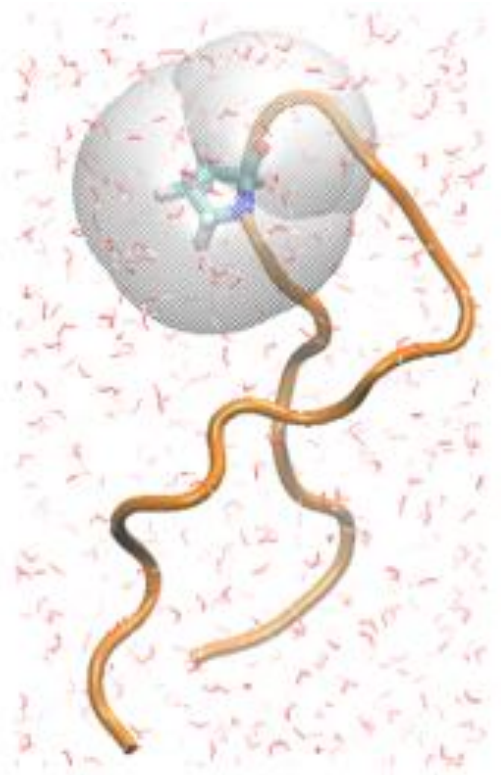
σ_i : charge

$l_B = 561.6 \text{ nm}$: Bjerrum length

Tau and Traumatic Brain Injury



Overhauser Dynamic Nuclear Polarization (ODNP) experiments show a reduction in hydration water dynamics around 301 site for the P→L mutant (jR2R3-P301L)



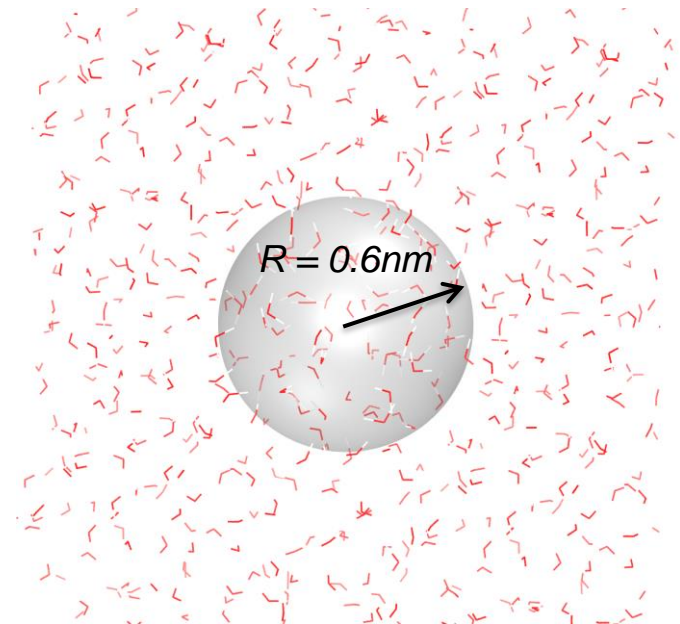
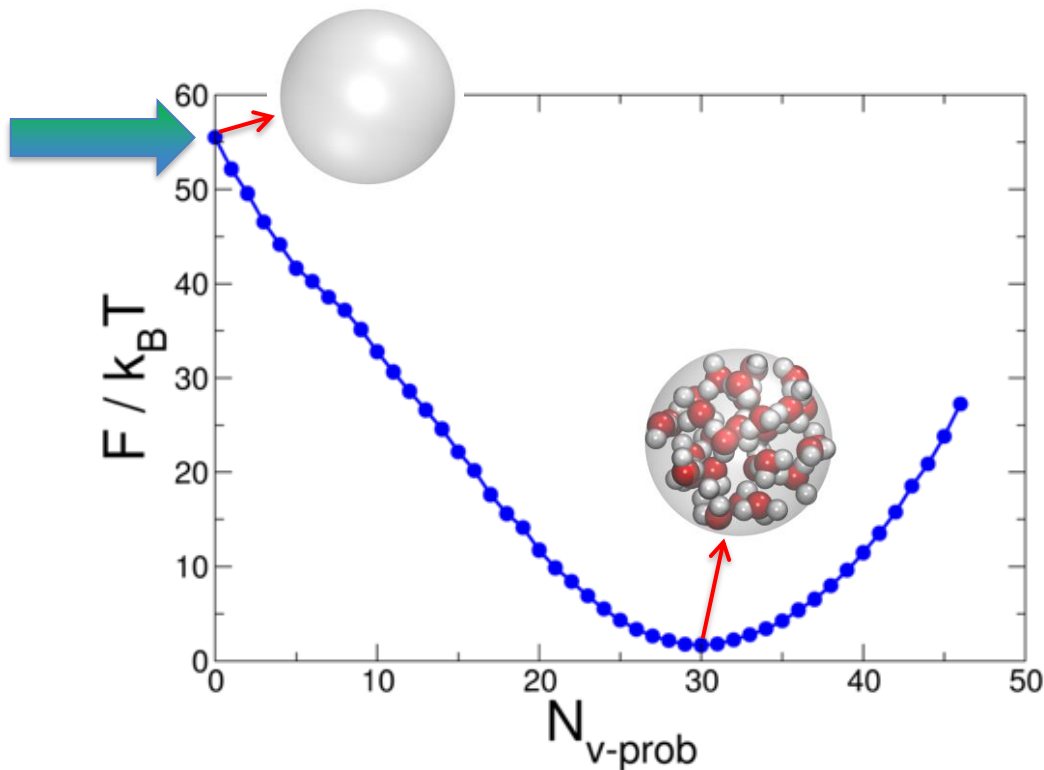
Increased ordering of water around mutation site

→ locally more hydrophobic

Probing Hydrophobicity Computationally through Umbrella Sampling (INDUS)

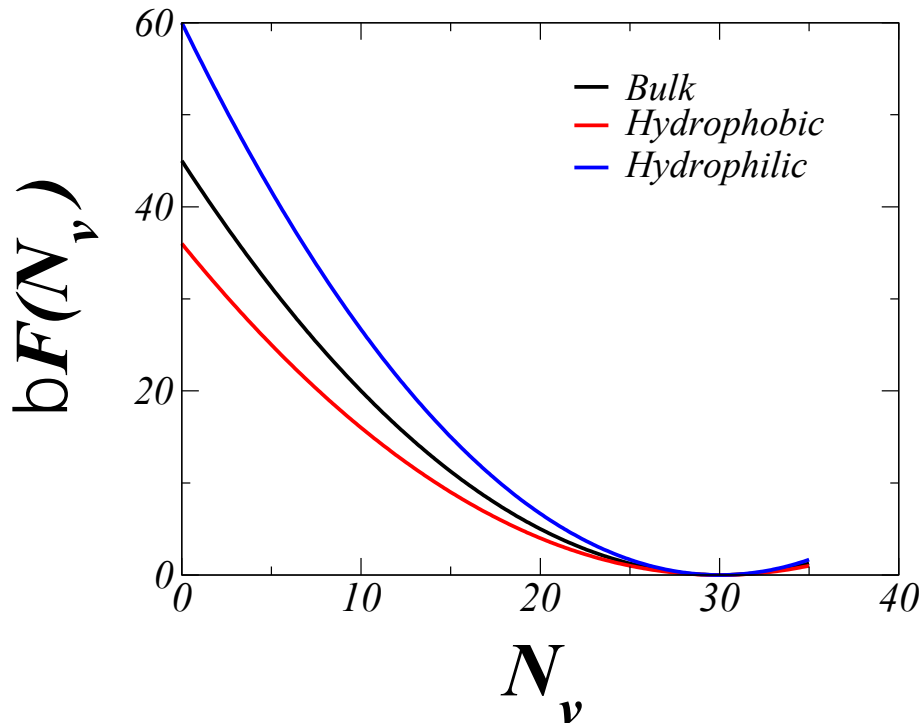
Free energy of dewetting a spherical volume in bulk

$$\mu_{\text{ex}} = \mathbf{F}(\mathbf{0}) = -\ln \mathbf{P}_{\mathbf{v}}(\mathbf{0})$$

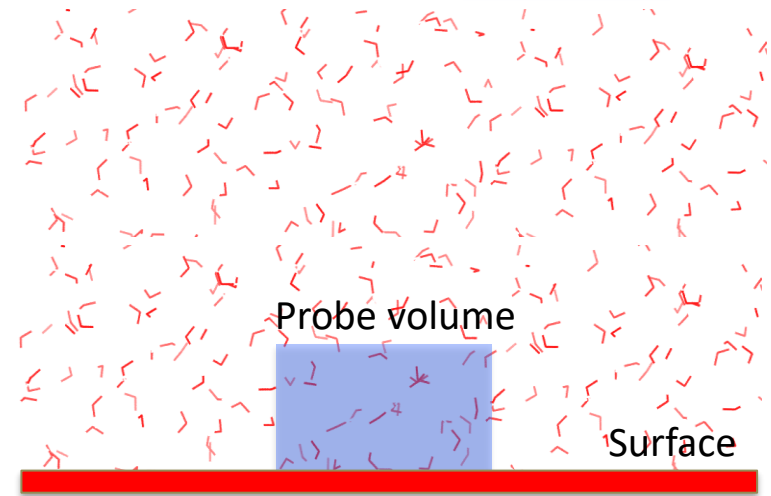


Free energy of dewetting the probe volume in vicinity of a surface

Excess chemical potential is an indication of hydrophilicity or hydrophobicity of the surface

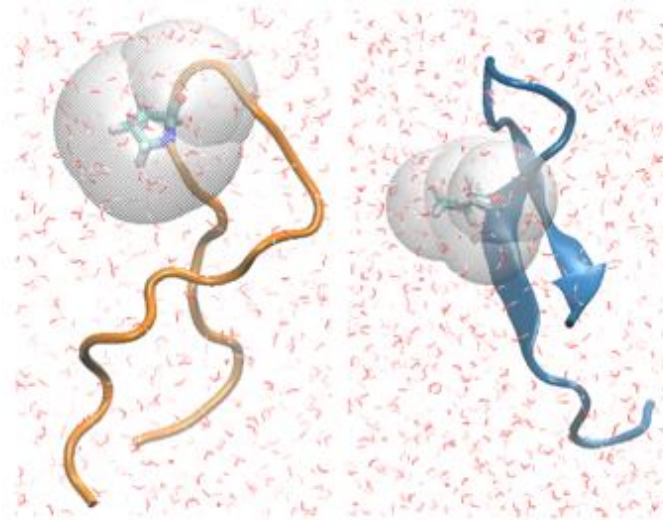


$$\mu_{\text{ex}}^{\text{phil}} > \mu_{\text{ex}}^{\text{bulk}} > \mu_{\text{ex}}^{\text{phob}}$$



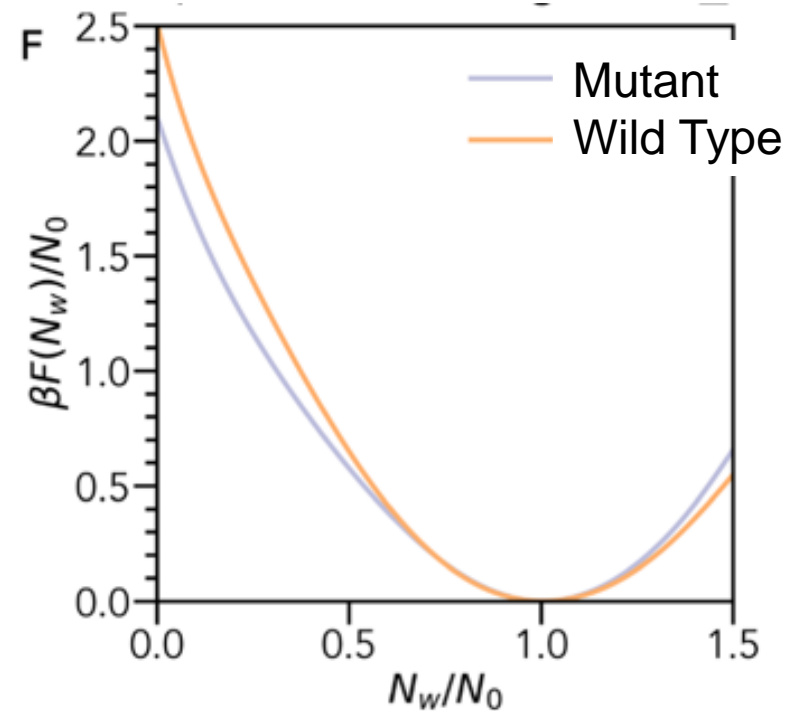
$$\mu_{\text{ex}} = \mathbf{F}(\mathbf{0}) = -\ln P_v(\mathbf{0})$$

Free energy of dewetting lower for jR2R3-P301L: an additional factor favoring association of jR2R3-P301L

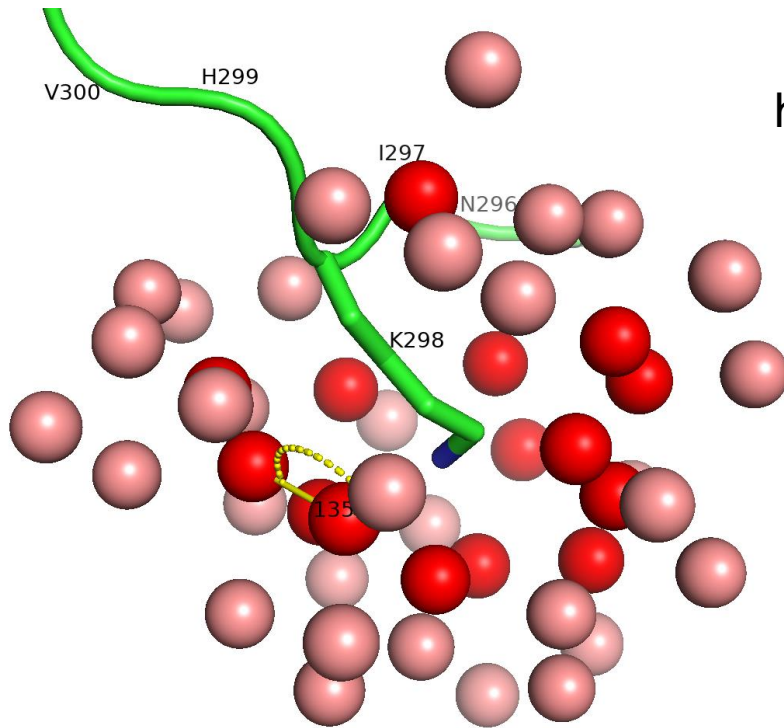


Wild Type

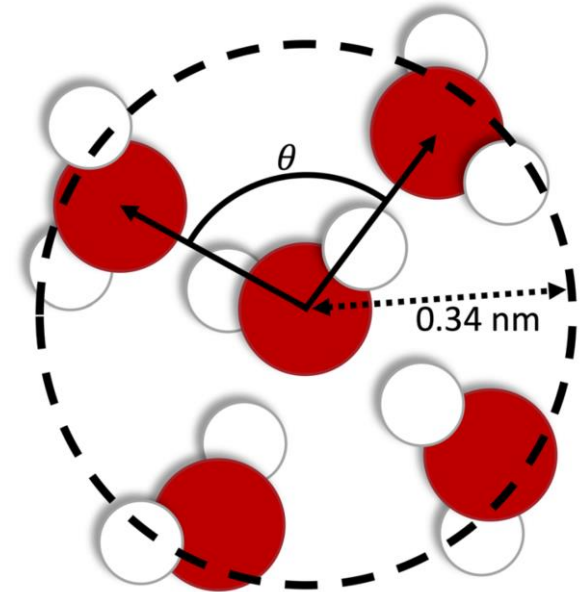
Mutant



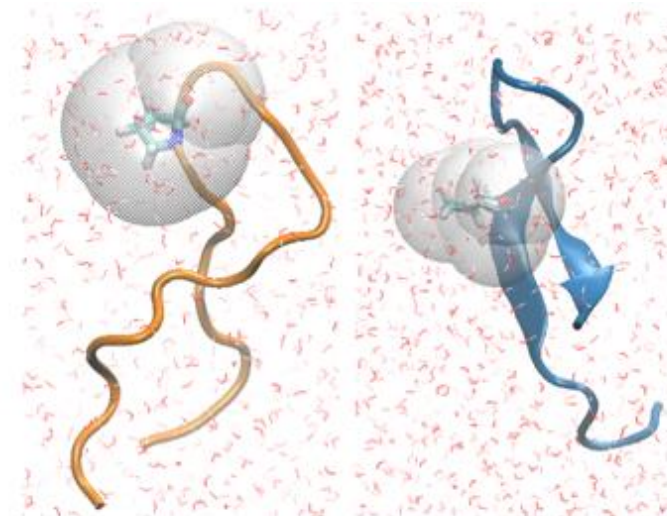
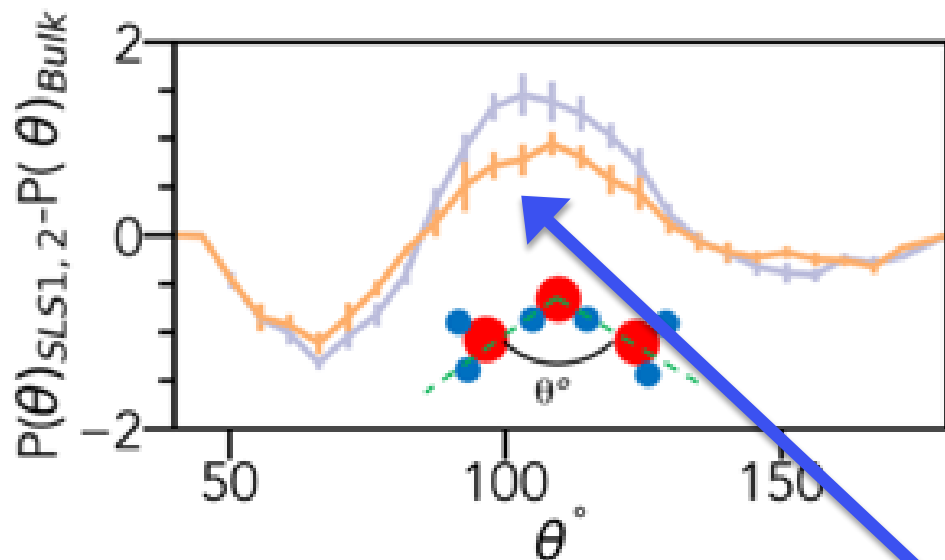
Quantifying Water Structure: *water triplet distribution*



histogram
the
angles



Increased tetrahedral ordering of hydration waters near the L301 (mutant) compared to P301 (wild type)



Wild Type

Mutant

TETRAHEDRAL
“hydrophobic”

Dimer Simulations of jR2R3 and JR2R3-P301L



jR2R3

6.4%



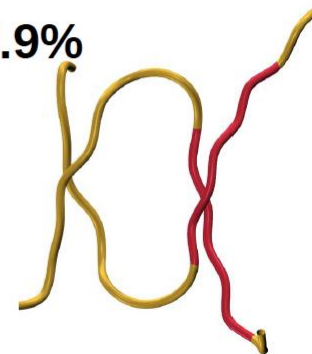
6.1%



5.6%

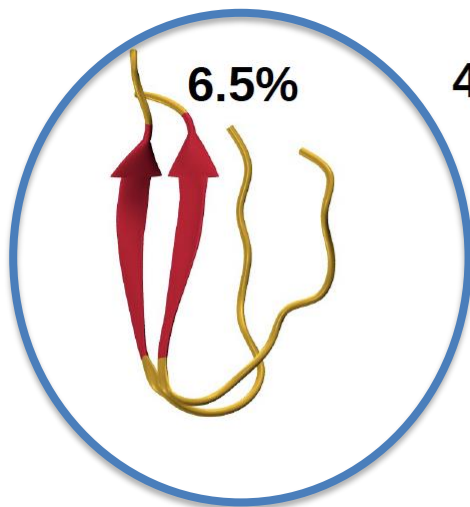


2.9%



jR2R3-
P301L

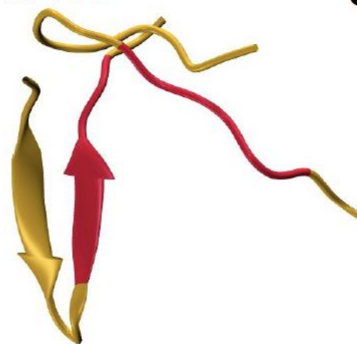
6.5%



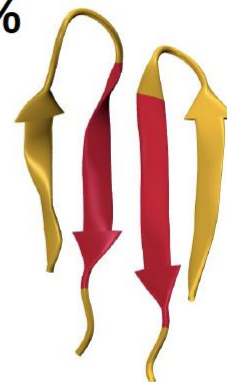
4.8%



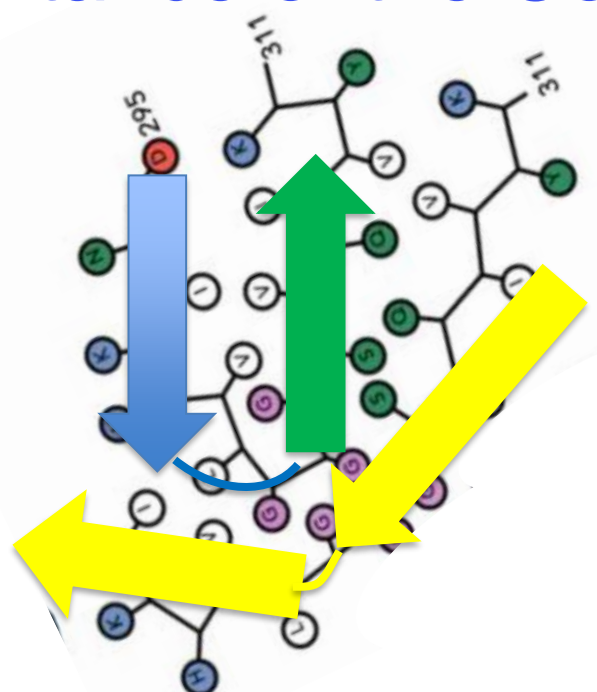
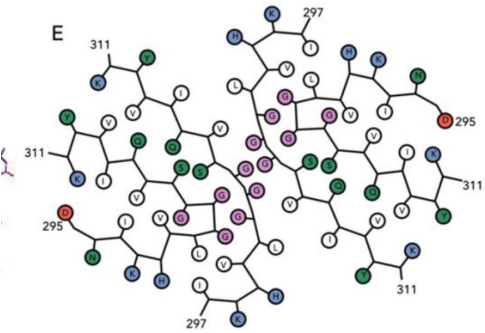
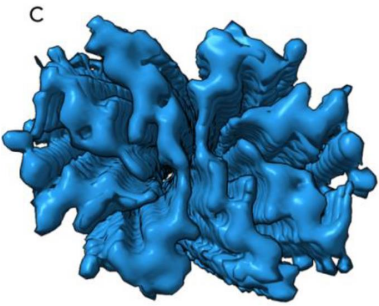
4.4%



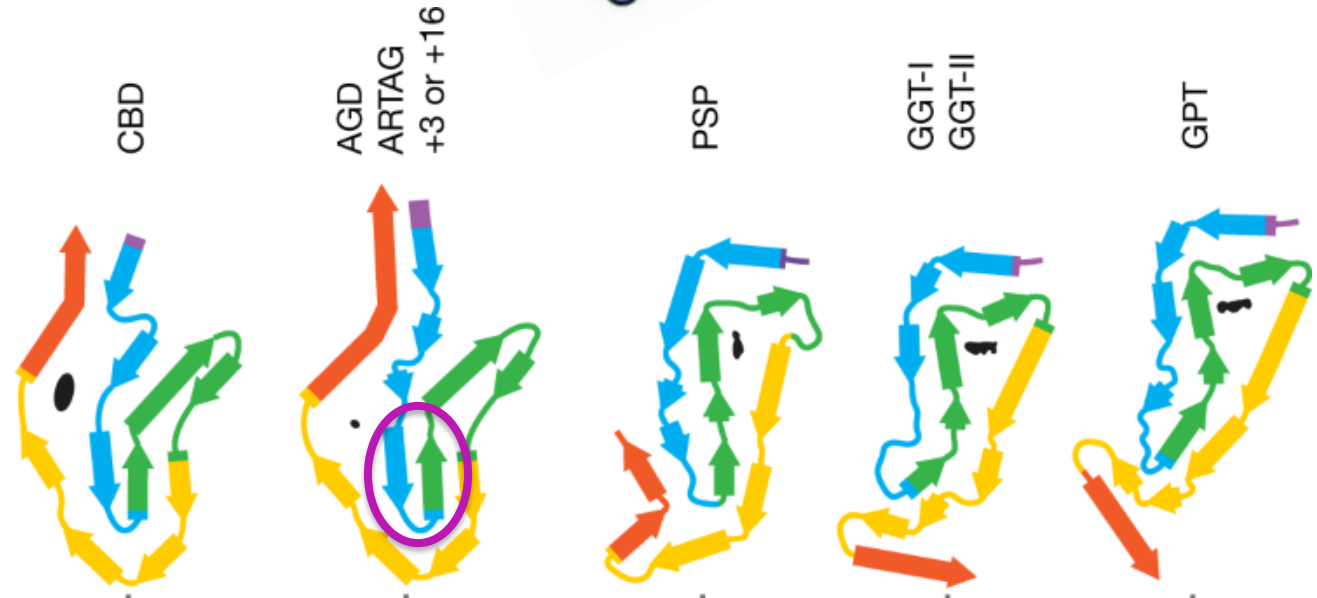
3.5%



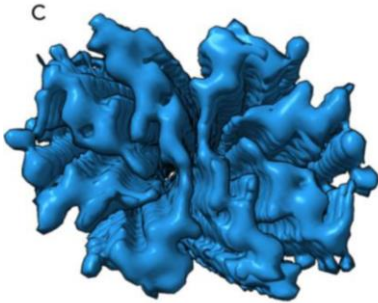
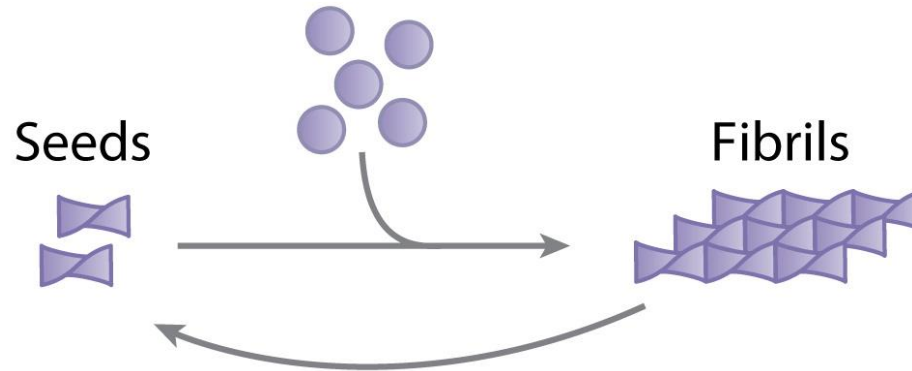
Importance of the Counter-Strand



jR2R3-P301L

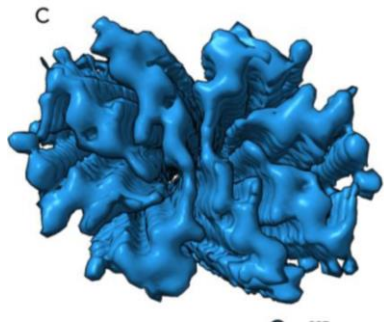


Seeding



Can jR2R3-P301L seed the fibrillization of full length Tau?

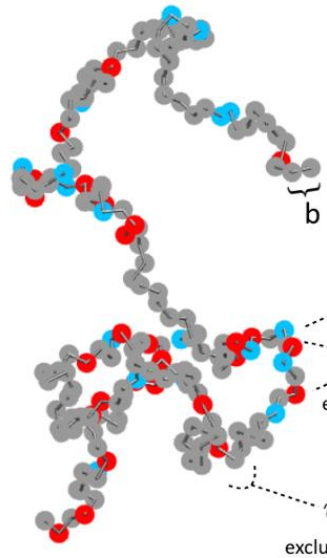
jR2R3-P301L can seed the fibrillization of full length Tau in Vitro



Fibril of Tau
Fragment
jR2R3-P301L

DNIKHV**L**GGS
VQIVYK

+



Full length Tau

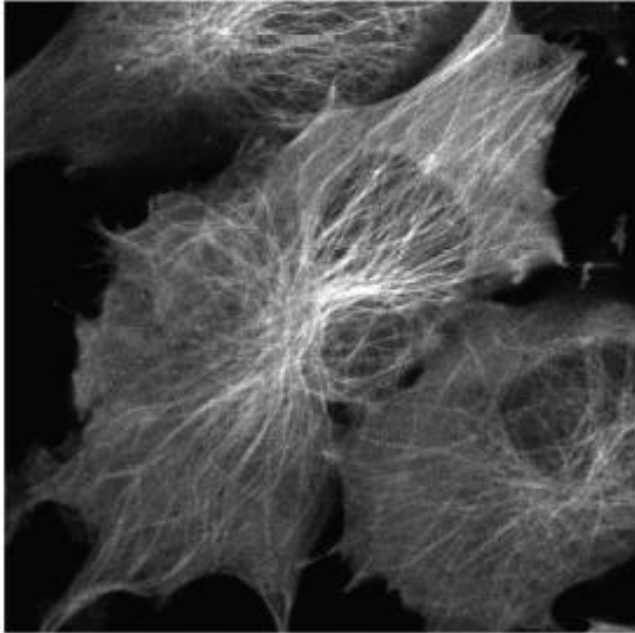


Full Length Tau
Fibrils

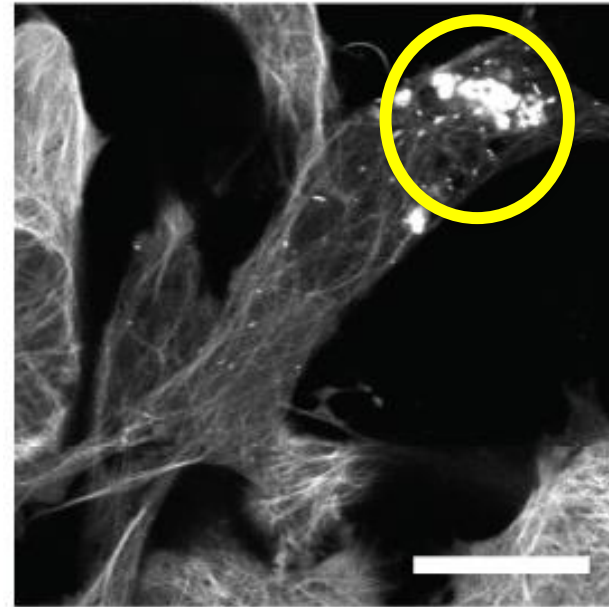
	272	GGK	274	R1
275	VQI	IINKKLDLS-NVQSKCGSKDNIKHVPGGGS	305	R2
306	VQIVYK	PVDLS-KVTSKCGSLGNIHHKPGGGQ	336	R3
337	VEVKSEK	LDLDFKDRVQSKIGSLDNITHVPGGGN	368	R4
369	KKIETHK	LPRENAKAKTD	387	C

jR2R3-P301L can seed the fibrillization of full length Tau in Vivo

Before jR2R3 P301L

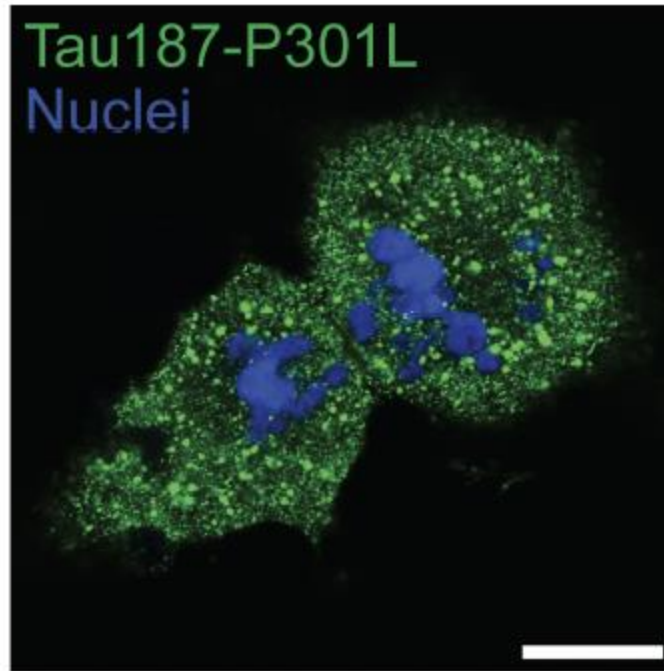


After jR2R3 P301L



Cells expressing mClover3-Tau187-P301L seeded with jR2R3-P301L fibrils

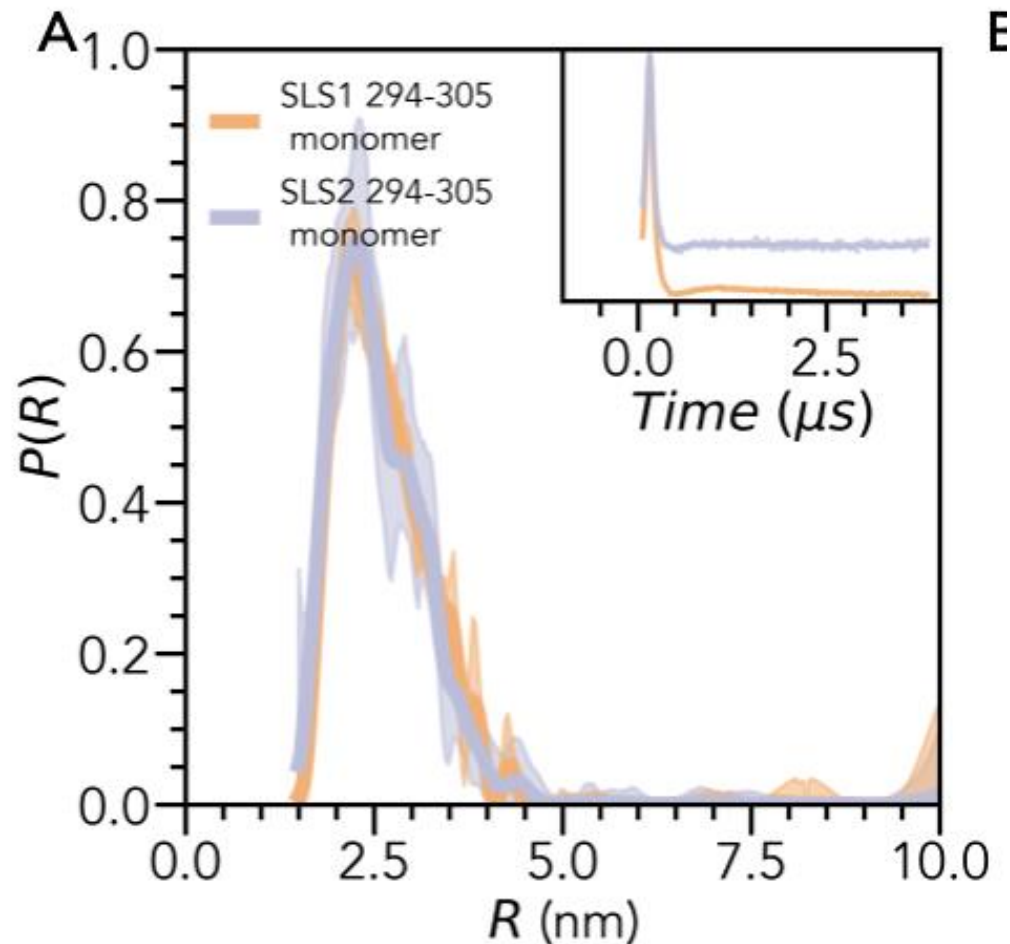
jR2R3-P301L acts as a prion: propagates the strain



Prof. Ken Kosik, UCSB

Cells seeded with jR2R3-P301L fibrils undergo division and propagate aggregates to daughter cells

Double Electron-Electron Resonance (DEER) Spectroscopy cannot distinguish between wild type and mutant



Simulations of jR2R3 and JR2R3-P301L (Replica Exchange; Charmm36m)

jR2R3



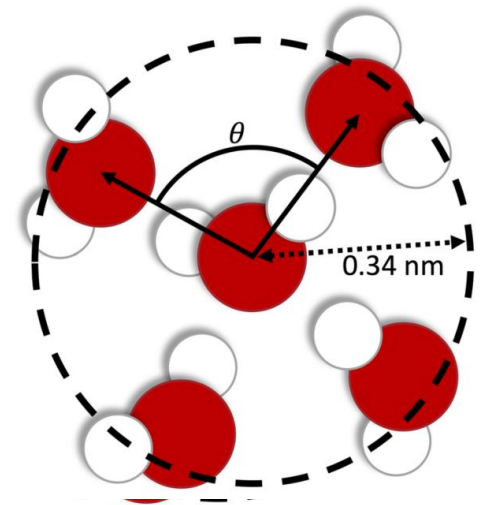
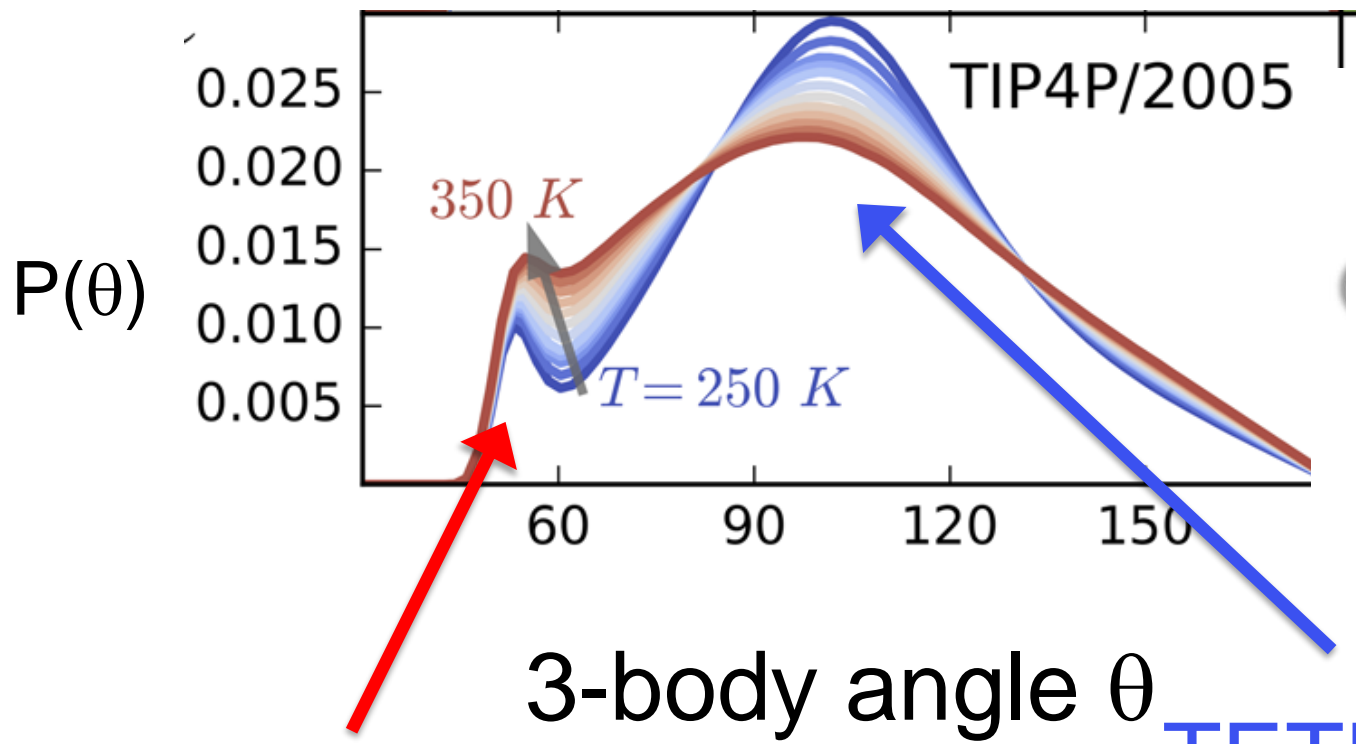
jR2R3-P301L

LITTLE DIFFERENCE



Pritam Ganguly

Water Triplet Distribution



“hydrophilic”

TETRAHEDRAL
“hydrophobic”